Light-front Hamiltonian field theory

covariance and renormalization

VRIJE UNIVERSITEIT

Light-front Hamiltonian field theory
covariance and renormalization

ACADEMISCH PROEFSCHRIFT

ter verkrijging van de graad van doctor aan
de Vrije Universiteit te Amsterdam,
op gezag van de rector magnificus
prof.dr. E. Boeker,
in het openbaar te verdedigen
ten overstaan van de promotiecommissie
van de faculteit der natuurkunde en sterrenkunde
op maandag 23 september 1996 te 15.45 uur
in het hoofdgebouw van de universiteit,
De Boelelaan 1105

door

Norbert Emiel Ligterink
geboren te Enschede

Promotor:	prof.dr. H.J. Boersma
Copromotor:	dr. B.L.G. Bakker
Referent:	prof. S.J. Brodsky

This work was supported by the Stichting voor Fundamenteel Onderzoek der Materie (FOM), which is financially supported by the Nederlandse Organisatie voor Wetenschappelijk Onderzoek (NWO). The text is typeset in LaTeX.

Contents

Outline

In this thesis we establish the relation between covariant field theory and light-front Hamiltonian field theory. The results of covariant field theory can be derived in a light-cone time-ordered[1] formulation despite the formal difficulties that exist in the framework where the time-direction is chosen light-like. Our results put some of the features of light-front field theory in a different perspective.

Chapter 1: Introduction

We give a general discussion of field theory and argue that the Hamiltonian formulation of field theory is more appropriate for the study of bound-state problems. We give a simple example to illustrate the special features of light-cone time-ordered perturbation theory.

Chapter 2: Partial differential equations and light-front field theory

In this chapter we examine some properties of the partial differential equations and the consequences of the choice of initial conditions on the light-front for field theory. Two important results are discussed: non-uniqueness and singular solutions. The null-solutions, which are solutions that vanish at the light-front, are explicitly constructed for the Klein-Gordon equation and the Dirac equation. The complete solution of the partial differential equation with given boundary conditions can be determined up to such null-solutions. It is also shown that the existence of singular solutions makes the set of integrable solutions smaller on the light-front than on any other hypersurface, because the singularities propagate in light-like surfaces. These problems make quantization of light-front field theory and the consequent renormalization difficult.

Chapter 3: Equivalence of light-front and covariant field theory

In this chapter we discuss the relation between the standard covariant quantum field theory and light-front field theory. We define covariant theory by its Feynman diagrams, whereas light-front field theory is defined in terms of light-cone time-ordered diagrams. A general algorithm is proposed that produces the latter from any Feynman diagram. The procedure is illustrated in several cases. Technical problems that occur in the light-front formulation and have no counterpart in the covariant formulation are identified and solved.

[1] We talk about light-cone time, since time is a direction and is defined in the affine space. The light-cone time direction lies on the light-cone. The hyperspace perpendicular to light-cone time is the light-front. Our states and our Hamiltonian are formulated with variables on this light-front and hence we use the term light-front Hamiltonian.

Chapter 4: A different approach to dimensional regularization

We have combined elements of dimensional regularization, dimensional analysis and differentiation with respect to external variables to a renormalization scheme. The method does not use regulators and gives finite integrals. The method is manifestly covariant, but designed especially to be used outside the realm of manifestly covariant theories. In particular, we are interested in time-ordered perturbation theory. We also discuss some aspects of dimensional regularization. We apply our method to the nucleon self-energy.

Chapter 5: Renormalization of light-front Hamiltonian field theory

We propose a regularization of light-front field theory which does not make a distinction between transverse and longitudinal coordinates. It consists of a subtraction of low order terms in the Taylor expansion of an amplitude with respect to external momenta, similar to the regularization in the BPHZ-scheme, which has some advantages that do not exist in covariant field theory. Instantaneous parts and other longitudinal singularities are automatically removed irrespective of their explicit form. We argue therefore that these parts are meaningless. The local counterterms are equal to those of covariant field theory. We demonstrate the method in a number of examples, recovering the covariant results.

Chapter 6: The relativistic Hamiltonian in the bound-state problem

We discuss the relation between covariant field theory and Hamiltonian field theory and show that the Hamiltonian corresponding to a local Lagrangian density has nonlocal phase-space factors in the interaction. We apply these results in the weak coupling limit to scalar electrodynamics and derive the relativistic version of the Coulomb-Schrödinger equation. In the light-front formalism we analyze the higher Fock state contents of a bound state and find that the higher Fock states are suppressed kinematically.

1

Introduction

This thesis deals with some aspects of the Hamiltonian formulation of quantum field theory, in particular light-front Hamiltonian field theory. Light-front Hamiltonian field theory uses a light-like direction as time direction.

Since the discovery of particle creation and annihilation, field theory is considered the correct formulation to describe quantum-mechanical processes at small scales. In field theory separate degrees of freedom are expressed in the field strengths of different fields at a point. The field strength at a space-time point can only be defined in a formal manner, but the notion of a point is relevant, since, if we go to higher and higher energies, we will look at smaller and smaller scales approaching a point scale. However, the field strength at a point remains an enigma: the impossible measurement. Still, it seems that nature uses this point scale since almost local intermediate states, such as extremely heavy particles in the intermediate state, contribute finite amounts to the low energy states ($e.g.$, the heavy Higgs particle which generates the fermion masses).

From a theoretical viewpoint the local theory, which contains only interactions among fields at the same space-time point, has many advantages: a point is relativistically invariant and therefore a local theory can be expressed independently of a coordinate frame. A quantum field theory is usually derived from the canonical commutation relations which are the natural extension of the quantum-mechanical commutation relations of systems with a finite number of degrees of freedom. The corresponding degrees of freedom in field theory are $\phi(\vec{x})$ and $\partial_t\phi(\vec{x})$, where $\phi(\vec{x})$ is the field strength of the field ϕ at $(t,\vec{x})$:

$$\begin{aligned}[\phi(\vec{x}),\phi(\vec{x}')]_{t=0} &= 0,\\ [\partial_t\phi(\vec{x}),\partial_t\phi(\vec{x}')]_{t=0} &= 0,\\ [\partial_t\phi(\vec{x}),\phi(\vec{x}')]_{t=0} &= i\hbar\delta^3(\vec{x}-\vec{x}').\end{aligned} \tag{1.1}$$

The commutation relations link space-time functions with Fock-space operators. The degree of freedom is the field at a point, and we label the degrees of freedom by their space coordinates. It is hard to deal with a theory where at each space-time point fields are created and annihilated. If we use each space-time point as a separate point we can deal with scattering theory at finite orders in perturbation theory in a straightforward manner. At a finite number of space-time points specific interactions occur, and particles propagate freely between those points. The propagation amplitude is given by the expectation value of creating a particle at one point and

annihilating it at another and the amplitude is determined by the phase rotation due to the action of a straight line trajectory between the two points. A particle is labeled by a coordinate, and although we are far from the classical notion of a particle we still use its coordinate in field theory. The Feynman rules tell us how to calculate a scattering amplitude perturbatively.

The concept of a state is obscured in this picture. Asymptotic scattering theory can be viewed as time-independent perturbation theory; in-states and out-states are free states which are projected on the nth order approximation of an eigenstate which results from an analytical expansion of the eigenstate in the coupling constant. If the coupling constant is zero the eigenstate is the free state, and if the coupling constant is nonzero the free states form only a basis for the true eigenstate and other free states mix with the initial state. However, in the scattering amplitude these intermediate eigenstates of the interacting theory are no longer manifest. The idea of an interacting eigenstate is obscured by the space-time approach and in the asymptotic in-states and out-states.

In order to deal with bound states we need to know more about the interacting eigenstates. Scattering theory, which uses free states as asymptotic states, gives us only indirect information about the bound state: "the bound state is a pole in the S matrix." A bound state can only be an interacting eigenstate, therefore in the free theory a bound state cannot exist. In scattering theory the scattering of constituents which form the lowest Fock component of the bound state is considered. The concept of scattering is extended to a kinematical region in which scattering cannot occur; the particles are off-shell. If other particles contribute to a nontrivial content of the bound state we can only hope to gain some information about that. For example, in charged states in QED we find that the infrared divergences tell us that we neglected the possible presence of soft photons in the asymptotic states. If these soft photons are included, the theory will become finite. If soft photons need to be included in the asymptotic states we might expect they are a nontrivial part of the bound state.

A bound state is a stationary state. A stationary state is a state which changes only its phase with time. At least in nonrelativistic quantum mechanics this is the case: the eigenstates of the Schrödinger equation are stationary states. In relativistic quantum field theory we lack a framework in which such an equation can be formulated. The Bethe-Salpeter equation comes closest to such an equation, starting with a scattering kernel it finds the fixed point of successive off-shell to off-shell scatterings. Given the constituents it produces a pole in the S matrix.

Any nontrivial content of the bound state, such as mass, energy or spin, carried by the exchanged particles cannot be recovered in the Bethe-Salpeter formalism. Since that would demand for intermediate particles to be included in the "asymptotic state". Therefore the Bethe-Salpeter equation becomes useless for stronger interactions. The sea particles which are an important part in the analysis of deep-inelastic scattering of hadronic bound states are awkward to handle in the Bethe-Salpeter formalism.

In order to establish a framework in which we can formulate a bound-state eigenvalue equation we have looked at time-ordered theories, where in each intermediate state we have a specific Fock-state content, or particle content. A critical advantage of light-cone time-ordered theories is the suppression of higher Fock-states due to the spectrum condition which restricts the longitudinal momenta of the particles to a positive fraction of the total longitudinal momentum. In order to make sense of such a formulation we have looked at its connection with covariant field theory. We shall show that the same results as in covariant field theory can be obtained in a time-ordered, or Hamiltonian, theory.

One major problem of finding a stationary eigenvalue equation is the divergences. The

expressions in the perturbative expansion are ill-defined when two, or more, interactions occur at the same space-time point. In a local theory infinites occur frequently since it allows for a continuously infinite number of intermediate states, each contributing only an infinitesimal amount but adding up to an infinite contribution. In covariant field theory renormalization of the infinities, such that one ends up with a finite physical theory, is well established, but in the time-ordered theory only ad hoc methods exist. We will consider how dimensional regularization can be made applicable to time-ordered theories. We have also designed a renormalization scheme which maintains covariance in light-front Hamiltonian perturbation theory. Covariance guarantees the locality of the counterterms which in the noncovariant framework of time-ordered theories can only be inferred indirectly.

The infinities are the result of switching on the interaction; the interaction generates the masses of the particles and the screening of charges. In order to obtain results in the interacting theory we have to make an enormous detour from free states of the free theory to free states with large, regularized, masses and small, regularized, charges of the interacting theory, to finite free states, and finally, to finite interacting states. It would be desirable to have a method in which the finite free states of the interacting theory will lead immediately to the finite effects of interaction on the free states of the interacting theory. However, such a method does not exists.

The usual manner in which a Schrödinger equation is obtained from field theory consists of a number of steps. Starting with the Bethe-Salpeter equation, one removes the dependence on the internal energy variable by: heavy mass limit, quasi-potential approximation, Wick rotation (which treats the time variable as a space coordinate) or a vierbein construction (where only coordinates orthogonal to the four-velocity are used as internal degrees of freedom). Afterwards, one integrates out the degrees of freedom associated with the exchanged particles, usually restricted to one or two particles and often only those that are exchanged between two constituents. Finally, one has a linear eigenvalue equation that can be solved with standard techniques under the proper approximations. The integrated degrees of freedom result in a nonlocal potential between the constituents.

In the sixth chapter we shall derive the Coulomb-Schrödinger equation from the lowest nontrivial Fock-state truncation of the time-ordered field theory. The truncation is the only approximation in this Hamiltonian formalism, while in the covariant formulation one has not only to deal with the awkward relative time coordinate but also with the antiparticle components which are present in the covariant propagators.

We argue that our mechanism of binding can be extended. Therefore one has to keep the Fock state picture intact but instead approximate the kinematics. We shall show that such a study of binding in feasible.

1.1 Conventions

We use wave equations and time-ordered theory. Therefore, we will use the Minkowski metric in this thesis. In the cases that we use the Euclidean metric we will state this explicitly.

$$x = (x^0, x^1, x^2, x^3); \quad x^2 = (x^0)^2 - \vec{x}^2 = (x^0)^2 - (x^1)^2 - (x^2)^2 - (x^3)^2. \tag{1.2}$$

The light-front variables, $x^{\pm}$, are combinations of x^0 and x^3.

$$x^{\pm} = x_{\mp} = \frac{1}{\sqrt{2}}\left(x^0 \pm x^3\right), \tag{1.3}$$

with the metric tensor: $g^{+-} = g^{-+} = 1$; $g^{11} = g^{22} = -1$ and all other entries zero.

$$x^2 = 2x^+x^- - (x^1)^2 - (x^2)^2 = 2x^+x^- - \vec{x}_\perp^2 = 2x^+x^- - x_\perp^2. \tag{1.4}$$

In Euclidean space these two directions are orthogonal, but in Minkowski metric these vectors are light-like. The length of a light-like vector is zero in Minskowski metric. Therefore, given the length and the direction of a light-like position vector, the position is indefinite. Since $x^+ = x_-$, we will use only the contravariant vectors, with the upper indices, in order to avoid confusion throughout this thesis. We define the time-direction in the x^+ direction which makes p^- the time-evolution operator, the Hamiltonian, of our system.

Note also that the gamma matrices have the properties one would expect:

$$\gamma^{\pm} = \frac{1}{\sqrt{2}}\left(\gamma^0 \pm \gamma^3\right), \quad \gamma^{\pm}\gamma^{\pm} = 0, \quad \gamma^+\gamma^- + \gamma^-\gamma^+ = 2g^{+-} = 2. \tag{1.5}$$

For the inner-product of a momentum and gamma matrices we will always use the Lorentz metric: $\not{k} = \gamma^0 k^0 + \vec{\not{k}} = \gamma^+ k^- + \gamma^- k^+ + \gamma_\perp \cdot k_\perp$. The $\gamma^{\pm}$ matrices are singular. This is one of the features which make light-front field theory special, and the quantization of fermion fields tricky. Our conventions are the same as those of Mustaki (Mustaki, 1990; Mustaki et al., 1991).

1.2 A simple example

In order to give some flavor of the subject, we discuss the scalar one-loop self-energy in ϕ^3 theory in this section. See fig. 1.1. This diagram is calculated in most text-books on field theory and plays a central role in many discussions. The covariant amplitude is

$$\mathcal{F}(p^2) = \frac{g^2}{2(2\pi)^4}\int \mathrm{d}^4k \frac{1}{((p-k)^2 - m^2 + i\epsilon)(k^2 - m^2 + i\epsilon)}. \tag{1.6}$$

A factor g occurs for each vertex, a factor $(2\pi)^{-1}$ for each integration and a factor $\frac{1}{2}$ for symmetry. The diagram itself is divergent. However, we can renormalize the amplitude and calculate the finite part. (Details of the calculations can be found in sect. 4.11.2.) The result is

$$\mathcal{F} = \frac{ig^2}{16\pi^2}\left(1 - \sqrt{\frac{p^2-4m^2}{p^2}}\operatorname{arctanh}\sqrt{\frac{p^2}{p^2-4m^2}}\right). \tag{1.7}$$

The covariant diagram sums two specific processes separated by the time ordering of the two vertices. We can see this if we look at the propagator, which contains actually two propagators; one for each pole:

$$\frac{1}{p^2 - m^2 + i\epsilon} = \frac{1}{2E_p}\left(\frac{1}{p^0 - E_p + i\epsilon} - \frac{1}{p^0 + E_p - i\epsilon}\right), \tag{1.8}$$

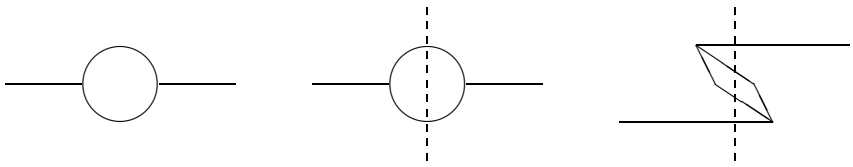

Figure 1.1: The scalar loop; covariant, forward and backward diagram.

where $E_p = \sqrt{\vec{p}^2 + m^2}$.

If we separate the different poles in the scalar loop, the poles combine only in two cases to a nonvanishing contribution. One pole must be at each side of the real axis to give a contribution to the contour integral. The integration over the energy is equivalent to summing all processes for different relative times between the occurrences of the two vertices. If we integrate over the energy variable k^0, we will have only these two contributions, corresponding to different time orderings of the two vertices. We denote the two time orderings as the forward diagram:

$$\frac{-ig^2}{2(2\pi)^3}\int \mathrm{d}^3k \frac{1}{4E_{p-k}E_k}\frac{1}{(p^0 - E_{p-k} - E_k)}, \tag{1.9}$$

and the backward diagram:

$$\frac{-ig^2}{2(2\pi)^3}\int \mathrm{d}^3k \frac{1}{4E_{p-k}E_k}\frac{1}{(p^0 + E_{p-k} + E_k)}, \tag{1.10}$$

respectively. See fig. 1.1. The meaning of the backward diagram has been the subject of many discussions. We see it is necessary to recover a covariant amplitude. The backward diagram is also referred to as a vacuum diagram or Z-diagram. It is believed to signify the contributions due to vacuum fluctuations. The particle is annihilated by an antiparticle created from the vacuum. For fermions it is also said that the vacuum is suppressed by the Pauli principle due to the presence of extra fermions. However, this does not explain the same diagram for bosons.

The backward diagram is absent in light-front perturbation theory. If we introduce the light-front variables: $p^{\pm} = (p^0 \pm p^3)/\sqrt{2}$ and integrate over the light-front energy k^- we will only find one contribution:

$$\frac{-ig^2}{2(2\pi)^3}\int_0^{p^+} \mathrm{d}k^+\mathrm{d}^2k_\perp \frac{1}{4(p^+ - k^+)k^+}\frac{1}{\left(p^- - \frac{(p_\perp - k_\perp)^2+m^2}{2(p^+-k^+)} - \frac{k_\perp^2+m^2}{2k^+}\right)}. \tag{1.11}$$

The integration domain in the longitudinal variable is determined by the value of the longitudinal momenta for which there is a pole on each side of the real axis. The integral gives the covariant result (see sect. 5.3.1). This is a very subtle result. The covariant propagator can be written in light-front coordinates:

$$\frac{1}{p^2 - m^2 + i\epsilon} = \frac{1}{2p^+}\left(\frac{\theta(p^+)}{p^- - \frac{p_\perp^2+m^2}{2p^+} + i\epsilon} + \frac{\theta(-p^+)}{p^- - \frac{p_\perp^2+m^2}{2p^+} - i\epsilon}\right). \tag{1.12}$$

The residue integration restricts the four-dimensional integration to an integration over a three-dimensional mass hyperbola. This integral is equivalent for light-front and ordinary coordinates; variable substitution relate one to the other. However, in light-front coordinates we are able to combine the results from the different residues.

The different contributions give the same expressions but the domains in k^+ space are different. The (standard) forward diagram gives the integrand integrated over the domain $k^+ \in [0, \infty)$, while the (standard) backward diagram gives the opposite contribution in the domain $k^+ \in [p^+, \infty)$. The net result is a forward diagram in the domain $k^+ \in [0, p^+]$. If we look at the light-front variables in standard coordinates we will see that the integration over k^3 is not over the full space but over a domain where a parabola is cut from the three-dimensional space:

$$k^+ < p^+ \quad \Rightarrow \quad \vec{k}_\perp^2 + m^2 < 2(p^+)^2 - 2\sqrt{2}\, p^+ k^3 \ . \tag{1.13}$$

It seems that the backward diagrams are incorporated in light-front field theory as the restriction of the kinematical domain. The forward part of the propagator has the opposite behavior for large momenta as the backward part. Light-front field theory uses this feature and subtracts the two contributions in an efficient way such that only the forward parts remain. In chapter 3 we will see that this holds for any part of an amplitude expressed in Feynman diagrams.

2

Partial differential equations and light-front field theory

In the theory of partial differential equations there are two major research areas: the study of the local solutions and of the global solutions, respectively. The approaches for both are quite different. The global theory integrates the differential equation and tries to analyze qualitatively the behavior of the solution. The results might differ depending on the space in which the initial conditions are defined. Apart from general mathematical interest and the construction of counterexamples the global theory is necessary to check the stability of a numerical algorithm used to solve a partial differential equation.

The local theory only looks at the behavior around a point. It uses an analytical expansion around that point. Or, more general, it refers back to the analytical expansion. The Cauchy-Kovalevskaya and the Holmgren theorems are general results (Hörmander, 1963) in this case. Field theory is more closely related to the local theory.

In field theory we feel that the behavior at far distances should not interfere with the outcome of an experiment. Therefore specific behavior of the initial conditions at far distances, as imposed by insisting that the initial conditions should be in a specific mathematical space, are not strictly imposed in a physical model. Also, quantum field theory is only properly defined as perturbation theory therefore we will seldom recover some of the striking features of the classical nonlinear wave equations which lie at the basis of the field theory. The nonlinear terms in the Lagrangian poses many problems upon quantization. Most of these problems are circumvented if we consider these nonlinear terms as perturbations. The global effects which have found their way in quantum field theory as topological effects, specifically in gauge theories, are rarely observed experimentally.

To define the perturbative expansion in quantum field theory we do need some knowledge of the free field theory which includes the knowledge of the differential equations which determine the free solutions. This is necessary to define the propagators which relate the fields at different space-time points. There turn out to be some subtle differences between the standard case where the initial conditions are defined on an equal time surface and initial conditions defined on the light-front surface, or null plane, $z+ct = constant$. These differences manifest themselves in the quantization procedure and at a technical level when we try to use operators which have singular behavior.

In this chapter we study the classical free wave equation with the light front as initial surface. Part of the results can be found in the mathematical literature, some explicit solutions are derived here.

The quantization of a field theory requires some basic knowledge of the classical theory. First, the knowledge of the independent variables with which a state, a specific field configuration, is described. Second, a Hamiltonian which governs the dynamics of the system: the time-dependent behavior. The Hamiltonian gives the evolution of the state in time and so indirectly the evolution of all physical quantities. If we cannot determine either, we have a problem. It turns out that classical light-front field theory, which corresponds to the classical wave equation with light-like boundary values is ill-defined in both ways in a mathematical sense. This makes it doubtful whether a consistent canonical quantization exists. The problems people encounter upon quantization of light-front field theory are often considered as practical problems, but more likely they are the signatures of an ill-defined mathematical problem.

2.1 Motivation

Relativistic covariance is a necessary property for a realistic description of many physical systems. Quantum field theory (QFT) offers a formalism that describes interacting particles in a covariant way. Light-front field theory (LFFT) has been proposed as a version of QFT that has advantages over the usual formulation. The main point is that the vacuum has a simpler structure in LFFT. Many results in LFFT have been derived by methods which work in ordinary QFT, or by plain application of results of ordinary QFT in LFFT. However, in the light-front formulation problems arise that may invalidate some of these results. In this chapter we go back to the classical theory of partial differential equations where some of these problems are already present:

- Boundary conditions on a light-like surface don't give a *unique* solution.
- There exist *singular solutions* with singularities on the light front. (The singularities are of a higher order on the light front than on any other hypersurface.)

These problems become important if perturbation theory and renormalization are considered. Then we are interested in uniqueness, completeness and the behavior of singular solutions of the field equations.

The particle interpretation of QFT hinges on the possibility to construct wave packets that are normalized. On the light front, $x^+ = 0$, such a wave packet cannot be constructed in an invariant way[1], because a wave packet has to be independent of the x^- coordinate (Nakanishi & Yamawaki, 1977).

The ordinary causal propagator is singular on the light-cone, so it is singular on a line in the light front (Kogut & Soper, 1970) from which we wish to "propagate". Therefore this propagator is ill-defined for a Hamiltonian theory and cannot arise from quantization on this surface. Another approach is to construct a propagator out of independent free fields only (with the spectrum condition $p^+ \geq 0$). This gives a *non-covariant* propagator (Yan, 1973a).[2]

[1] This problem is different from the inconsistency between particle interpretation and localization as noticed by (Newton & Wigner, 1949).

[2] The interaction Hamiltonian also has extra terms in this case, because the eliminated dependent fields contained interaction, which has to be included.

Also, one can let the propagator satisfy the constraint, that is: the non-propagating part is local in the time direction (Hagen & Yee, 1976) (which is only constructed in the case of a massless theory). Different requirements lead to different results, so either the demands are inconsistent, or there is an underlying principle which connects the approaches. We conjecture that the different definitions follow from the singular nature of the propagator and the ambiguity should be resolved by requiring covariance.

2.2 Relevant theorems

The mathematical theorems about partial differential equations (PDE) stand as unrefutable facts. Nevertheless, their connection with QFT is unclear. Many of the theorems constitute nothing but a formal proof of existence.

Most of the theorems and proofs can be found in the books by Hörmander, *e.g.*, (Hörmander, 1963). The mathematical theory of partial differential equations examines some of the strange effects which might be expected if we use a light-like surface as boundary on which we define the initial field (the initial surface). A light-like surface is the *characteristic* surface of the wave equations we are considering. Here we state some of the relevant theorems, but for proofs we refer to the mathematical literature. In this chapter we will look at some aspects of *characteristic partial differential equations* more closely.

The solutions of differential equations have a number of special properties, often independent of the fact whether we deal with *massive* or *massless* fields:

Theorem : The Cauchy problem is non-unique

It is possible to have a solution which vanishes at the light front (together with an arbitrary number of derivatives) which is non-zero in the half-space we are considering. For the massless case this is trivial: simply take any function of the x^+-coordinate only, which vanishes at the boundary. For the massive case it is more complicated, but still true. So it is fundamentally impossible to determine the evolution of a solution if one knows it at a light front, since one can add any null-solution (i.e. a solution vanishing at the boundary), unless one imposes additional conditions. This is as true for the Klein-Gordon equation as it is for the Dirac equation.

Theorem : Singular solutions exist on the light-cone

If a PDE has a singular solution, the singularity propagates in a light-like surface. It only has to satisfy a supplementary condition $P^+\phi = 0$, where P^+ is the differential operator along the light-like direction in the light-front, which shows the two features of these solutions:

1. The condition on the eigenvalue $p^+ = 0$ allows more solutions than only the vacuum (namely all kinds of singular solutions).

2. Since we don't know how to interpret these states, normalization and regularization require more caution.

Theorem : Every PDE with constant coefficients has a Greens function

A Greens function $G(\mathbf{R}^n)$ satisfies:

$$P(D)\,G(x) \equiv \left(\sum_{ij} a_{ij}\partial^i\partial^j + \sum_i b_i\partial^i + c\right) G(x) = \delta^n(x) \tag{2.1}$$

A Greens function is not necessarily a propagator with the right properties (e.g. CPT). This theorem only tells us that *formally* we can construct a solution.
A Greens function allows one to give symbolically the evolution of a field, a method which became more appreciated with the functional methods. However, the Greens function doesn't say much about uniqueness of the evolution of a solution.

2.3 Null-solutions

Null-solutions are defined as the non-zero solutions which vanish at the boundary $x^+ = 0$. The existence of null-solutions is not apparent in momentum representation, since there it is related to the analytical continuation of the characteristic relation: $p^2 - m^2 = 0$. However, in configuration space it follows easily from invariant solutions of the Klein-Gordon equation, which are functions of the invariant length only. Let ψ be an invariant solution of the (massive) wave equation, then it is a function of the invariant length s. So assume a solution $\psi(s)$ where $s = 2x^+ x^- - (x^1)^2 - (x^2)^2$, then we can construct a set of solutions, which are zero on the light front $x^+ = 0$ namely:

$$(\partial^+)^n \psi(s) = (2x^+)^n \psi^{(n)}(s), \tag{2.2}$$

which is zero on the light front if ψ is not singular in $s = 0$. But we will see that the space of null-solutions is even bigger than this.

One of the solutions which satisfy the wave equation, $(\Box + m^2)u = 0$, is the Bessel-function:

$$J_0(m\sqrt{2x^+ x^-}) \equiv \sum_{i=0}^{\infty} \frac{\left(-\frac{1}{2}m^2 x^+ x^-\right)^i}{i!\, i!}, \tag{2.3}$$

which is an analytical function on the whole space (an *entire* function). We can extend this trivially to include transverse coordinates by multiplying the Bessel-function with a plane wave in the perpendicular coordinates, and changing the argument of the Bessel-function slightly:

$$J_0(\sqrt{k_\perp^2 + m^2}\ \sqrt{2x^+ x^-}\,)\ \mathrm{e}^{ik_\perp \cdot x_\perp}, \tag{2.4}$$

which is again a solution of the wave equation. Instead of an analytical solution one can also use a bounded ($\mathcal{L}^1_{\mathrm{loc}}(\mathbf{R}^4)$) solution, which is given by: $(\theta(x^+)\theta(x^-) - \theta(-x^+)\theta(-x^-))J_0$, with J_0 as above. We can also construct an invariant solution, since we can use *any* Fourier-transformable function in the perpendicular coordinates. This invariant solution is: $\frac{2}{m\sqrt{s}} J_1(m\sqrt{s})$.

A set of null-solutions (N_ν) is given by:

$$N_\nu(\mu, x^+, x^-) = \sum_{i=0}^{\infty} \frac{(-\frac{1}{2}\mu^2)^{i+\frac{\nu}{2}} (x^+)^{i+\nu} (x^-)^i}{i!\,\Gamma(i+\nu+1)} = \left(\sqrt{\frac{-x^+}{x^-}}\right)^{\nu} J_\nu(\mu\sqrt{2x^+ x^-}), \tag{2.5}$$

where $\mu = \sqrt{k_\perp^2 + m^2}$. Again we can include any function in the perpendicular coordinates, since the $(x^+)^\nu$ factor causes the functions to vanish at $x^+ = 0$ for $\nu > 0$. These solutions can be related to each other by step operators: $\mathbf{P}^+, \mathbf{P}^-$, $(\nu \notin \mathbf{Z}^-)$

$$\mathbf{P}^+ N_\nu = -i\frac{\sqrt{2}}{\mu}\partial^+ N_\nu = N_{\nu+1}\ , \quad \mathbf{P}^- N_\nu = -i\frac{\sqrt{2}}{\mu}\partial^- N_\nu = N_{\nu-1}, \tag{2.6}$$

(with the exception: $\mathbf{P}^- N_0(x^+, x^-) = N_1(x^-, x^+)$, where the variables are interchanged, which shows the special nature of $\nu \in \mathbf{N}$.) The functions, N_ν, where ν are integers, together with those with interchanged arguments (N'_ν) can be related to plane wave solutions. The solutions form a basis for an analytical expansion on $x^+ = 0$ and $x^- = 0$ around the origin. Therefore, this expansion on a finite domain can be expanded in plane waves, since they both form a basis for smooth functions on a finite domain. If one first restricts oneself to a countable basis, the convergence will be bad. In the "$\{N_\nu, N'_\nu\}$-basis" only half of the solutions have non-vanishing boundary values. So one can conclude that the light-front boundary determines only half of the degrees of freedom.

The existence of null-solutions is related to z-boost symmetry. If we assume a solution analytical in x^+ and x^-, we can construct a whole set of new solutions which also satisfy the Klein-Gordon equation; If u is a solution then any sequence $\{b_i\}_{-\infty}^{\infty}$ will lead to a new solution (not bothering about convergence):

$$u = \sum_{i,j} a_{ij} (x^+)^i (x^-)^j \qquad \Rightarrow \qquad \tilde{u} = \sum_{i,j} a_{ij} b_{(i-j)} (x^+)^i (x^-)^j. \tag{2.7}$$

This is the massive analogue of the two dimensional massless case where a solution is *any* function $u(x^+, x^-) = f(x^+) + g(x^-)$.

2.3.1 Null-solutions of the Dirac equation

Once the null-solutions (N_ν's) for the Klein-Gordon equation are known then those for the Dirac equation follow relatively easily. We just project these null-solutions on spinor-states:

$$u = (-i\partial\!\!\!/ + m)N \quad \Rightarrow \quad (-i\partial\!\!\!/ - m)u = -(\Box + m^2)N = 0. \tag{2.8}$$

But we must be cautious with the constraints. Since not the whole Dirac equation involves the x^+-time derivative, we have additional relations which have to be satisfied[3]. Formally implementing the constraints on the *free* Dirac equation, where one assumes $(\partial^+)^{-1}$ to be a proper one-to-one operator on the space of physical solutions, leads to two independent "Klein-Gordon" fields ($\frac{1}{2}\gamma^-\gamma^+\psi = \psi^+$ fields) distinguished by their spinor directions.

This hardly changes the construction of the null-solutions for the Dirac equation, because then one just has to restrict the projection on the independent part only: ($N_\nu \to \frac{1}{2}\gamma^-\gamma^+ N_\nu$).

2.4 Singular solutions

The wave equation can have singular solutions. These are associated with *shock waves* or *wave front* solutions. One important feature of these solutions is that the singularities propagate in a characteristic, or light-like, surface. This has an important impact, because if we are constructing a space of solutions we like to take only integrable solutions. These solutions can be integrable on any ordinary hypersurface, but not on a characteristic surface.

[3]Its analogue for the Klein-Gordon equation is unfamiliar, but since the Klein-Gordon equation is a second order equation, one has to give u and $\partial^- u$ at the boundary, which leads to a consistency condition: $\partial^+[\partial^- u] = (\Delta - m^2)u$ (after quantization the particle interpretation replaces the second boundary condition).

Compare this with the massless case: a solution is $u(x^+, x^-) = g(x^+) + f(x^-)$. One can take for $g(x^+)$ any singular solution, so as a special case one can take singular solutions which are integrable on $t = 0$ over z: $g(\frac{t+z}{\sqrt{2}})$, but not integrable on $x^+ = 0$ over x^-, for instance: $g(x^+) = (x^+)^\alpha$ with $-1 < \alpha < 0$ are $\mathcal{L}^1_z$ but not $\mathcal{L}^1_{x^-}$. The comparison between the massless case and the massive case goes further than one might expect at first glance: for any (differentiable) solution of the massive wave equation there exists an analytical expansion that has the leading terms $g(x^+)$ and $f(x^-)$ (the only terms that survive at boundaries $x^+ = 0$ and $x^- = 0$). This doesn't mean we have something "going with the speed of light".

The massive case is similar. Let's assume a singular solution of the form ($\alpha < 0$):

$$u(x^+, x^-, \vec{x}_\perp) \equiv (x^+)^\alpha U(x^-, \vec{x}_\perp) + \ \textit{less singular terms}. \tag{2.9}$$

The Klein-Gordon equation gives a recurrence relation between terms of different order, where we get a condition for the leading term:

$$(\Box + m^2)u = 0 \quad \Rightarrow \quad \partial^+ U = 0. \tag{2.10}$$

These solutions are also of the form N_ν, containing a Bessel-function, but with $\nu < 0$. (J_ν exists for all $\nu \ : \ \nu < 0 \ \ \wedge \ \ \nu \notin \mathbf{Z}$.)

This aspect is related to the (group)-structure of space-time: all points[4], except those on the light cone, are smoothly related by Lorentz transformations to each other (the light cone is invariant under transformations). If one starts with one smooth solution (like a plane wave) then all other solutions can be obtained by Lorentz transformations, so they are also smooth except at the light cone against which solutions get "crushed" with boosts approaching the velocity of light. Remember that the idea of a Lorentz metric originally comes from the wave equation, and that the distance is zero in Minkowski metric on the light cone with respect to the apex of the cone.

Although one can treat the space and time coordinates in many respects in the same manner, there remain subtle differences between the two. This can best be illustrated by two features:

1. On a space-like boundary one cannot have proper boundary values to guarantee existence and uniqueness.
2. A PDE as $(\partial^2_\sigma + \partial^2_\tau - \partial^2_x - \partial^2_y)u = f$ cannot be solved (generally) with Fourier-Laplace techniques, because it has two "time" directions.

2.5 The causal propagator

The causal propagator, or Feynman propagator, is derived in the literature in many different ways with many different argumentations. The propagator expresses the effect of a source. If a source is located at the origin it will tell us how a solution of the wave equation propagates outward. In fact, this is not the only option. A solution can also propagate inward and let the source act as a sink. A propagator, or Greens function, does not even have to be spherically symmetric.

[4]This is of course true for each domain within the forward light cone, backward light cone, and outside the light cone separately

In this section we derive the causal propagator in configuration space from the main conditions; spherical symmetry and causality. This derivation is short and simple, and the result is expressed as a boundary of a holomorphic functions. In the later chapters we will refer to this result.

Since the propagator is not unique we have to impose extra conditions. Spherical symmetry means that the propagator is only a function of r and not of x, y and z separately. Causality insures that all particles, denoted by their wave number, have a positive energy. The negative energy solutions approach the origin from negative time direction (inward), and the positive energy solutions leave the origin in a positive time direction (outward).

Bogoliubov and Shirkov (Bogoliubov & Shirkov, 1959) calculate the causal propagator by explicitly calculating the transcendental functions in each of the space-time domains. They find:

$$D^c(s) = \frac{1}{4\pi}\left[\delta(s) - \theta(s)\left(\frac{m}{2\sqrt{s}}H_1^{(-)}(m\sqrt{s})\right) - \theta(-s)\left(\frac{m}{\pi i\sqrt{-s}}K_1(m\sqrt{-s})\right)\right], \quad (2.11)$$

where

$$K_1(z) = \frac{\pi}{2}H_1^{(-)}(-iz), \quad (2.12)$$

$$H_1^{(-)}(z) = J_1(z) - iN_1(z). \quad (2.13)$$

The causal propagator is an analytical function of the invariant length. The delta function is the imaginary part of the pole in the Hankel function. In momentum space causality restricts the $i\epsilon$ prescription uniquely:

$$\frac{1}{p^2 - m^2 + i\epsilon} = \frac{1}{2\sqrt{\vec{p}^2 + m^2}}\left(\frac{1}{p^0 - \sqrt{\vec{p}^2 + m^2} + i\epsilon} - \frac{1}{p^0 + \sqrt{\vec{p}^2 + m^2} - i\epsilon}\right). \quad (2.14)$$

The pole for the positive energy solutions $p^0 = \sqrt{\vec{p}^2 + m^2}$ lies inside the integration contour for the Fourier transform of the propagator for times greater than zero, the opposite is true for the negative energy solutions. So we see that the propagator is finite for positive imaginary values of p^2. The Fourier transformation of an analytical function of p^2 is an analytical function of s in the opposite half plane, since

$$\mathrm{e}^{ix\cdot p} f(p^2) \to \mathrm{e}^{ix\cdot(L\cdot p)} f(p \cdot L^T \cdot L \cdot p) = \mathrm{e}^{i(L^T\cdot x)\cdot p} f(p^2), \quad (2.15)$$

where L is an arbitrary Lorentz transform, which does not alter an invariant solution. Therefore the time coordinate has the opposite (Wick) rotation as the energy ($0 < \phi < \frac{1}{2}\pi$):

$$p^0 = \mathrm{e}^{i\phi}|p^0|, \quad (2.16)$$

$$x^0 = \mathrm{e}^{-i\phi}|x^0|. \quad (2.17)$$

From the two invariant solutions of the wave equation there is one combination that exists in the lower half plane: the second Hankel function $H_1^{(-)}$, therefore it follows that

$$D^c(s) = \frac{-m}{8\pi\sqrt{s - i\epsilon}}H_1^{(-)}(m\sqrt{s - i\epsilon}). \quad (2.18)$$

This result coincides[5] with Bogoliubov and Shirkov.

2.5.1 Uniqueness for a $t = 0$ initial surface

The discussion above makes one wonder why these problems do not occur in the usual case. In the ordinary case, where one uses an instantaneous hypersurface as initial surface, one can easily prove the uniqueness of the solutions of the field equations. If we know *all* time *derivatives* of the field on the initial surface then we can continue the solution into the half space by a Taylor-expansion.

Uniqueness of a solution is equivalent to the fact that vanishing boundary conditions give a zero solution in the half space, since if two different solutions exist with the same boundary values, the difference is also a solution, which has vanishing boundary conditions:

$$u = 0 \quad , \quad \partial_t u = 0 \quad \text{and} \quad (\partial_t^2 - \Delta + m^2)u = 0. \tag{2.19}$$

Now we can construct higher derivatives:

$$\left.\begin{array}{c} \partial_t^2 u = (\Delta - m^2)u = 0 \\ \partial_t^3 u = (\Delta - m^2)\partial_t u = 0 \\ \partial_t^4 u = (\Delta - m^2)\partial_t^2 u = (\Delta - m^2)(\Delta - m^2)u = 0 \end{array}\right\} \quad etc. \tag{2.20}$$

For the Dirac equation the proof is similar: the main condition for the uniqueness is the existence of an inverse of the group element or gamma matrix which is associated with the time derivative ($(\gamma^0)^{-1} = \gamma^0$). Note that in the case of light-front dynamics, where x^+ is the "time", the corresponding gamma matrix, γ^+, is singular, so it has no inverse ($2\gamma^+\gamma^+ = \gamma^0\gamma^0 + \gamma^3\gamma^3 + \{\gamma^3, \gamma^0\} = 0$).

2.5.2 Propagators and the $i\,\epsilon$-Prescription

In Fourier-transformed[6] space it is more easy to construct homogeneous solutions and Greens functions, since the differential equation transforms to a polynomial in several variables (e.g. $p^2 - m^2$).

Propagators are Greens functions with specific boundary conditions (or discrete symmetries). The difference between different propagators is a homogeneous solution, which is the result of different regularizations[7] ($i\epsilon$ prescriptions). These homogeneous solutions belong to the span of the plane waves. The null-solutions are also homogeneous solutions, so the propagators are not uniquely determining the evolution of the field.

In the Fourier-transformed space, non-uniqueness is related to the existence of a homogeneous solution for $p^+ \to 0$ and $p^- \to \pm\infty$. This looks more simple than it is, because one must perform the analytic continuation of the variables in a complex domain and consider areas of convergence of the Fourier transform.

[5] Some authors use the opposite branch of the square root and the first Hankel function which lead to the same result.

[6] Actually the transformation to be considered is more general than the Fourier transform only, since many solutions of PDE's don't have a Fourier-transform, but a Fourier-Laplace transform in some complex variable with the same symbolic calculus (see for instance (Leray, 1953)).

[7] Different regularizations are the result of different particle interpretations, for instance "the positron" and "the backward going electron" as, respectively, interpretations of the retarded and the Feynman propagator.

3

Equivalence of light-front and covariant field theory

It has often been stated that time-ordered perturbation theory is equivalent to covariant perturbation theory. The work of Dyson and Wick constitutes the only direct proof of this statement, and even this proof is rather formal. It is formulated in terms of creation and annihilation operators on a Hilbert space, although there is not a proper Hilbert space at the basis of field theory.

In fact, only the formulation of time-ordered perturbation theory as given by Weinberg (Weinberg, 1966) is equivalent to the covariant perturbation theory. Weinberg introduces some ad hoc phase-space factors which were not present in earlier formulations. He motivates these factors by covariance, but this cannot truly account for their presence.

Because the light-front field theory is plagued by conceptual problems we found it a useful exercise to derive the light-cone time-ordered perturbation theory from covariant perturbation theory. It turned out to be a bit more than an exercise. Many technical problems had to be solved before we could say that both expansions are equivalent mathematical expressions. Along the way we encountered many of the ambiguities that plague light-front perturbation theory. In our different approach we are able to shed some light on these problems, and in some cases covariance made us favor a specific treatment of an ambiguity.

In this chapter we deal with the problem of equivalence of covariant and light-cone time-ordered perturbation theory. After some simple examples to illustrate our method we give a discussion of the technical problems we encounter. The general proof is the last part of this chapter.

3.1 Introduction

Dirac's paper (Dirac, 1949) on forms of relativistic dynamics opened up a whole field of investigation: the study of different ways of quantizing and the relationship between different forms of dynamics. Three forms were identified, the instant form, that corresponds to ordinary time ordered theories, the point form, that will be of no concern to us here, and the front form, where the dynamical variables refer to physical conditions on a plane advancing with

the velocity of light. (Such surfaces are called null planes or light fronts.) The latter form has the advantage that it requires only three dynamical operators, "Hamiltonians", the other seven (kinematical) generators of the Poincaré group containing no interaction. The other advantage noted by Dirac was that there is no square root in the Hamiltonians, thus avoiding the degeneracy of the free field solutions. (Particles and anti-particles cannot have the same kinematical momenta.)

Dirac published his paper right in the middle of the period in the development of quantum electrodynamics, when old-fashioned perturbation theory was replaced by the covariant formalisms of Feynman, Schwinger and Tomonaga (Schwinger, 1958). Only much later were his ideas taken up again[1]. Quantum electrodynamics held center stage for a long time, not only for its unparalleled phenomenological success, but also because it functioned as a role model for many new theories, notably the gauge theories of the weak and the strong interactions.

A new development occurred when the infinite-momentum frame, which had appeared in connection with current algebra (see *e.g.* De Alfaro et al. (de Alfaro et al., 1973)), was proposed by Weinberg (Weinberg, 1966) as a tool in the study of scalar theories, because it simplifies the vacuum structure in those theories. Not long after Weinberg's paper was published, it was suggested (Chang & Ma, 1969) that the use of a new set of variables, *viz*,

$$x^+ = \frac{x^0 + x^3}{\sqrt{2}},\ x^- = \frac{x^0 - x^3}{\sqrt{2}},\ x^1,\ x^2 \tag{3.1}$$

would provide the advantages which are present in the use of the infinite-momentum frame. In such a description, x^+ plays the role of "time", *i.e.*, the evolution parameter, and the connection to Dirac's front-form of dynamics seems immediate. (We will use the terminology light-cone time (l.c.t.) for this variable.) However, the connection between the rest frame and the infinite-momentum frame involves a limiting procedure of Lorentz transformations. Therefore, the equivalence of descriptions in those frames cannot be derived using arguments based on Lorentz invariance alone.

So the question concerning the relationship between different forms of dynamics remains difficult to answer. In particular, the connection between the manifestly covariant formulations and the front form is not yet fully clear. The main reason is that quantization using planes $x^+ = \tau$ as surfaces on which the initial conditions are specified–initial surfaces–is beset with difficulties, that occur already at the classical level in scalar theories. It is a well established result from the theory of partial-differential equations (Hörmander, 1963) that the Cauchy problem with an initial surface that contains a light-like direction, is ill-posed. See also chapter 2.

Attempts to formulate light-front field theory in close relationship with covariant field theory were made by *e.g.* Chang *et al.*, (Chang et al., 1973), Schmidt, Robertson and McCartor, and Brodsky and Langnau (Schmidt, 1974; Robertson & McCartor, 1992; Brodsky & Langnau, 1993; Kadyshevsky, 1964; Karmanov, 1988). However, in these approaches one encounters some difficulties, *e.g.*, the ill-posedness of the Cauchy problem, discussed above, the occurrence of ill-defined space-time objects like $\epsilon(x^- - y^-)\delta^2(x_\perp - y_\perp)$ in the operator $1/p^+$, and the closely related problem of noncovariantly normalized states (Nakanishi & Yamawaki, 1977)

This disturbing fact might hinder the development of a Hamiltonian formulation of front-form field theory, if it could not be circumvented. A possible way out was shown by Chang

[1] Leutwyler and Stern (Leutwyler & Stern, 1978) extended Dirac's analysis to include two more forms of dynamics. A review on the present situation can be found in (Lev, 1993).

and Ma (Chang & Ma, 1969) and later by Kogut and Soper (Kogut & Soper, 1970): one may attack the problem at the level of Feynman diagrams. If one follows that line, one must show that the usual Feynman rules can be reformulated in terms of the new variables, eq. (3.1), or their conjugate momenta

$$p^+ = \frac{p^0 + p^3}{\sqrt{2}},\ p^- = \frac{p^0 - p^3}{\sqrt{2}},\ p^1,\ p^2. \tag{3.2}$$

In the present chapter we use their approach. We avoid the problems of quantization and assume that covariant quantization is correct. Then we show that the perturbative expansion in covariant terms—Feynman diagrams—is equivalent to an expansion in light-cone time-ordered terms for theories describing spinless particles. We show in sect. 3.2 how to derive light-cone time-ordered (l.c.t.-ordered) diagrams from a given Feynman diagram by integrating over the l.c. energy p^-. The general algorithm is illustrated there by applying it to the box diagram. On the way to the proof of equivalence we encounter questions of regularization. For scalar theories they are not more difficult to answer than in the manifestly covariant formulation.

The true difficulty lies in theories containing spinning particles. In the case of spin-1/2 particles one encounters the following expression for the free propagator (Kogut & Soper, 1970)

$$\frac{i(\not{p} + m)}{p^2 - m^2 + i\epsilon} = \frac{i(\not{p}_{on} + m)}{p^2 - m^2 + i\epsilon} + \frac{i\gamma^+}{2p^+} = \sum_\alpha \frac{iu^{(\alpha)} \otimes \bar{u}^{(\alpha)}}{p^2 - m^2 + i\epsilon} + \frac{i\gamma^+}{2p^+} \tag{3.3}$$

where p_{on} is the on-shell value of the four momentum of the spin-1/2 particle with mass m, if its components p^+, p^1 and p^2 are given. The component p^-_{on} is computed from

$$p^2 = 2p^+p^- - p_\perp^2 = m^2 \tag{3.4}$$

and so

$$p^-_{on} = \frac{p_\perp^2 + m^2}{2p^+}. \tag{3.5}$$

The occurrence of the nonpropagating part $i\gamma^+/2p^+$ makes the treatment of fermions in front-form field theories much more difficult, as it gives rise to integrals that are much more singular than the corresponding integrals in time-ordered or manifestly covariant formulations. In sect. 3.3 the general case of spin-1/2 particles is discussed. As an illustration a box diagram, describing two fermions exchanging scalar bosons, is reduced to a set of l.c.t.-ordered diagrams.

The algorithm we propose demonstrates the equivalence of Feynman diagrams to sets of x^+-ordered diagrams in the case of scalar and spin-1/2 fields. (In a way, this is the reverse of Wick's theorem for time-ordered perturbation theory. The fact that the Cauchy problem with a null-plane as initial surface is ill posed makes the Wick theorem in front-form dynamics a strictly formal result. Different interpretations have lead to different perturbative expansions (Kogut & Soper, 1970; Chang & Yan, 1973).) The popular belief that massive fields do not have these problems is a misconception. The leading behavior of the fields near the light front is independent of the mass.

A brief discussion on the extension of our treatment to diagrams with several loops is given in sect. 3.4.

In the course of our investigation we encountered several technical difficulties. They are discussed in sect. 3.5, where solutions are given too. In particular we argue that there is

no problem concerning zero modes, if the p^--integrals are regularized properly, *viz*, using a regularization that preserves covariance. But it shows that Feynman diagrams give rise to terms in the perturbative expansion of the S-matrix that act on $p^+ = 0$-states.

The next section (sect. 3.6) is concerned with the many mathematical details that were left out from the preceding sections, lest the main line of argument be blurred.

We close with a discussion of our results and compare them to some of the literature on light-front field theory.

3.2 Equivalence

Before we proceed with the equivalence proof, we define what we mean by equivalence. By application of the Feynman rules as ordinarily understood, one obtains manifestly-covariant expressions[2] for terms in the perturbative expansion of S-matrix elements, expressed in terms of four-momenta, masses, spins, and dynamical ingredients: coupling constants. Wick's theorem can be understood as asserting that the S-matrix elements could be calculated as well in time-dependent perturbation theory, and as giving us an algorithm to combine the terms found in the latter case into manifestly-covariant expressions. Thus Wick's theorem establishes the equivalence of time-dependent ("old-fashioned") and covariant perturbation theory.

In this thesis we use the word equivalence in a similar way: each term in covariant perturbation theory–Feynman diagram–can be written as the sum of amplitudes that can be *interpreted* as terms in a l.c.t.-ordered perturbation series. (In the interest of brevity, we will use the terminology l.c.t.-ordered diagrams.) In fact, those amplitudes are expressed in momentum-energy-space quantities, however, it is a straightforward matter to translate them into space-time language, thus justifying our terminology.

By taking Feynman diagrams as our point of departure, we avoid the problems of front-form quantization mentioned before. Besides, we also side-step the problem of identifying the independent degrees of freedom and the determination of commutation relations between them for a constrained system.

The splitting of a Feynman diagram into l.c.t.-ordered ones results in amplitudes of the form

$$V_\alpha \frac{1}{P^- - H_0} V_\beta \frac{1}{P^- - H_0} \cdots \frac{1}{P^- - H_0} V_\sigma \frac{1}{P^- - H_0} V_\omega. \tag{3.6}$$

(See also eq. (6.13).) Here, P^- plays the role of the "energy" variable, conjugate to the light-cone time x^+. H_0 is again the energy, however, now expressed in terms of the kinematical components p^+ and $p_\perp$ of the momenta of the particles in the intermediate state between two interactions. The objects V are the vertices that correspond to the local interactions. As we will show, expressions of this form arise naturally upon integration of a Feynman diagram over the minus-component of the integration variable. In general, a number of l.c.t.-ordered diagrams are derived from a single Feynman diagram. This is directly analogous to old-fashioned perturbation theory, where $n!$ time-ordered diagrams sum up to one Feynman diagram with n vertices. However, there exists an important difference: in l.c.t.-ordered theory there are less diagrams owing to the linearity of the denominator of the single-particle propagator in the p^-

[2] Except for noncovariant gauge terms in a noncovariant gauge like the light-cone gauge.

variable

$$\frac{1}{p^2 - m^2 + i\epsilon} = \frac{1}{2p^+[p^- - \frac{p_\perp^2 + m^2 - i\epsilon}{2p^+}]}. \tag{3.7}$$

Consequently, to every propagator there corresponds only one pole in p^- and its location in the complex p^--plane depends on the sign as well as the magnitude of p^+. This property, already alluded to by Dirac (Dirac, 1949), allows us to pose the condition that in any state $p^+ > 0$. In the past the status of this so-called "spectrum condition" has remained somewhat unclear. We shall demonstrate that it follows directly from our splitting procedure and from a natural reinterpretation of amplitudes, quite similar to the reinterpretation of negative-energy states as states of positive energy of anti-particles in time-ordered perturbation theory. In fact, our reduction algorithm shows that the l.c.t.-ordered diagrams have the property that the internal lines carry positive p^+-momentum only. Therefore a better terminology might be *spectrum property*, however, we stick to the term spectrum condition, because it is commonly used. In case one would like to formulate diagram rules in l.c.t.-ordered perturbation theory, one could use the spectrum condition as a limitation of all intermediate states to states where every particle has positive p^+-momentum.

The spectrum condition is intimately related to causality. When the causal single-particle propagator eq. (3.7) is Fourier transformed, one finds that the sign of p^+ determines whether one can extend the integral over the p^--axis to an integral along a closed contour in the complex p^--plane by adding a semi-circle at infinity for positive or negative $\mathbf{Im}p^-$: $p^+ > 0$ corresponds to positive x^+-evolution. States with positive energy go forward in time and states with negative energy go backward in time.

One can argue formally that the spectrum condition holds for all intermediate states. As a result of the completeness of the physical Hilbert-space each state is a superposition of free states and thus has a positive p^+ momentum. Any particle in a free state with positive p^+ has positive energy and goes forward in time. The conservation of kinematical momentum $(p^+, p_\perp)$ restricts the creation of particles in a Hamiltonian formulation, which is not the case in the equal-time formulation. We will show that this property indeed holds for the l.c.t.-ordered perturbative expansion.

This result seems rather obvious for spin-0 bosons, however, to our knowledge, its proof has never before been given. For spin-1/2 particles, there are complications due to the non-propagating part $i\gamma^+/2p^+$ of the fermion propagator. These render the equivalence proof in this case more difficult.

There is an important point worth mentioning: the pole moves in the complex p^--plane as a function of p^+, and even crosses the real axis at infinity for $p^+ = 0$. This makes the propagator undefined as it stands. The crossing at infinity gives rise to so-called "zero-modes" which will be dealt with later (see sect. 3.5.1).

3.2.1 Examples

As a pedagogical example we reduce the box diagram and the crossed-box diagram in ϕ^3-theory[3] to the associated l.c.t.-ordered diagrams. This gives us the opportunity to show the working of the reduction algorithm in great detail. Later on we will give the general form of the algorithm.

[3]The type of theory is not essential for the arguments, the presence of a loop is.

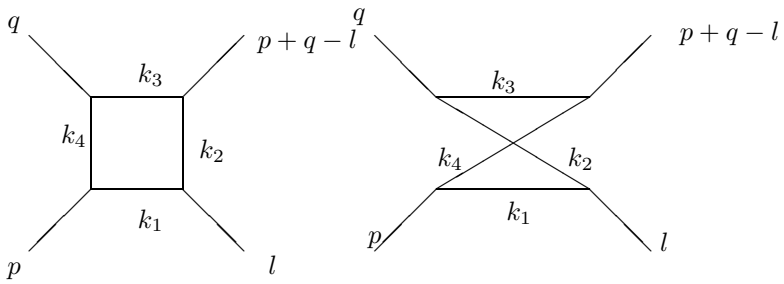

Figure 3.1: Box and crossed-box diagrams.

Box diagram

The box diagram consists of four propagators: (see Fig. 3.1)

$$\begin{aligned} FD_\Box &= \int \frac{\mathrm{d}k^+\mathrm{d}^2k_\perp}{(2\pi)^3} D_\Box, \\ D_\Box &= \int \frac{\mathrm{d}k^-}{2\pi} \frac{1}{(k_1^2-m^2+i\epsilon)(k_2^2-m^2+i\epsilon)(k_3^2-m^2+i\epsilon)(k_4^2-m^2+i\epsilon)}, \end{aligned} \tag{3.8}$$

with incoming momenta p and q and outgoing momenta l and $p+q-l$. The four momenta in the loop are: $k_1 = k$, $k_2 = k-l$, $k_3 = k-p-q$ and $k_4 = k-p$. We can rewrite the integral in terms of energy denominators and phase space factors. We define the quantities $\{H_i\}_{i=1}^4$ as

$$\begin{aligned} H_1 &= \frac{k_\perp^2+m^2-i\epsilon}{2k^+}, \\ H_2 &= l^- + \frac{(k_\perp-l_\perp)^2+m^2-i\epsilon}{2(k^+-l^+)}, \\ H_3 &= p^- + q^- + \frac{(k_\perp-p_\perp-q_\perp)^2+m^2-i\epsilon}{2(k^+-p^+-q^+)}, \\ H_4 &= p^- + \frac{(k_\perp-p_\perp)^2+m^2-i\epsilon}{2(k^+-p^+)}. \end{aligned} \tag{3.9}$$

Then the k^--integral can be written as

$$D_\Box = \int \frac{\mathrm{d}k^-}{2\pi\phi} \frac{1}{(k^- - H_1)(k^- - H_2)(k^- - H_3)(k^- - H_4)}. \tag{3.10}$$

The phase-space factor is given by $\phi = 16k^+(k^+-l^+)(k^+-p^+-q^+)(k^+-p^+)$.

The positions of the poles in the complex k^- plane depend on the values of the external momenta and the value of k^+. To calculate the time ordered diagram we must set the values

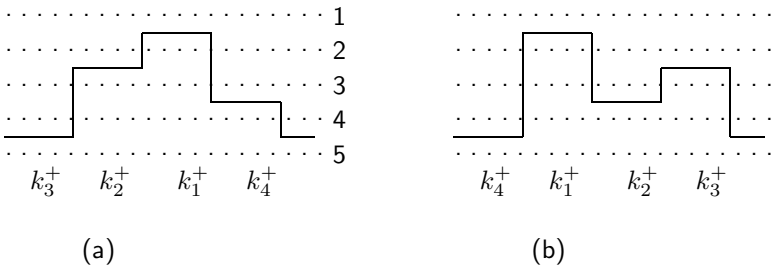

(a) (b)

Figure 3.2: The relative values of the longitudinal momenta, for the box diagram (a), and the crossed box diagram (b). All other box diagrams follow from these two through discrete symmetries. The absolute scale for the k_i^+'s is set by the value of k^+, the loop momentum.

of the external momenta p^+, q^+ and l^+. For specific values of k^+, the poles cross the axis and end up in the opposite half plane. When that happens, the integral changes discontinuously. The order in which the different poles cross the real axis depends on the values of the external momenta. In order to make our example definite, and without loss of generality, we assume $p^+ > l^+$. Then we have five regions on the k^+-axis:

1. $k^+ < 0$; $\mathbf{Im}H_i > 0$, (i=1,2,3,4);
2. $0 < k^+ < l^+$; $\mathbf{Im}H_1 < 0, \mathbf{Im}H_i > 0$, (i=2,3,4);
3. $l^+ < k^+ < p^+$; $\mathbf{Im}H_1, \mathbf{Im}H_2 < 0, \mathbf{Im}H_4, \mathbf{Im}H_3 > 0$;
4. $p^+ < k^+ < q^+ + p^+$; $\mathbf{Im}H_3 > 0, \mathbf{Im}H_i < 0$, (i=1,2,4);
5. $p^+ + q^+ < k^+$; $\mathbf{Im}H_i < 0$, (i=1,2,3,4).

(see fig. 3.2) with respectively zero, one, two, three, and four poles below the real axis. Each region corresponds with a different process in light-cone time. This observation leads naturally to the definition of a *skeleton graph*. Each physical region in k^+ corresponds to one skeleton graph. It is a graph that is topologically equivalent to the original Feyman diagram, however, it has its internal lines graded $+$ or $-$ corresponding to the signs of the $\mathbf{Im}H_i$, associated with the internal momenta k_i^μ.

In the first and the last case all the poles are at the same side of the real axis so the integral over k^- vanishes. Cases 2 and 4 are similar to each other. The integrals are calculated by closing the contour in the upper (lower) half-plane of complex k^--values. The application of the residue theorem gives for case 2

$$D_\Box^2 = \frac{i}{\phi} \frac{1}{(H_4 - H_1)(H_3 - H_1)(H_2 - H_1)}, \tag{3.11}$$

and for case 4

$$D_\Box^4 = \frac{i}{\phi} \frac{1}{(H_3 - H_1)(H_3 - H_4)(H_3 - H_2)}. \tag{3.12}$$

Case 3 is the most interesting one. Straightforward application of the residue theorem gives the result

$$D^3_\Box = \frac{-i}{\phi}\frac{(H_1-H_2)(H_4-H_3)(H_4+H_3-H_1-H_2)}{(H_4-H_1)(H_3-H_1)(H_1-H_2)(H_4-H_3)(H_4-H_2)(H_3-H_2)}, \tag{3.13}$$

which can be split into two parts

$$D^3_\Box = -\frac{i}{\phi}\frac{1}{(H_4-H_1)(H_4-H_2)(H_3-H_2)} - \frac{i}{\phi}\frac{1}{(H_4-H_1)(H_3-H_1)(H_3-H_2)}. \tag{3.14}$$

A point to be clarified is the meaning of the denominators $(H_i - H_j)$. We choose the sign such that in these denominators $\mathbf{Im}H_i > 0$, corresponding to backward moving particles, while H_j has a negative imaginary part and refers therefore to forward moving particles.

Four-momentum conservation gives $k_4 = k_1 - p$. We set $k \equiv k_1$ and consider the case $\mathbf{Im}H_1 < 0$, $\mathbf{Im}H_4 > 0$, which means that $0 < k^+ < p^+$. Then, according to the residue theorem, we have a factor $H_4 - H_1$ in the denominator corresponding to this diagram. This factor can be written as

$$H_4 - H_1 = p^- - \frac{(p_\perp - k_\perp)^2 + m^2}{2(p^+ - k^+)} - \frac{k_\perp^2 + m^2}{2k^+} \tag{3.15}$$

The interpretation of the factor $H_4 - H_1$ is facilitated by cutting the diagram. We cut it first by a line cutting the legs of the loop with momenta k_1 and k_4 and all incoming lines except p. For every internal line, we define an on-shell value of the corresponding minus-component as

$$k^-_{i,on} = \frac{k_{i\perp}^2 + m^2}{2k_i^+}. \tag{3.16}$$

We define H_0 as the sum of the on-shell minus-momenta on the lines cut. In our example we find for the internal lines 1, 4 and the external line q

$$H_0(1,4) = q^- + \frac{k_\perp^2 + m^2}{2k^+} + \frac{(p_{1\perp} - k_\perp)^2 + m^2}{2(p^+ - k^+)}. \tag{3.17}$$

The cutting line defines an intermediate state with total minus momentum $P^- = p^- + q^-$ and total on-shell minus momentum $H_0(1,4)$. The difference between these two is just $H_4 - H_1$, eq. (3.15). Up till now, the direction of the internal four momenta is determined by the direction in which the loop is passed. If we reverse the direction of k_4, the momentum with negative plus component, *viz*, $k^+ - p^+$ eqs. (3.15, 3.16), is replaced by $p^+ - k^+$, which is then correctly interpreted as the plus component of the momentum of the particle corresponding to line 4.

If we consider a cut through k_1, k_3 and p, q, we will find $k_3 = k - p - q$. The same algebra that led to the result eq. (3.17), will now give

$$\begin{aligned} P^- - H_0(1,3) &= p^- + q^- - \left(\frac{k_\perp^2 + m^2}{2k^+} + \frac{(p+q-k)_\perp^2 + m^2}{2(p^+ + q^+ - k^+)}\right) \\ &= H_3 - H_1 \end{aligned} \tag{3.18}$$

It is clear that this procedure can be followed until the cut considered is cutting outgoing external lines only. There it stops. So, we conclude that we have the general result that any factor $(H_i - H_j)$ is equal to the difference of the minus-component of the total momentum $P^- = p^- + q^-$, and the on-shell minus-component of the momentum carried by the lines cut. Generally this holds for all combinations i and j such that $\mathbf{Im}H_i > 0$ and $\mathbf{Im}H_j < 0$ since the imaginary part is related to the sign of the on-shell momentum.

The l.c.t.-ordered box-diagrams can be interpreted as fourth order diagrams in l.c.-perturbation theory, having the form

$$V_4 \frac{1}{P^- - H_0} V_3 \frac{1}{P^- - H_0} V_2 \frac{1}{P^- - H_0} V_1 \tag{3.19}$$

In order to systematize the reduction of $D_\Box$ to a sum of residues that correspond to l.c.t.-ordered diagrams, it is appropriate to consider both the algebraic structure and the connection of residues with diagrams.

First, we demonstrate the use of some concepts that will be of crucial importance for the proof of equivalence of the Feynman-diagram approach and l.c.t.-ordered perturbation theory in the simple case of the box diagram. (The general proof is to be found in sect. 3.6).

The first object of interest is the Vandermonde determinant of order k:

$$\Delta(H_1, \ldots, H_k) = \begin{vmatrix} H_1^{k-1} & \cdots & H_1^2 & H_1 & 1 \\ \vdots & & \vdots & \vdots & \vdots \\ H_k^{k-1} & \cdots & H_k^2 & H_k & 1 \end{vmatrix} \tag{3.20}$$

The second one is $W_{n,m}(H_1, \ldots, H_n | H_{n+1}, \ldots, H_{n+m})$ defined as

$$W_{n,m}(H_1, \ldots, H_n | H_{n+1}, \ldots, H_{n+m}) = (-1)^m \begin{vmatrix} H_1^{n+m-2} & \cdots & H_1^2 & H_1 & 0 & 1 \\ \vdots & & \vdots & \vdots & \vdots & \vdots \\ H_n^{n+m-2} & \cdots & H_n^2 & H_n & 0 & 1 \\ H_{n+1}^{n+m-2} & \cdots & H_{n+1}^2 & H_{n+1} & 1 & 0 \\ \vdots & & \vdots & \vdots & \vdots & \vdots \\ H_{n+m}^{n+m-2} & \cdots & H_{n+m}^2 & H_{n+m} & 1 & 0 \end{vmatrix} \tag{3.21}$$

By direct computation one verifies easily the following statements:

$$\frac{W_{1,n}(y | x_1, \ldots, x_n)}{\Delta(y, x_1, \ldots, x_n)} = \frac{(-1)^n}{\prod_{i=1}^n (y - x_i)}, \tag{3.22}$$

$$\frac{W_{n,1}(x_1, \ldots, x_n | y)}{\Delta(x_1, \ldots, x_n, y)} = \frac{-1}{\prod_{i=1}^n (x_i - y)}. \tag{3.23}$$

Straightforward application of our rules gives for the skeleton graphs the following corresponding amplitudes:

$$D^2 = -\frac{i}{\phi} \frac{W_{3,1}(H_2, H_3, H_4 | H_1)}{\Delta(H_2, H_3, H_4, H_1)}, \tag{3.24}$$

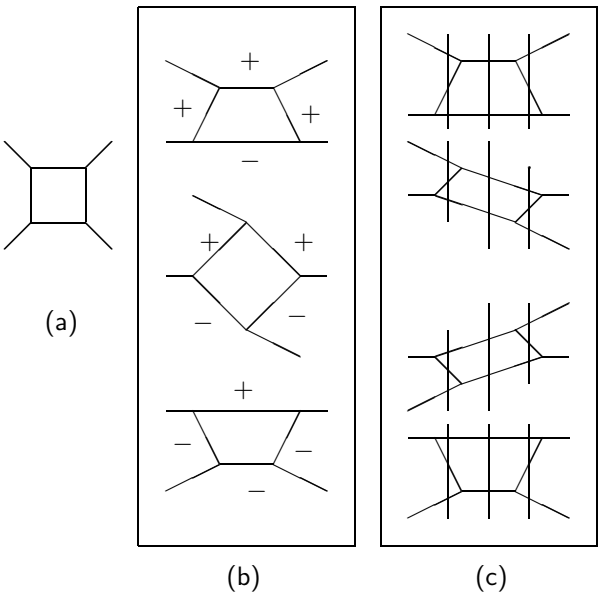

Figure 3.3: The plane box. (a) Feynman diagram, (b) skeleton graphs, and (c) l.c.t.-ordered diagrams.

$$D^4 = -\frac{i}{\phi}\frac{W_{1,3}(H_3|H_1,H_2,H_4)}{\Delta(H_3,H_1,H_2,H_4)}. \tag{3.25}$$

In case 3 we have

$$D^3 = -\frac{i}{\phi}\frac{W_{2,2}(H_4,H_3|H_1,H_2)}{\Delta(H_4,H_3,H_1,H_2)}. \tag{3.26}$$

D^3 needs to be rewritten such that energy denominators appear. The energy denominator $(H_4 - H_1)^{-1}$ should appear in all l.c.t.-ordered diagrams associated with D^3. It can be extracted as

$$\frac{W_{2,2}(H_4,H_3|H_1,H_2)}{\Delta(H_4,H_3,H_1,H_2)} = \frac{1}{(H_4-H_1)}\left(\frac{W_{1,2}(H_3|H_1,H_2)}{\Delta(H_3,H_1,H_2)} + \frac{W_{2,1}(H_4,H_3|H_2)}{\Delta(H_4,H_3,H_2)}\right) \tag{3.27}$$

and upon using eq. (3.22) we recover the final expression (3.14). The proof in sect. 3.6 demonstrates how this type of reduction can be carried out in the general case.

Secondly, we describe the relation of this algebraic procedure with l.c.t.-ordered diagrams. We begin with the Feynman-diagram and enumerate the possible configurations of poles in the complex k^--plane. (Cases $1,\ldots,5$.) A pictorial representation of those cases where the contour integral over k^- does not vanish (Cases 2, 3 and 4) is given by diagrams where the sign of $\mathbf{Im}H$ is indicated. (See fig. 3.3.)

The box diagram is relatively easy to reduce to l.c.t.-ordered diagrams because in any associated skeleton graph there are at most two vertices that need to be ordered with respect

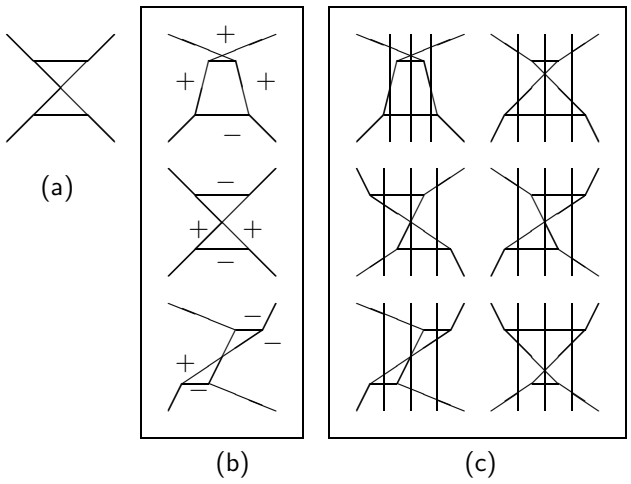

Figure 3.4: The crossed box. (a) Feynman diagram, (b) skeleton graphs , and (c) l.c.t.-ordered diagrams.

to each other. There are only two internal lines which connect an incoming line with an outgoing line. Generally we call this kind of diagrams *flat*. The box diagram being flat, it does not show all the possible complications. Therefore, we also discuss the crossed box.

Crossed box diagram

The difference between the flat box and the crossed box is clearly visible in the sign patterns, for the imaginary parts of the denominators, one encounters when going around the loop. In the flat box one encounters the sign patterns $+--$, $++--$ and $+++-$. In the crossed box, however, the sign patterns are $+---$, $+-+-$ and $+++-$. When there are two poles on either side of the real k^-axis, two sign changes occur, which can be seen as "bends" in the internal line, from backward to forward and vice versa. The skeleton graphs with signatures $+--$ and $+++-$ are treated in the same way as the corresponding flat ones. The case $+-+-$ leads to four l.c.t.-orderings, which we explain now. There are two possible orderings of the two vertices with incoming external lines. Having chosen one ordering, we follow one of the internal lines until we reach a vertex with an outgoing external line. Either of the two vertices with outgoing lines can come first. This gives a total of four l.c.t.-ordered diagrams. The corresponding diagrams are depicted in fig. 3.4. We choose again $p^+ > l^+$. The algebra for the $+-+-$ case, given by the interval $q^+ - l^+ < k^+ < l^+$, gives the residue

$$\frac{W_{2,2}(H_4,H_2|H_1,H_3)}{\Delta(H_4,H_2,H_1,H_3)} = \frac{1}{(H_4-H_1)}\left(\frac{W_{1,2}(H_2|H_1,H_3)}{\Delta(H_2,H_1,H_3)} + \frac{W_{2,1}(H_4,H_2|H_3)}{\Delta(H_4,H_2,H_3)}\right) \qquad (3.28)$$

that can be reduced to

$$\frac{1}{(H_4-H_1)(H_2-H_3)(H_4-H_3)}+\frac{1}{(H_4-H_1)(H_2-H_3)(H_2-H_1)}. \tag{3.29}$$

In order to expose the four l.c.t.-orderings, we write the two energy denominators next to the vertices with incoming lines as sums of two terms , *e.g.*,

$$\begin{aligned}\frac{1}{(H_4-H_1)(H_2-H_3)} &= \frac{1}{(H_2-H_3)(H_4+H_2-H_3-H_1)}\\ &+ \frac{1}{(H_4-H_1)(H_4+H_2-H_3-H_1)}\end{aligned} \tag{3.30}$$

Inserting these two denominators in the above expression gives four l.c.t.-ordered diagrams:

$$\begin{aligned}D^2_\times &= \frac{i}{\phi}\frac{1}{(H_2-H_3)(H_4+H_2-H_3-H_1)(H_4-H_3)}\\ D^3_\times &= \frac{i}{\phi}\frac{1}{(H_4-H_1)(H_4+H_2-H_3-H_1)(H_4-H_3)}\\ D^4_\times &= \frac{i}{\phi}\frac{1}{(H_2-H_3)(H_4+H_2-H_3-H_1)(H_2-H_1)}\\ D^5_\times &= \frac{i}{\phi}\frac{1}{(H_4-H_1)(H_4+H_2-H_3-H_1)(H_1-H_2)}.\end{aligned} \tag{3.31}$$

The l.c.t-ordered diagrams D^1 and D^6 are obtained in a similar way as in the case of the box diagram. Now we can easily answer the question why the number of l.c.t.-ordered diagrams is smaller than the number of ordinary time-ordered diagrams. In the latter case, a loop with 4 vertices leads to $4!=24$ diagrams. For the l.c.t.-ordered diagrams the number is reduced, because of the smaller number of poles. We can also interpret it as the *spectrum condition*. The spectrum condition restricts the plus-component of any momentum on any line, internal as well as external, to nonnegative values. Internal lines with negative plus-momentum correspond to poles with positive imaginary part and are interpreted as anti-particles. By reversing the direction of the momenta on these internal lines while maintaining four-momentum conservation, these lines can be again associated with particles. So, conservation of plus-momentum then provides the limitation of possible diagrams. The number of diagrams however, does depend on the external momenta; it is four in the case of the box diagram and six for the crossed box diagram.

3.2.2 General case

In a typical Feynman diagram on encounters several single-particle propagators. Following the same line of reasoning as used in the two examples given above, one will find that the corresponding poles in the loop variable k^- are located at different sides of the real k^--axis, depending on the value of k^+. To illustrate this fully general property, we consider a one-loop diagram with N vertices, N internal and N external lines. The number of incoming lines is N_1; there are $N_2=N-N_1$ outgoing lines. Suppose we call our integration variable k and identify it with k_N (see fig. 3.5). Four-momentum conservation takes the form

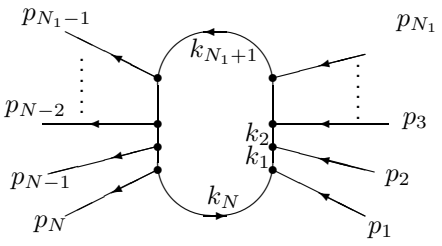

Figure 3.5: One-loop diagram

$$k_i^\mu = k^\mu + K_i^\mu(p_1^\mu, ..., p_N^\mu), \tag{3.32}$$

where the functions $K_i^\mu(p_1^\mu, ..., p_N^\mu)$ are linear. It is obvious that for arbitrary, but fixed external momenta all $k_i^+ < 0$ ($k_i^+ > 0$) for $k^+ \to \infty$ ($k^+ \to -\infty$). So, we can divide the real k^+-axis into different regions, a semi-infinite region where all $k_i^+ < 0$, another where all $k_i^+ > 0$ and $N-1$ finite regions where some of the k_i^+ are positive, the others being negative.

We will use here again the concept of a skeleton graph, as we did in the cases of the box and crossed box diagrams. For any Feynman diagram with given values of the external momenta, and for every interval in the loop variable k^+, one draws a graph that is topologically equivalent to the original Feynman diagram and has its internal lines graded either $+$ or $-$, corresponding to the signs of the imaginary part of the poles H_i. In the one-loop case we thus find for $k^+ \to -\infty$ the skeleton graph with all lines graded $+$; there are $N-1$ skeleton graphs with lines graded $+$ as well as lines graded $-$ and, finally, for $k^+ \to \infty$, a skeleton graph with all lines graded $-$. From our discussion of the causal single-particle propagator it becomes immediately clear that lines graded $-$ ($+$) correspond to particles moving forward (backward) in x^+-evolution. This justifies the terminology we adopt: if two vertices in a skeleton graph are connected by a line with internal momentum say $k_i^+ > 0$, then the vertex from which the momentum k_i^μ is flowing is said to be *earlier* than the vertex into which k_i^μ is flowing.

Apparently, each skeleton graph corresponds to a (partial) l.c.t.-ordering of the vertices in a Feynman diagram. The graphs with all lines graded $+$ or all graded $-$ correspond to a cyclic l.c.t.-ordering of the vertices that contradicts logic. Fortunately, these graphs are associated with the situation that all poles in k^- are lying at one side of the real k^--axis, in which case the amplitude vanishes. In all other graphs there is at least one vertex with an outgoing internal line with positive plus-momentum and an incoming internal line with a negative plus-momentum, and at least one vertex where the situation is reversed. The former vertices are called *early*, the latter *late* vertices. A sign change in the skeleton graph corresponds with an early or a late vertex, the other vertices are called *trivial*. (see fig. 3.6) If only one early and one late vertex are present in a given skeleton graph, the partial ordering is complete after the trivial vertices are ordered. This was the case for the flat box diagram. Otherwise, the different early vertices must be ordered with respect to each other and with respect to the late vertices. This additional ordering produces several l.c.t.-ordered diagrams associated with a single skeleton graph. In this way, a single Feynman diagram gives rise to a number of consistently l.c.t.-ordered diagrams. At this stage one reverses the directions of the four-momenta k_i^μ on all

Figure 3.6: The sign change in $\mathbf{Im}H_i$ correspond to early or late vertices. Both lines go in the same time direction. The sign of $\mathbf{Im}H_i$ is opposite to the sign of k_i^+.

those lines i where $k_i^+ < 0$. One sees immediately that as a result early vertices have only outgoing internal momenta, whereas late ones have only incoming internal momenta.

We use the late vertices in a different way than the early vertices. Starting from an early vertex, all vertices on the lines going out from this vertex are ordered relatively to this vertex. However, vertices lying on different lines are not yet ordered relative to each other. For two lines starting at different early vertices and connected at a late vertex, we can fix the relative ordering of the intermediate vertices, since all vertices on both lines must occur before the late vertex. When all late vertices have been encountered, their relative ordering determines the complete ordering of the full diagram.

The last point to be clarified is the form of the amplitudes corresponding to l.c.t.-ordered diagrams. We consider again the one-loop diagram and write the covariant amplitude as

$$FD = \int \frac{\mathrm{d}^4k}{(2\pi)^4} \frac{1}{[k_1^2 - m_1^2 + i\epsilon]\cdots[k_N^2 - m_N^2 + i\epsilon]} \tag{3.33}$$

where for the sake of simplicity we have put all vertex functions equal to unity. Using eq. (3.32) we can write for a typical factor in the denominator:

$$\begin{aligned} k_i^2 - m_i^2 + i\epsilon &= 2k_i^+ \left(k_i^- - \frac{k_{i\perp}^2 + m_i^2 - i\epsilon}{2k_i^+} \right) \\ &= 2k_i^+ \left(k^- + K_i^- - \frac{(k+K_i)_\perp^2 + m_i^2 - i\epsilon}{2k_i^+} \right) \\ &\equiv 2k_i^+ (k^- - H_i) \end{aligned} \tag{3.34}$$

The poles in k^-, H_j, are functions of the kinematical components of k^μ and the external momenta p_j^μ. The imaginary part of H_i, $\mathbf{Im}H_i$, is determined by the sign of k_i^+. Now suppose that for given external momenta k^+ is such that m pole positions are located in the upper half plane ($\mathbf{Im}H_i > 0$) and $n = N - m$ in the lower half plane ($\mathbf{Im}H_j < 0$). In order to simplify the discussion, we renumber the lines such that $\mathbf{Im}H_i > 0$ for $1 \le i \le m$, $\mathbf{Im}H_j > 0$ for $m+1 \le j \le N = m+n$. Consider the k^--integral by itself:

$$D_{m,n} = \int \frac{\mathrm{d}k^-}{2\pi 2^N k_1^+ \cdots k_N^+} \frac{1}{[k^- - H_1]\cdots[k^- - H_N]} \tag{3.35}$$

After performing the integral by closing the contour in either $\mathbf{Im}k^- > 0$ or $\mathbf{Im}k^- < 0$ one obtains a rational function of the H_i's:

$$D_{m,n} = \frac{i}{2^N k_1^+ \cdots k_N^+} \frac{W_{m,n}(H_1, \cdots, H_m | H_{m+1} \cdots H_N)}{\Delta(H_1, \cdots, H_N)} \tag{3.36}$$

Details on the functions $W_{m,n}$ and Δ are given in sect. 3.6. As we argued before, the k^+ integration splits into $N+1$ intervals, $(-\infty, k^+(0)), (k^+(0), k^+(1))$, $\cdots$, $(k^+(N-1), +\infty)$, where the boundaries $k^+(i)$ are defined such that in the interval $(k^+(r-1), k^+(r))$ there are, for finite r, precisely r H_i's with $\mathbf{Im}H_i > 0$. In each of the finite intervals one skeleton graph is present corresponding to one k^--integral $D_{m,n}$. The full Feynman diagram is recovered by summing $D_{m,n}$ over m from 1 to $N-1$, integrating over k^+ over the appropriate finite interval, and over $k_\perp$. For either n or m different from 1, $D_{m,n}$ does not have the desired form eq. (3.6). A further reduction, corresponding to the transition from the partially ordered skeleton graphs to the completely ordered diagrams must be performed. The heuristics that help us to do so is provided by the space-time concepts. Take any early vertex and identify it with an *event* at some l.c.t. $x^+ = \tau_0$. Suppose H_1 and H_{m+1} are the poles corresponding to the outgoing and incoming internal lines resp. at this vertex. The intermediate state with momenta k_1 and k_{m+1} corresponds to the l.c.-energy denominator $H_1 - H_{m+1}$. We can convince ourselves that this is correct if the reversal of four momenta on lines with $k_j^+ < 0$ is effected. We find

$$H_1 - H_{m+1} = P^- - \frac{k_{1\perp}^2 + m_1^2}{2k_1^+} - \frac{k_{m+1\perp}^2 + m_{m+1}^2}{2k_{m+1}^+}. \tag{3.37}$$

The identification of P^- becomes clear when one uses the surface τ to cut the internal and external lines. We can close the surface by cutting all the external lines attached to the piece of the Feynman diagram out of which the p^+ momentum flows. The momentum flow through this first cut plane τ_0 equals the flow through the second cut plane τ since energy-momentum is conserved locally in a Feynman diagram. The flow of P^- through the internal lines equals the initial flow into the diagram minus the flow through the external lines cut at τ. The loop momenta do not contribute because they go into the τ cut plane as well as out of the cut plane, so there is no net contribution of these momenta. (We stress here that this interpretation is correct only after reversal of the four momenta on the lines with $\mathbf{Im}H_j > 0$.) For brevity we call denominators of the form $H_i - H_j = P^- - H_0(i,j)$ *energy denominators*. These cut planes can be interpreted as equal-time surfaces.

Now the strategy is clear. For every skeleton graph one uses the surface $x^+ = \tau$ to cut lines that give rise to energy denominators. That this is possible is the content of our proof of equivalence. Indeed, as we demonstrate in sect. 3.6, we have

$$\begin{aligned} \frac{W_{m,n}(H_1, \cdots, H_m | H_{m+1}, \cdots, H_N)}{\Delta(H_1, \cdots, H_N)} &= \frac{1}{H_1 - H_{m+1}} \times \\ \left(\frac{W_{m-1,n}(H_2, \cdots, H_m | H_{m+1}, \cdots, H_N)}{\Delta(H_2, \cdots, H_m, H_{m+1}, \cdots, H_N)} \right. &+ \left. \frac{W_{m,n-1}(H_1, \cdots, H_m | H_{m+2}, \cdots, H_N)}{\Delta(H_1, \cdots, H_m, H_{m+2}, \cdots, H_N)} \right) \end{aligned} \tag{3.38}$$

That this identity leads to a recurrence follows from the fact that the two terms in the r.h.s. of eq.(3.38) have the same form as the original one. The reduction stops if either n or m is reduced to 1.

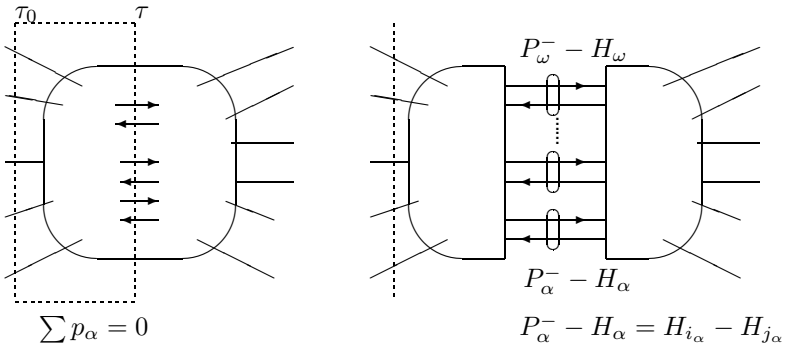

Figure 3.7: Illustration of the cut-procedure in a general n-leg diagram. For each cut area there is four-momentum conservation in a Feynman diagram. We can use this to make general statements for an intermediate state. The minus-momentum transferred across the intermediate state is equal to the incoming minus-momentum. The sum of energy denominators contains the sum of all external minus-momenta minus the sum of all on-shell values of the particle lines. Loop momenta drop out because these go in and out of the cut area.

There remains one loose end that we tie up now. If several early vertices occur, we have to consider all l.c.t.-orderings of them. (This happens if $n \geq 2$.) Moreover, we may have to consider l.c.t.-orderings such that some late vertices occur before some, but not all, early vertices. In all those cases the number of internal lines cut by an $x^+ = \tau$ surface is greater than two, but always even: for every line going into this surface there is a corresponding outgoing line. We have seen that a pair of lines, one incoming, the other outgoing, that connect in an early (or late, for that matter) vertex, gives rise to an energy denominator, say $H_i - H_j$. When two pairs of such lines occur, there will be two energy denominators, which we call *simultaneous parts*. A simple example illustrates this. Let the two early vertices be α and β, and p^μ_α and p^μ_β the momenta on the two corresponding incoming external lines. The reduction algorithm gives two factors, one corresponding to the vertex α, of the form $1/(H_{i_\alpha} - H_{j_\alpha})$, the other being $1/(H_{i_\beta} - H_{j_\beta})$. As before, we can rewrite such factors, upon reversing the backward flowing momenta, in the form $1/(P^-(\beta) - H_0(\beta))$ and $1/(P^-(\alpha) - H_0(\alpha))$, where $P^-(\gamma), \gamma = \alpha, \beta$ is the total net external minus momentum flowing into vertex γ. A simple algebraic identity

$$\begin{aligned} \frac{1}{P^-(\alpha) - H_0(\alpha)} \times \frac{1}{P^-(\beta) - H_0(\beta)} \quad &= \\ \frac{1}{P^-(\alpha) + P^-(\beta) - H_0(\alpha) - H_0(\beta)} \quad &\times \quad \left(\frac{1}{P^-(\alpha) - H_0(\alpha)} + \frac{1}{P^-(\beta) - H_0(\beta)} \right) \end{aligned} \tag{3.39}$$

combines the two factors in the correct way. The first factor can be rewritten as $1/(P^-(\alpha \cup \beta) - H_0(\alpha \cup \beta))$, which we recognize as an energy denominator for the intermediate state with

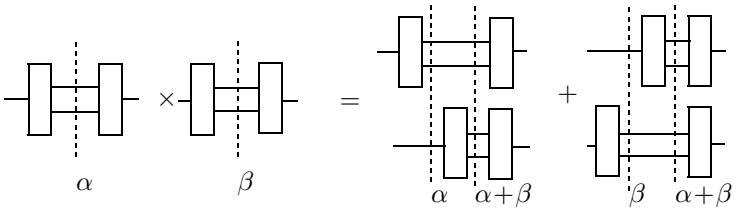

Figure 3.8: The product of two time orderings is the sum of the relative orderings.

the four internal lines i_α, j_α, i_β and j_β. The combination $1/(P^-(\alpha) - H_0(\alpha))(P^-(\alpha \cup \beta) - H_0(\alpha \cup \beta))$ corresponds to the l.c.t.-ordered diagram where the vertex α comes before vertex β, the other part of the r.h.s. of eq.(3.39) corresponding of course to vertex β preceding vertex α (see fig. 3.8). Clearly, the splitting formula works also recursively, so it applies to any number of pairs of internal lines.

With this observation we end our general discussion of the reduction algorithm. We stress that the l.c.t.-ordered language used here has heuristic value only, but does not replace a strict proof. The algebraic details are provided in section 3.6.

3.3 Spin-1/2 particles

In the previous sections we dealt with scalar particles only, thus avoiding complications due to summations over spin degrees of freedom in intermediate states. Here, we discuss these complications for spin-1/2 particles. The reduction algorithm in this case is partly identical to the algorithm for scalar particles. However, we now have to include in our treatment not only the energy denominators, but also the numerators. Consider the Feynman propagator for a single particle. The spin sum $\not{p} + m$ depends on p^-, so we have to account for that when we define the skeleton graphs corresponding to a Feynman diagram. It has been argued before (Kogut & Soper, 1970) that one can split the Feynman propagator into two pieces, one that is independent of p^-, the *instantaneous part*, and another piece, the *propagating part*, where p^- occurs in the denominator only:

$$\frac{\not{p} + m}{p^2 - m^2 + i\epsilon} = \frac{\not{p}_{\rm on-shell} + m}{p^2 - m^2 + i\epsilon} + \frac{\gamma^+}{2p^+} = \sum_\alpha \frac{u^{(\alpha)}(p) \otimes \bar{u}^{(\alpha)}(p)}{p^2 - m^2 + i\epsilon} + \frac{\gamma^+}{2p^+}, \tag{3.40}$$

with the obvious definition $p^\mu_{\rm on-shell} = (p^-_{\rm on-shell}, p^+, p_\perp)$, where $p^-_{\rm on-shell} = (p_\perp^2 + m^2)/(2p^+)$. The spin sum $\sum_\alpha u^{(\alpha)}(p) \otimes \bar{u}^{(\alpha)}(p)$ runs over a complete basis in spin space, *viz*, particles and anti-particles. In a loop p^+ can take any value, positive or negative. There are two spin polarizations, however, for a particle with negative momentum and a given polarization, this correspond to the anti-particle with the opposite polarization. There are two equivalent ways to interpret the sum; either as sum over particles and anti-particles with two spin degrees of freedom, or as particles with two spin polarization which travels forward or backward in time. We will show that the last interpretation is consistent with the spectrum condition.

In order to illustrate the differences between the purely scalar case and the situation where spin-1/2 particles occur, we discuss in the next subsection the flat box diagram with two bosons and two fermions.

3.3.1 Example: fermion box diagram

Consider the case of two spin-1/2 fermions exchanging spinless bosons. A Feynman diagram for the fourth order in perturbation theory is shown in fig. 3.9, (a). The momenta are defined similar to the scalar case, fig. 3.1. Before the associated skeleton graph can be drawn, one must split the fermion propagators for the intermediate states into the two parts: instantaneous and propagating. This results in four different diagrams shown in fig. 3.9 (b). In these four, the p^--dependence of the propagators is present in the denominators only. Therefore, one can apply the methods described in the previous section immediately, since the numerator does not depend on the integration variable. Doing so, one obtains the eight skeleton graphs drawn in panel (c). These graphs form the basis of the splitting into l.c.t-ordered diagrams. After this has been achieved one can combine certain diagrams into a single diagram by adding the propagating part to the instantaneous part of the fermion propagator. This regrouping of diagrams is represented graphically in the last panel of this figure. The formulae associated with the four final diagrams are

$$\begin{aligned}
D^{(1)} &= \int \frac{\mathrm{d}k^+\mathrm{d}^2k_\perp}{(2\pi)^3\phi} \frac{\gamma^a\Lambda_3\gamma^b\otimes\gamma^c\Lambda_1\gamma^d}{(P^- - H_0(1,4))(P^- - H_0(1,3))(P^- - H_0(1,2))} \\
&+ \int \frac{\mathrm{d}k^+\mathrm{d}^2k_\perp}{(2\pi)^3\phi} \frac{\gamma^a\gamma^+\gamma^b\otimes\gamma^c\Lambda_1\gamma^d}{(P^- - H_0(1,4))(P^- - H_0(1,2))} \\
&= \int \frac{\mathrm{d}k^+\mathrm{d}^2k_\perp}{(2\pi)^3\phi} \frac{\gamma^a\Omega_3\gamma^b\otimes\gamma^c\Lambda_1\gamma^d}{(P^- - H_0(1,4))(P^- - H_0(1,3))(P^- - H_0(1,2))}, \\
D^{(2)} &= \int \frac{\mathrm{d}k^+\mathrm{d}^2k_\perp}{(2\pi)^3\phi} \frac{\gamma^a\Lambda_3\gamma^b\otimes\gamma^c\Omega_1\gamma^d}{(P^- - H_0(1,4))(P^- - H_0(1,3))(P^- - H_0(2,3))}, \\
D^{(3)} &= \int \frac{\mathrm{d}k^+\mathrm{d}^2k_\perp}{(2\pi)^3\phi} \frac{\gamma^a\Omega_3\gamma^b\otimes\gamma^c\Omega_1\gamma^d}{(P^- - H_0(1,4))(P^- - H_0(2,4))(P^- - H_0(2,3))}, \\
D^{(4)} &= \int \frac{\mathrm{d}k^+\mathrm{d}^2k_\perp}{(2\pi)^3\phi} \frac{\gamma^a\Lambda_3\gamma^b\otimes\gamma^c\Lambda_1\gamma^d}{(P^- - H_0(1,4))(P^- - H_0(1,3))(P^- - H_0(2,3))}.
\end{aligned} \tag{3.41}$$

The objects Λ and Ω are defined as

$$\Lambda_i = \not{k}_{i,on} + m_i, \tag{3.42}$$

and

$$\Omega_i = \not{k}_i + m_i = \Lambda_i + \gamma^+(k_i^- - k_{on}^-). \tag{3.43}$$

The on-shell values of the minus components have been defined before, see eq. (3.5). The energy denominator $P^- - H_0(1,2)$ is of course

$$\begin{aligned}
P^- - H_0(1,2) &= p^- + q^- - k_{1,on}^- - k_{2,on}^- - q_{on}^- \\
&= p^- - \frac{k_{1\perp}^2 + m_1^2}{2k_1^+} - \frac{k_{2\perp}^2 + m_2^2}{2k_2^+},
\end{aligned} \tag{3.44}$$

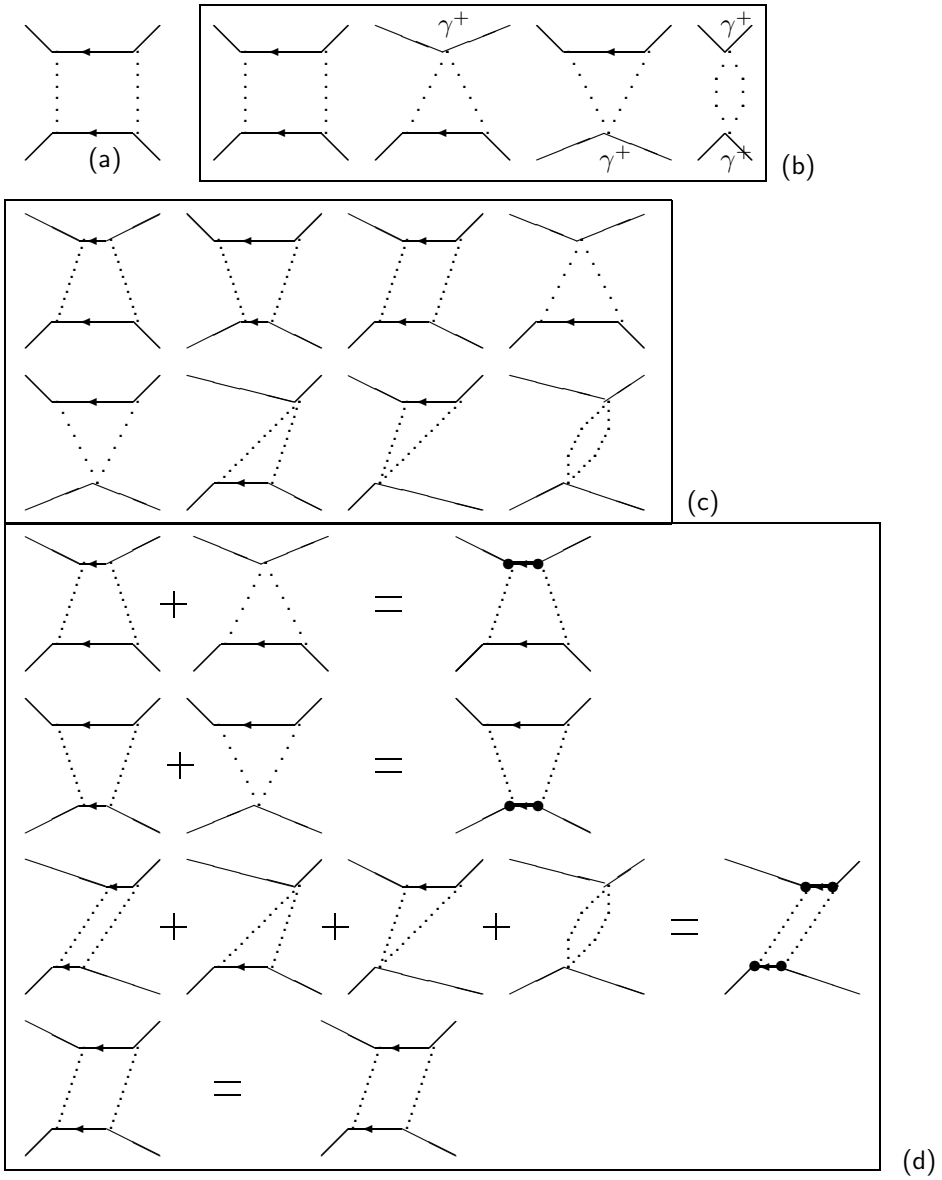

Figure 3.9: (a) The Feynman diagram, (b) the corresponding diagrams with on-shell spinor projections or instantaneous parts, (c) the skeleton graphs, (only the tilted box leads to two l.c.t.-ordered diagrams) (d) the summed l.c.t-ordered diagrams, which yields the adjusted blink propagators (with the points at beginning and end of a line).

and the other ones are defined similarly. The phase-space element ϕ has also been given before, below eq. (3.10).

The flat fermion box shows clearly the peculiar complications caused by spin. Because the numerators and the denominators of the fermion propagators depend both linearly on the integration variable k^-, one has to perform a Laurent expansion in order to identify the pole terms. This leads to a number of "intermediate amplitudes", equal to 2^F, where F is the number of internal fermion lines. These amplitudes give rise to skeleton graphs that can be reduced to l.c.t.-ordered diagrams in the, by now, familiar way. The l.c.t.-ordered diagrams in which an element $\gamma^+/2k_i^+$ occurs, are special, because associated to every one of them there occurs a diagram where the element $\gamma^+/2k_i^+$ is replaced by $\Lambda_i/(2k_i^+(P^- - H_0))$. This happens only in those cases where the on-shell value $H_i = (k_i^2 + m_i)/2k_i^+$ occurs in a single energy denominator. These are the states that begin and end with the creation and the annihilation of the same particle. We call an internal line with this property a *blink*. In the case considered above: $D^{(1)}$ contains H_3 in only one factor in the denominator, the same holds for $D^{(2)}$ and H_1, whereas $D^{(3)}$ contains the blinks H_1 and H_3. If a blink occurs, one can recombine, after the l.c.t.-ordering has been performed, the propagating part and the instantaneous part into a complete propagator. This is done in the diagrams $D^{(1)}$, $D^{(2)}$ and $D^{(3)}$ eq. (3.41), and illustrated in fig. 3.9(d), where the thick lines beginning and terminating in dots symbolize complete propagators.

3.3.2 Including the instantaneous terms

By now, it is relatively easy to formulate the general reduction algorithm. It has four steps.

(i) For a given Feynman diagram, perform the Laurent expansion of the fermion propagator, *i.e.*, split the propagator into a propagating part and an instantaneous part;

(ii) Determine the skeleton graphs for all diagrams obtained in step (i);

(iii) Perform the reduction of all skeleton graphs in exactly the same way as it was done in the scalar case;

(iv) Identify the blinks and sum the diagrams corresponding to the same blink in order to obtain amplitudes with complete spin sums.

In order to understand why we recommend step (iv) we consider the general case. Let k_i^μ be the four momentum of a blink. The two corresponding diagrams, partly shown in fig. 3.10, contain the factors[4]

$$\begin{aligned} G_i &= \frac{1}{2k_i^+}\frac{\Lambda_i}{P^- - (\cdots H_i \cdots)}, \\ \Lambda_i &= \gamma^+ H_i + \gamma^- k_i^+ + \gamma_\perp \cdot k_\perp + m_i, \\ H_i &= (k_{i\perp}^2 + m_i)/2k_i^+, \\ g_i &= \gamma^+/2k_i^+. \end{aligned} \tag{3.45}$$

[4]We define $\gamma_\perp = (0, \gamma_1, \gamma_2, 0)$, $k_\perp = (0, k_1, k_2, 0)$ and $\gamma_\perp \cdot k_\perp = -(\gamma_1 k_1 + \gamma_2 k_2)$.

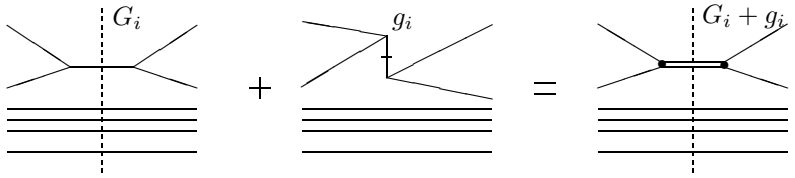

Figure 3.10: The state begins and ends with the creation and annihilation of the same particle. The singularity in this diagram cancels against the same singularity in the instantaneous diagram.

We see that both G_i and g_i become singular at $k_i^+ = 0$. These two singularities appear to cancel. We can see this most clearly if we realize that the denominator $P^- - (\cdots H_i \cdots)$ can be rewritten as $k_i^- - H_i$. If $k_i^+ \to 0$, then $H_i \to \infty$, so we see that in this limit G_i behaves as

$$G_i \overset{k_i^+ \to 0}{\sim} \frac{1}{2k_i^+} \frac{\gamma^+ H_i}{k_i^- - H_i} \sim -\frac{\gamma^+}{2k_i^+} = -g_i. \tag{3.46}$$

Therefore, the sum of the two contributions is finite for $k_i^+ \to 0$.

$$\begin{aligned} G_i + g_i \quad &= \quad \frac{1}{2k_i^+} \frac{\gamma^+ H_i + \gamma^- k_i^+ + \gamma_\perp \cdot k_\perp + m_i}{k_i^- - H_i} + \frac{\gamma^+}{2k_i^+} \\ &= \quad \frac{\gamma^+ k_i^- + \gamma^- k_i^+ + \gamma_\perp \cdot k_\perp + m_i}{2k_i^+ (k_i^- - H_i)} \\ &\overset{k_i^+ \to 0}{\sim} \quad -\frac{\gamma^+ k_i^- + \gamma_\perp \cdot k_\perp + m_i}{k_{i\perp}^2 + m_i^2}. \end{aligned} \tag{3.47}$$

This expression appears *after* the integration of the energy variable. Then k_i^- is a function of the external variables only and represents the p^--flow through the intermediate state under consideration.

3.3.3 General case

We have seen that singularities in l.c.t-ordered diagrams cancel similar singularities in instantaneous terms. See also (Brodsky et al., 1973). The instantaneous terms might contain other divergences that are cancelled by lower-order terms with additional instantaneous terms. The question remains whether this procedure ends, or whether we are left with terms which contain only instantaneous singularities that do not cancel each other. In the section on divergent contour integration (sec. 3.5.2) we show that the proper treatment of the shift of poles to infinity removes all singularities from each residue. So after the recombination of terms we won't have a residual term in the form of instantaneous parts.
Although we are not concerned with gauge theories explicitly, we note that most of these terms drop in a gauge theory with the (naive) light-cone gauge, and in theories with scalar and pseudo-scalar coupling, due to $\gamma^+\gamma^+ = \gamma^+\gamma^5\gamma^+ = 0 = \gamma^+\gamma^i\gamma^+$.

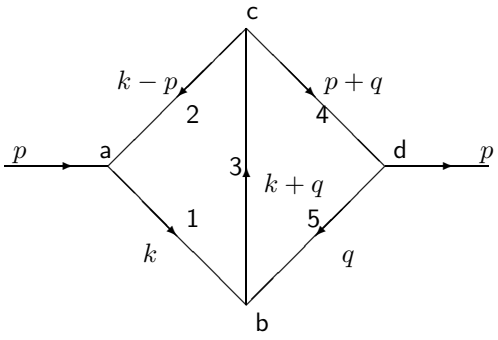

Figure 3.11: The two-loop diagram.

3.4 Multi-loop diagrams

The extension of the reduction algorithm from Feynman diagrams with one loop to Feynman diagrams with several loops is not difficult, but there are some points that need to be clarified. The loop integrations can be done one after another since the structure of a l.c.t.-ordered diagram is not essentially different from a Feynman diagram. We will illustrate the procedure with a simple example in the section below.

3.4.1 Two-loop diagram

We consider the scalar diagram with two loops, depicted in fig. 3.11. The corresponding integral is :

$$D = \int \frac{\mathrm{d}q^- \mathrm{d}k^-}{(2\pi)^2 \phi} \frac{1}{(k^- - H_1)(k^- - H_2)(k^- + q^- - H_3)(q^- - H_4)(q^- - H_5)} \tag{3.48}$$

Where the phase factor $\phi = 2^5 k^+(k^+ - p^+)(k^+ + q^+)q^+(q^+ + p^+)$ and the poles are given by:

$$\begin{array}{rcll} H_1 & = & \frac{k_\perp^2 + m^2}{2k^+} & -\frac{i\epsilon}{k^+} \\ H_2 & = & p^- + \frac{(p_\perp - k_\perp)^2 + m^2}{2(k^+ - p^+)} & -\frac{i\epsilon}{k^+ - p^+} \\ H_3 & = & \frac{(k_\perp + q_\perp)^2 + m^2}{2(k^+ + q^+)} & -\frac{i\epsilon}{k^+ + q^+} \\ H_4 & = & -p^- + \frac{(q_\perp + p_\perp)^2 + m^2}{2(q^+ + p^+)} & -\frac{i\epsilon}{q^+ + p^+} \\ H_5 & = & \frac{q_\perp^2 + m^2}{2q^+} & -\frac{i\epsilon}{q^+} \ . \end{array} \tag{3.49}$$

There are twelve sectors in $k^+ \otimes q^+$-space corresponding to twelve skeleton graphs. These sectors are depicted in fig. 3.12, where also the signatures of the skeleton graphs are shown. The amplitude D vanishes if either the integral over k^- or the one over q^- vanishes. The former happens if $\mathbf{Im}H_1, \mathbf{Im}H_2$ and $\mathbf{Im}H_3$ have the same sign, the latter if this happens for $\mathbf{Im}H_3, \mathbf{Im}H_4$ and $\mathbf{Im}H_5$. We read off from fig. 3.12 that there are two sectors remaining,

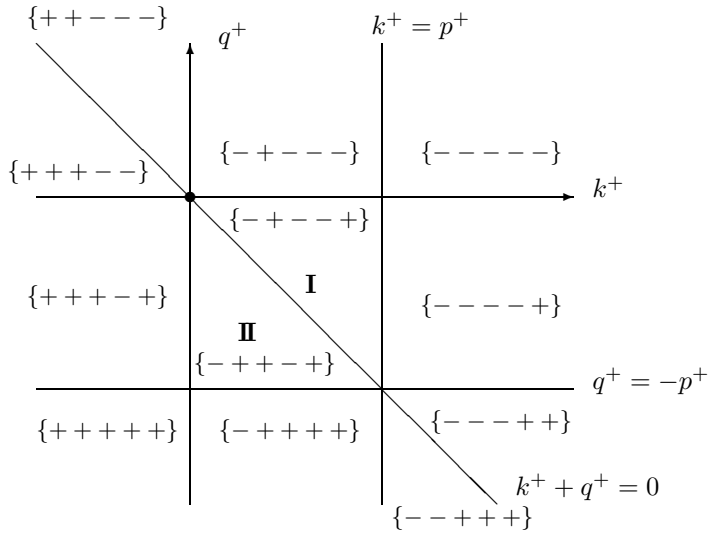

Figure 3.12: The imaginary signs of $\{H_1, H_2, H_3, H_4, H_5\}$ for the different sectors in $k^+ \otimes q^+$ space. Only the inner regions **I** and **II** correspond to integrals and skeleton graphs.

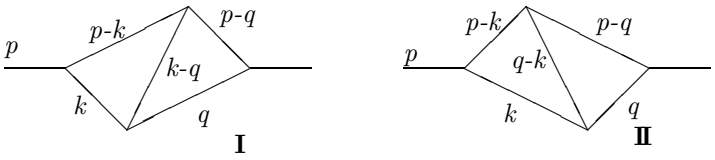

Figure 3.13: The two l.c.t-ordered diagrams that follow from the two-loop diagram.

denoted as **I** and **II**. In sector **I** we have $H_1, H_3, H_4 < 0$ and $H_2, H_5 > 0$. The reduction algorithm gives the l.c.t.-ordered diagram **I** of fig. 3.13, with l.c.t. ordering $a < b < c < d$. In sector **II** we have $H_1, H_4 < 0$ and $H_2, H_3, H_5 > 0$. The corresponding l.c.t. ordering is $a < c < b < d$. The only difference between the two diagrams is the sign of $\mathbf{Im}H_3$, that is linked to the two different l.c.t. orderings of the vertices b and c. For the sake of completeness we give the algebraic expressions for the two l.c.t. ordered diagrams. Upon integration over k^- we obtain:

$$\begin{aligned} D_{\mathbf{I}} &= \frac{i}{2\pi}\int \frac{\mathrm{d}q^-}{\phi}\frac{1}{(H_2-H_1)(q^-+H_2-H_3)(q^--H_4)(q^--H_5)} \\ D_{\mathbf{II}} &= \frac{i}{2\pi}\int \frac{\mathrm{d}q^-}{\phi}\frac{1}{(H_2-H_1)(q^-+H_1-H_3)(q^--H_4)(q^--H_5)}. \end{aligned} \tag{3.50}$$

The q^- integration is straightforward and gives the result:

$$\begin{aligned} D_{\mathbf{I}} &= \frac{1}{\phi}\frac{1}{(H_2-H_1)(H_2+H_4-H_3)(H_4-H_5)} \\ D_{\mathbf{II}} &= \frac{1}{\phi}\frac{1}{(H_2-H_1)(-H_5-H_1+H_3)(H_4-H_5)} \end{aligned} \tag{3.51}$$

After reversing the directions of the lines corresponding to negative k_i^+, *viz*, $k_2 = k - p$ and $k_5 = q$ in $D_{\mathbf{I}}$ and k_2, $k_3 = k + q$ and $k_4 = p + q$ in $D_{\mathbf{II}}$ we obtain the l.c.t.-ordered diagrams depicted in fig. 3.13. As before, every factor in the denominators of eq. (3.51) can again be written in the form $P^- - H_0(i,j)$, where $H_0(i,j)$ is the sum of the energies on the lines i and j.

We see again that the integrations over k^+ and q^+ are limited to finite regions. After reversing the lines with negative $\mathbf{Im}H_i$, one sees that the diagrams obtained have the spectrum property.

3.4.2 General multi-loop diagrams

In an arbitrary Feynman diagram with L loops, one must first identify the independent integration variables, say $q_1^-, \ldots, q_L^-$. Then one can characterize the different types of pole positions in an L-dimensional space with coordinates $(q_1^+, \ldots, q_L^+)$. The different signatures $(\mathbf{Im}H_1, \ldots, \mathbf{Im}H_N)$ divide this space into a number of sectors, each sector being associated with its particular skeleton graph. The sectors where the pole positions in all variables q_i^- are distributed over both half planes, $\mathbf{Im}q_i^- > 0$ and $\mathbf{Im}q_i^- < 0$ resp., are necessarily finite. This is so, because for any loop i, all poles H_k occurring in this loop will have $\mathbf{Im}H_k < 0$ ($\mathbf{Im}H_k > 0$) if the integration variable q_i^+ goes to infinity ($-$infinity). Therefore, the sectors in $(q_1^+, \ldots, q_L^+)$-space which are semi-infinite in either of the q_i^+ do not contribute to at least one of the integrals over the q_i^- variables.

So, in general we will have a finite number of skeleton graphs that each give rise to a finite number of l.c.t.-ordered diagrams. Each and every one of them has the spectrum property. In the case of spin-1/2 particles, one can duplicate this algorithm, provided the full Feynman diagram, containing F fermion lines, is first split into 2^F intermediate diagrams according to the division of the spin-1/2 propagator into instantaneous and propagating parts. Then the reduction algorithm is applied to each of the intermediate diagrams, giving rise to the appropriate skeleton graphs and finally to the l.c.t.-ordered diagrams, as was demonstrated in the one-loop case in the previous subsection. Of course, in the multi-loop case blinks may occur as well as in the one-loop case. They are treated in exactly the same way as before. Thus we see that the multi-loop Feyman diagrams, although algebraically more involved than the one-loop cases, can be reduced to l.c.t.-ordered diagrams using precisely the same algorithm as was used for one-loop Feyman diagrams.

A final remark concerning the $i\epsilon$-prescription is in order here. It is used to define the deformed integration contours in all variables q_i^- simultaneously. After the residue theorem is applied to perform the contour integrals, the real parts of the poles are substituted in formulae like eqs. (3.50, 3.51) ($\epsilon = 0$). If one would substitute complex poles in eq. 3.50, ambiguities might arise in the values of the imaginary parts of the poles in q^-.

Figure 3.14: Two cases where the energy integral is ambiguous: (a) If the k^+ momentum along the loop is constant. (b) If there is one pole left in the k^--integration; the pole of the boson accompanied by the instantaneous part of the fermion propagator.

3.5 Technical difficulties

In the previous sections we dealt with the equivalence between Feynman diagrams and l.c.t-ordered diagrams when the integration over k^- is well-defined. There are two types of special cases were the k^- integration is not well-defined. We can best illustrate these with simple examples. Consider a scalar loop like in ϕ^3 theory. If the external line has positive p^+ then the integration domain in k^+ is the interval $0 < k^+ < p^+$ (see fig. 3.14 (a)). One may wonder what will happen if $p^+ = 0$, because in that case the measure of the integration interval is zero. The poles in the two propagators cross the real axis in the k^--plane for the same value of k^+: $k^+ = 0$. If this diagram is finite, there must occur a delta function like contribution in k^+. In cases where $p^2 \leq 0$, one can approach $p^+ = 0$ by performing a Lorentz-transformation (that, however, does not belong to the stability group of the null plane) and take the limit. Such a Lorentz-transformation is always possible for a space-like external momentum, and there are situations where the momenta on three space-like external lines can be transformed to have $p^+ = 0$ simultaneously. In other cases, like in (generalized) tadpoles, the measure of the integration domain is rigorously zero. We will consider a general approach which holds in all cases and give the same answer as a covariant calculation in the limit $p^+ = 0$. Tadpoles have a close relation with the ordering of operators in the Hamiltonian, therefore we see that the $\delta(k^+)$ contributions have a relation with the ordering.

The other case where the k^- integration is ill-defined, occurs if at most one pole is present in the k^- integration. This happens for all Feynman diagrams with at most one boson propagator and at least one fermion propagator in the loop. Then the intermediate diagrams with an instantaneous part of the fermion propagator combined with a boson propagator needs regularization. Other examples are diagrams with at least two instantaneous terms, which also lead to divergent integrals. The first order correction to the fermion self energy in a theory of scalar bosons and fermions with Yukawa coupling, is a simple example (see fig. 3.14 (b)). The fermion propagator has an instantaneous part such that the only k^--dependence of the integrand resides in the boson propagator. This integral is not defined, so we need a way to deal with this type of integrals in a consistent way. We are primarily interested in a treatment which does not interfere with the algebraic rules, so the regularization must be a linear operation. In addition we require it to be homogeneous in the integration variables. In both cases,

one where tadpoles are present and the other where instantaneous parts give rise to infinities, we are lead by covariance in our choice of regularization. Other arguments do not restrict the regularization to a unique method, while covariance does.

3.5.1 "Zero modes" from energy integration.

One of the integrals which show the presence of zero modes in a time-ordered formulation has been discussed already by Yan (Yan, 1973b):

$$\lim_{k^+\to 0}\int \mathrm{d}p^- \frac{1}{(2(p^+-k^+)p^- - m^2+i\epsilon)(2p^+p^- - m^2+i\epsilon)} = \int \mathrm{d}p^- \frac{1}{(2p^+p^- - m^2+i\epsilon)^2} \overset{\text{covariant}}{=} \frac{i\pi\delta(p^+)}{m^2}\ . \quad (3.52)$$

For $p^+ \neq 0$ there is one double pole either above or below the real axis so it was concluded that, since $p^+ = 0$ is an unphysical value (no free state can acquire $p^+ = 0$), the integral should vanish. A careful analysis shows that eq. (3.52) is an ambiguous expression, so one can get any value (including the covariant answer) and one needs to choose a regularization to get a well-defined integral. (The proper covariant value was obtained by Yan by taking the limits $p^+ \downarrow 0$ and $p^+ \uparrow 0$ in a special way.)

For $p^+ = 0$ the p^- integral diverges, so $(p^+ \to 0, p^- \to \infty)$ is the ambiguous point. If p^+ moves along the real axis and crosses $p^+ = 0$, the poles move through infinity and end up on the other side of the real axis. To deal with all singularities of this type at the same time, we introduce the variable $u = 1/p^-$ and study a general case:

$$D_n = \int \mathrm{d}p^- \frac{1}{(2p_1^+p^- - H_1^\perp + i\epsilon)(2p_2^+p^- - H_2^\perp + i\epsilon)\cdots(2p_n^+p^- - H_n^\perp + i\epsilon)} = \int \mathrm{d}u \frac{u^{n-2}}{(2p_1^+ - (H_1^\perp - i\epsilon)u)\cdots(2p_n^+ - (H_n^\perp - i\epsilon)u)}\ . \quad (3.53)$$

The integrand goes to zero like u^{-2} for $u \to \pm\infty$, therefore the integral is well-defined, unless the integrand has a singularity at $u = 0$. So the only divergence can occur if $u \to 0$ which gives a finite contribution only if all p^+-momenta vanish at the same time. The poles in the variable p^- that moved to infinity, now correspond to poles in the variable u that cross the real axis at $u = 0$ when either of the variables p_i^+ is zero. If all p_i^+ happen to be equal, the integrand is singular at $u = 0$. (The first example, eq. (3.52), is the special case with $n = 2; H_1^\perp = H_2^\perp = m^2$.) This gives a finite contribution to the integral of D over p^+, with support $p^+ = 0$, thus D contains a delta function in p^+.

The u coordinate regularization replaces all other arguments we might have to deal with this "zero-mode" problem. The choice of regularization determines the integral uniquely. Instead of treating the general expression, eq. (3.53), we regularize the case of a single pole in the integrand and use an algebraic relation to obtain the general expression. Consider the integral

$$D_1 = \int \mathrm{d}u \frac{1}{u(2p^+ - (H^\perp - i\epsilon)u)}. \quad (3.54)$$

This expression is ambiguous for two reasons: it has a pole at $u = 0$ and a double pole occurring for $p^+ = 0 \wedge u = 0$. The first ambiguity we remove by adding a small imaginary part to one factor u coming from the Jacobian. In order to obtain a covariant expression we must do this symmetrically:

$$\frac{1}{u} \to \frac{1}{2}\left(\frac{1}{u+i\delta} + \frac{1}{u-i\delta}\right). \tag{3.55}$$

We split the integral into two pieces; one just above the real axis and the other just below it. We do not give the singularities some strict nature, like principal value, which would lead to non-integrable singularities under multiplication such as the square of the principal value for u^{-2}. Generally we treat the energy as a complex variable (since each pole corresponds to a particle), and the kinematical variables are treated geometrically. The choice eq. (3.55) separates $p^+ > 0$ from $p^+ < 0$ for all positive values of ϵ and δ. Thus we find for the regularized integral:

$$\begin{aligned} D_1^{\rm Reg} &= \int \mathrm{d}u \frac{1}{2}\left(\frac{1}{u+i\delta} + \frac{1}{u-i\delta}\right) \frac{1}{(2p^+ - (H^\perp - i\epsilon)u)} \\ &= -\frac{\pi i\theta(p^+)}{2p^+ + i(H^\perp - i\epsilon)\delta} + \frac{\pi i\theta(-p^+)}{2p^+ - i(H^\perp - i\epsilon)\delta} \\ &= -\frac{2\pi i\theta(p^+)}{2p^+ + i(H^\perp - i\epsilon)\delta}. \end{aligned} \tag{3.56}$$

For $p^+ < 0$ we reversed its sign to obtain the last line. Integrating $D_1^{\rm Reg}$ over p^+ from 0 to a cutoff Λ and taking the limit $\epsilon \to 0$, gives $\pi(\ln(H^\perp) + \ln\delta + \pi i/2 - \ln 2\Lambda)$. We shall see that the constant part $\ln\delta + i\pi/2 - \ln 2\Lambda$ drops if we have two or more energy denominators. Using the algebraic relation

$$\frac{1}{\prod_{j=1}^n (2p^+p^- - H_i^\perp + i\epsilon)} = \sum_{k=1}^n \frac{1}{(2p^+p^- - H_k^\perp + i\epsilon)\prod_{j\neq k}(H_k^\perp - H_j^\perp)} \tag{3.57}$$

the regularized integral becomes:

$$\mathrm{R}\!\!\int \mathrm{d}p^- \frac{1}{(2p^+p^- - H_1^\perp + i\epsilon)\cdots(2p^+p^- - H_n^\perp + i\epsilon)} = \sum_{k=1}^n \frac{i\pi\delta(p^+)\ln(H_k^\perp)}{\prod_{j\neq k}(H_k^\perp - H_j^\perp)}\ . \tag{3.58}$$

The function $\delta(p^+)$ appears here, because the integral is strictly zero for $p^+ \neq 0$, although integration over p^+ gives a finite result. The result eq. (3.58) can also be obtained as a limiting case of eq. (3.53) in the simultaneous limits $p_i^+ \to p^+, \forall i$. One can check that eq. (3.58) is the same as the covariant result, using a Wick rotation such that $2p^+p^- - p_\perp^2 \to -|p|^2$. The limit for $H_i \to H_j$ is well-defined. The constant term has dropped since

$$\sum_{k=1}^n \frac{1}{\prod_{j\neq k}(H_k^\perp - H_j^\perp)} = 0\ , \tag{3.59}$$

which follows from the fundamental theorem of algebra.

We emphasize here that these zero modes appear in loops where the p^+ momentum is constant along the loop. Zero-modes can be interpreted as an infinite number of states (around $p^+ = 0$) which are infinitely off-shell ($p^-_{on} = \infty$), and thus have zero probability for propagation over a finite distance. The combination of both gives a finite contribution. This is reminiscent of the ultra-violet divergences, where the large number of high-energy states give an infinite contribution.

Although zero-modes are needed to obtain the covariant answer, they remain slightly artificial, which can be seen from the configurations were they occur. It seems that nature is telling us that the high density of states for high energy causes trouble: divergent integrals appear which have to be regularized, and zero-modes. Both result from singularities on the light-cone.

3.5.2 Divergences in the fermion loop

In the section on diagrams containing fermions we stated that they could be reduced to l.c.t.-ordered diagrams, provided no additional singularities would occur. In this section we deal with these singularities. We state that the regularization proposed here removes all of them. There remains one point to clarify, $i.e.$, whether the method of regularization does indeed produce a covariant result. The latter point, however, will not be discussed in this chapter but in the chapter on renormalization of light-front perturbation theory.

We now have the tools to deal with the singularities in the fermion loop. Earlier (sect. 3.3) we saw that a blink combines two singular terms in such a way that we get a nonsingular expression. However, in general the low-order terms, with several instantaneous contributions, are singular by themselves. We will show that the contribution from the contour at infinity leads to these singularities. After subtraction of the latter the singularities are gone and a proper recombination of terms will remove apparent singularities.

For Feynman diagrams with at most one boson propagator in a loop there are singular parts in the contour integration. Even if the diagram would be convergent in the ordinary sense, $i.e.$, in the covariant or instant-form, it will still be divergent in k^--integration. The singular behavior of the fermion propagator on the light front is to blame.

Also in the case of bosons an ambiguity occurred (see sect. 3.5.1). The result did depend on whether the contour was closed in the lower half plane or in the upper half plane. This problem could be resolved by choosing a particular combination of contours. We considered two contours, one consisting of the real axis and a semicircle in the upper half plane, the other one has the semicircle in the lower half plane. The integral over the real k^--axis was replaced by the average of the integrals over these two contours. This regularization turned out to have a number of desirable properties.

In the case of fermion loops the problem is more complex. A straightforward application of the residue theorem gives results that depends strongly on the choice of the contour. The integral is also more divergent than one would expect from naive power counting, and has noncovariant singularities. At the origin of these problems lies the contribution of the (semi-) circle at infinity to the contour integral. We have to subtract this contribution. In a sense we propose a regularization of the contour integral.

For an integral that converges on the real axis, it does not matter whether we close the contour in the upper or the lower half-plane. This means that the sum of all residues is zero:

$$\sum_i \mathrm{Res}_i = 0. \tag{3.60}$$

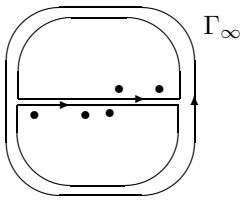

Figure 3.15: The difference between the upper-plane contour and the lower-plane contour is the contour at infinity Γ_∞.

If the integration is divergent we have contributions at infinity, which add differently to the two contours (see fig. 3.15). Therefore the two contours give different results. We denote this difference by Γ_∞. Then we have

$$\sum_i \mathrm{Res}_i = \Gamma_\infty. \tag{3.61}$$

To solve this problem we "regularize" the residues by subtracting fractions of Γ_∞ from them:

$$\sum_i \mathrm{Res}_i^{\mathrm{reg}} = \sum_i (\mathrm{Res}_i - \alpha_i \Gamma_\infty) = 0, \qquad \sum_i \alpha_i = 1. \tag{3.62}$$

We then find the desired result that closing the contour in the upper half plane gives the same result as closing it in the lower half plane. We will see that the α_i's can be chosen such that the singularities cancel.

The k^--integral corresponding to a general Feynman diagram with a fermion loop can be written as

$$D_n = \int \frac{\mathrm{d}k^-}{2^n k_1^+ \cdots k_n^+} \frac{(\gamma^+ k^- + \beta_1) \cdots (\gamma^+ k^- + \beta_n)}{(k^- - H_1) \cdots (k^- - H_n)}. \tag{3.63}$$

We wrote only the structure that depends on k^- and k^+ explicitly. We can consider one residue at a time, since the singularities of one residue are not canceled by another residue. The residue of the pole $(k^- - H_j)^{-1}$, and the contribution of the contour at infinity are:

$$\mathrm{Res}_j = \frac{1}{2^n k_1^+ \cdots k_n^+} \frac{(\gamma^+ H_j + \beta_1) \cdots (\gamma^+ H_j + \beta_n)}{(H_j - H_1) \cdots (H_j - H_n)} \tag{3.64}$$

$$\Gamma_\infty = \frac{1}{2^n k_1^+ \cdots k_n^+} \left((\sum_{i=1}^n H_i)(\gamma^+ \cdots \gamma^+) + (\beta_1 \cdots \gamma^+) + \cdots + (\gamma^+ \cdots \beta_n) \right) \tag{3.65}$$

The latter can best be calculated by changing the integration variable to $u = (k^-)^{-1}$ and integrating over a circle around the origin with a small radius, $|u| = \epsilon$. The residue Res_j has only singularities if $k_j^+ \to 0$, since then $H_j \to \infty$. In the limit $k_j^+ \to 0$ only a few terms survive. The surviving structure is precisely the contribution from the contour at infinity, which is independent of j

$$\lim_{k_j^+ \to 0} \mathrm{Res}_j = \Gamma_\infty \ . \tag{3.66}$$

If we decompose the contribution from the contour at infinity now in such a way that each term contains only one singular point ($k_j^+ \to 0$), we can subtract these terms from the residues with the same singularities, and the resulting regularized residues are finite. If we define the quantities q_j^+ and $H_j^\perp$ as $k_j^+ = k^+ - q_j^+$ and $H_j^\perp = 2k_j^+ H_j$, then we find that the following regularized residues are finite for $k_j^+ \to 0$

$$\mathrm{Res}_j^{\mathrm{reg}} = \mathrm{Res}_j - \left(\frac{1}{2^n (k^+ - q_j^+) \prod (q_j^+ - q_i^+)} H_j + \right.$$

$$\left. \sum_l \frac{H_l^\perp}{2^{n+1} (k^+ - q_j^+)(q_j^+ - q_l^+) \prod (q_j^+ - q_i^+)} + \frac{H_j}{2^n (q_j^+ - q_l^+) \prod (q_l^+ - q_i^+)} \right) (\gamma^+ \cdots \gamma^+) +$$

$$\frac{1}{2^n (k^+ - q_j^+) \prod (q_j^+ - q_i^+)} ((\beta_1 \cdots \gamma^+) + \cdots + (\gamma^+ \cdots \beta_n)) \tag{3.67}$$

Since each residue is now regular we know that there is a combination of l.c.t.-ordered diagrams where each term is convergent. The blink procedure tells us how to do this step-by-step. The argument above tells us that there are no singularities left.

We killed two birds with one stone: we resolved the ambiguity in the contour integration and removed the singularities. These two problems are intimately related since the singularity comes from the pinching of the contour at infinity between the "pole at infinity" and an ordinary pole.

Another advantage of this procedure is that only the physical sectors are nonzero, a property that would be destroyed by ordinary contour integration. It allows us to keep a simpler view of causality and unitarity, where each line is associated with a particle moving forward in l.c.-time. In nonphysical sectors all the poles are on the same side of the axis. Then formula (3.62) tells us that the result is zero. We do not know whether this regularization leads to the same amplitude as the covariant calculations.

Example; vacuum polarization

We will illustrate the procedure from the previous section with an example. The simplest diagram is the vacuum polarization diagram; a closed fermion loop with two fermion propagators.

$$D^{\mu\nu} = \int \frac{\mathrm{d}k^-}{2\pi i} \frac{Tr[\gamma^\mu (\gamma^+ k^- + \beta_1) \gamma^\nu (\gamma^+ k^- + \beta_2)]}{4k_1^+ k_2^+ (k^- - H_1)(k^- - H_2)}. \tag{3.68}$$

We deal with the physical sector so we can assume, without loss of generality $\mathbf{Im} H_1 > 0$ and $\mathbf{Im} H_2 < 0$. The result depends on the way the contour is closed. We will close the contour in the upper half plane. In terms of l.c.t.-ordered diagrams we have the ordinary diagram, with two propagating fermions, and the diagram with the instantaneous part associated with the pole H_2 in the lower half plane. Together they give the residue of the pole H_1, as expected.

$$D_1^{\mu\nu} = \frac{Tr[\gamma^\mu (\gamma^+ H_1 + \beta_1) \gamma^\nu (\gamma^+ H_1 + \beta_2)]}{4k_1^+ k_2^+ (H_1 - H_2)}. \tag{3.69}$$

If we would have chosen to close the contour in the lower half plane the result would be different. The difference is the result of a finite contribution of the semicircles. We still have to subtract the fraction of the contour at infinity which is given by (3.67):

$$\alpha_1\Gamma_\infty = \frac{Tr[\gamma^\mu\gamma^+\gamma^\nu\gamma^+]}{4k_1^+(k_2^+-k_1^+)}\left(H_1+\frac{k_2^+H_2}{k_2^+-k_1^+}+\frac{k_1^+H_1}{k_1^+-k_2^+}\right)+\frac{Tr[\gamma^\mu\beta_1\gamma^\nu\gamma^+]}{4k_1^+(k_2^+-k_1^+)}+\frac{Tr[\gamma^\mu\gamma^+\gamma^\nu\beta_2]}{4k_1^+(k_2^+-k_1^+)}. \tag{3.70}$$

The l.c.t.-ordered diagram obtained has no singularities, and is independent of the direction in which the contour is closed, since it is symmetric in H_1 and H_2:

$$D_1^{\mu\nu}-\alpha_1\Gamma_\infty = D_{\rm reg}^{\mu\nu} = \frac{Tr\left[\gamma^\mu\left(\left(\frac{k_2^+H_2-k_1^+H_1}{k_2^+-k_1^+}\right)\gamma^++\beta_1\right)\gamma^\nu\left(\left(\frac{k_2^+H_2-k_1^+H_1}{k_2^+-k_1^+}\right)\gamma^+ +\beta_2\right)\right]}{4k_1^+k_2^+(H_1-H_2)}. \tag{3.71}$$

This result could not be obtained if we would have taken a combination of an upper-plane semicircle and a lower-plane semicircle, this would give a singular, and thus an ambiguous, result. The contribution of the contour at infinity should be decomposed in a unique way to obtain a regular expression.
We will not calculate the amplitude here since the diagram is divergent and the comparison is with other results is spoiled by renormalization. After this regularization the k^+-integration is automatically finite, since the domain is finite and the integrand is regular. In chapter 5 we will see that this indeed leads to the covariant amplitude. The singularities which are removed here correspond to the meaningless divergences. To the contributions of the semicircle we cannot assign a proper Lorentz structure.

3.5.3 Dynamical spin

In a Hamiltonian theory we separate kinematical variables from dynamical ones. Starting from one equal-l.c.t surface, we evolve in the time direction to the next equal-l.c.t. surface. In a covariant formulation, different interaction points could be on the same equal-l.c.t surface. Constraints should, in a Hamiltonian formulation, account for these parts. A straightforward interpretation does not exist, the constraints "evolve" with the order in perturbation theory, and so does the physical Hilbert-space (constraints are imposed on the Hilbert space). We will illustrate this point with a Hilbert-space interpretation of the instantaneous interaction $\gamma^+/2p^+$.

The $(p^+)^{-1}$ singularity is ambiguous as it stands. We need a way to look at this part such that we avoid additional divergences which seem to appear. Note that the spinor-matrix elements of γ^+ are the same as those of p^+. Therefore we might suspect that the occurrence of γ^+ suppresses the singularity. To make this apparent we use the completeness of the physical Hilbert space. The physical Hilbert space is spanned by the free states. Therefore we can write the identity operator as the sum over all states:

$$\mathbb{1} = \sum_\alpha \int \mathrm{d}^3p\ |u^{(\alpha)}(p)\rangle\langle u^{(\alpha)}(p)|. \tag{3.72}$$

We use this abstract notation because we don't want to bother with conventions which are not

relevant. The normalization follows from the idempotency of the identity operator ($\mathbb{1} \cdot \mathbb{1} = \mathbb{1}$).

$$\langle u^{(\alpha)}(p)|u^{(\beta)}(p')\rangle = \bar{u}^{(\alpha)}(p)u^{(\beta)}(p')\langle p|p'\rangle = \delta^{\alpha\beta}\delta^3(p-p'). \tag{3.73}$$

We can project $\gamma^+/(2p^+)$ onto the physical states by applying the identity operator on both sides:

$$\begin{aligned} \mathbb{1} \cdot \frac{\gamma^+}{2p^+} \cdot \mathbb{1} &= \sum_{\alpha\beta} \int \mathrm{d}^3p' \mathrm{d}^3p |u^{(\alpha)}(p')\rangle\langle u^{(\alpha)}(p')| \frac{\gamma^+}{2p^+} |u^{(\beta)}(p)\rangle\langle u^{(\beta)}(p)| \\ &= \sum_{\alpha\beta} \int \mathrm{d}^3p' \mathrm{d}^3p |u^{(\alpha)}(p')\rangle \delta^{\alpha\beta} \frac{\delta^3(p-p')}{2m} \langle u^{(\beta)}(p)| = \frac{\mathbb{1}}{2m} \end{aligned} \tag{3.74}$$

There is no mixing between upper and lower components because they are spectrally separated.

$$\mathbb{1} = \left(\frac{\not{p} + m}{2m} + \frac{-\not{p} + m}{2m} \right) \theta(p^+) \tag{3.75}$$

Wherever $\gamma^+/(2p^+)$ appears we can replace it by $1/(2m)$, since eq. (3.74) is an operator identity on our space. The instantaneous interaction can be interpreted as nothing but a point interaction, $1/(2p^+)$ being the phase space that goes with it and γ^+ the vertex.

However, these arguments do not hold in a Feynman diagram. The spin plays a dynamical role. In contrast to the instant-form dynamics, where all components of the angular momentum are kinematical, in front-form dynamics only the z-component of the spin is a kinematical operator. The other components are involved in the interactions. It turns out that we can combine the $\gamma^+/(2p^+)$ singularity with the $1/p^+$ singularity that appears in a corresponding l.c.t.-ordered diagram with a propagating fermion line, such that the singularities of the two cancel. Thus we find that in a Hamiltonian approach to light-front field theory, there is an intimate interplay between the singularities of the propagators and a singular piece of the interaction. Interestingly enough, this piece occurs even for free particles. In old-fashioned ordinary time-ordered perturbation theory, *i.e.*, instant form dynamics, the amplitude of propagation depends on the off-shell energy only, not on the polarization.

3.5.4 Analyticity and covariance

A Feynman amplitude is an analytical function of scalar objects like p_i^2, $p_i \cdot p_j$. Often, the real values of the scalars are the boundary values of the complex domain on which this function is defined. We use these arguments in order to be able to apply the residue theorem to integration over the loop variables and to perform Fourier transformations. All contour integrals are finite (if we don't pinch the contour) and coincide for integrals convergent on the real axis with the integral along this axis. (A coordinate transformation $y = x^{-1}$, as used in the section on zero modes, doesn't alter the results, since it maps the real axis on the real axis.) We cannot use the exponential $\mathrm{e}^{i\,kx}$ to improve the convergence along the semicircle of the contour (Jordan's lemma).

If we integrate over one coordinate separately, manifest covariance is lost. In the case of integration over ordinary energy this was not much of a problem since we can consider

$\vec{p}^2 + m^2$ as real and then analyticity in p^0 is directly related to analyticity in $p_\mu p^\mu$. In light-front coordinates the situation is more complicated since $p^2 - m^2 = 2p^-p^+ - (p_\perp^2 + m^2)$. For real values of the scalar object the complex values of p^- and p^+ are related ($(p_\perp^2 + m^2)$ is real). The coordinates are each others complex conjugate. After Wick-rotation ($p^0 \to -ip^0$) this remains almost exactly true: $p^+ \to p,\ p^- \to -\bar{p}$. For a strip along the real axis we have: $p^-\mathbf{Im}p^+ = -p^+\mathbf{Im}p^-$. Singularities that occur in a complex function can be regularized, but the relation between the conjugate variables restricts the possibilities of regularization. Singularities of an integer order (like $1/x$) cannot be integrated by parts. But one can approach these singularities in parametric space $x^\alpha;\ \alpha \to -1$. The advantage of this dimensional regularization is that it does not interfere with algebraic rules; the regularized distributions satisfy the same relations as the singular ones, which is of great important for complex, analytical functions. For regularization of complex distributions one subtracts these poles as function of the order but with a fixed difference between the order of the singularity of p with respect to $\bar{p}$: $p^\alpha \bar{p}^{\alpha+k}$ with a fixed k (Gel'fand & Shilov, 1964).

We will follow a simpler approach with the same result. To avoid complications we define distributions of covariant objects only. Analyticity of the covariant object tells us the relation between p^+ and p^- at regularization. A homogeneous distribution is given by the partial integration of a singular, but integrable, function:

$$\left(\frac{1}{p^+}, \phi\right) = \int \mathrm{d}p^- \frac{1}{p^+}\phi = \int \mathrm{d}p^- \left[\frac{\partial}{\partial p^+}\ln(p^+p^-)\right]\phi. \tag{3.76}$$

We need p^+p^- for positive imaginary values. So we take the cut of the logarithm along the negative imaginary axis, therefore the logarithm has an imaginary part of the form $i\pi\theta(-p^+p^-)$. The homogeneous distribution is

$$\frac{1}{[p^+]} \equiv \frac{\partial}{\partial p^+}(\ln|p^+p^-| + i\pi\theta(-p^+p^-)) = \frac{1}{p^+ + i\epsilon\sigma(p^-)} = \mathrm{PV}\frac{1}{p^+} - i\pi\sigma(p^-)\delta(p^+), \tag{3.77}$$

where σ is the sign function. Therefore $\partial_{p^+}\partial_{p^-}\ln(p^+p^-) = \partial_{p^-}(p^+)^{-1} = 2\pi i\delta(p^-)\delta(p^+)$, which is nothing but the Mandelstam-Leibbrandt regularization (Leibbrandt, 1987). (The i can be accounted for through Wick rotating the z-variable.) After Fourier transformation the distribution $\ln(p^+p^- + i\epsilon)$ becomes a singular function which contains the intersection of the light cone with the null-planes $x^+ = 0 \vee x^- = 0$: $\mathcal{F}[\ln(p^+p^- + i\epsilon)] = \frac{i\delta^2(x_\perp)}{x^+x^- - i\epsilon} = -\delta^2(x)\delta^1(x^+x^-) + i\delta^2(x_\perp)\mathrm{PV}\frac{1}{x^+x^-}$. This fact is part of the reason why there exists confusion about the instantaneous term in the fermion propagator. In a Feynman diagram the integrands are treated as meromorphic functions in the complex plane. The real part is automatically complemented with an imaginary part. If we use a Hamiltonian approach, we will have constraints which relate real parts to real parts and we express one in terms of the other. Therefore we might loose some information concerning the behavior of the imaginary parts. To put it in other words: the off-shell behavior comes naturally in a Feynman diagram and this does not always happen in a l.c.t.-ordered diagram. This is another reason why we chose to define light-front field theory in close connection with a formulation in terms of Feynman diagrams.

3.6 Proof of equivalence

In this section we have collected several technical aspects of the proof of equivalence. In sect. 3.2 we gave some examples, in order to illustrate the general procedure. Therefore, we do not give any examples here.

3.6.1 Energy integration

We present here the proof of the basic theorem on the integration over p^-. First we discuss the case of a single loop. The proof for several loops comes next.

One loop

The integration of a Feynman diagram over one energy loop variable p^- gives the following expression for the p^+-interval corresponding to $\{(\mathbf{Im}H_i > 0 \wedge i \leq m) \vee (\mathbf{Im}H_i < 0 \wedge i > m)\}$:

$$FD(\vec{H}) = \int \frac{\mathrm{d}p^-}{2\pi} \frac{1}{2^N p_1^+ \cdots p_N^+ [p^- - H_1] \cdots [p^- - H_N]} = \frac{i(-1)^{N+1}}{2^N (p_1^+ \cdots p_N^+) \Delta(H_1, \cdots, H_N)} \begin{vmatrix} H_1^{N-2} & \cdots & H_1^2 & H_1 & 0 & 1 \\ H_2^{N-2} & \cdots & H_2^2 & H_2 & 0 & 1 \\ . & & & & . & . \\ H_m^{N-2} & \cdots & H_m^2 & H_m & 0 & 1 \\ H_{m+1}^{N-2} & \cdots & H_{m+1}^2 & H_{m+1} & 1 & 0 \\ . & & & & . & . \\ H_N^{N-2} & \cdots & H_N^2 & H_N & 1 & 0 \end{vmatrix} \tag{3.78}$$

The last factor is a complicated mixed symmetric polynomial in the H_i's that we denote by $(-1)^n W_{m,n}(H_1, \cdots, H_m | H_{m+1}, \cdots, H_{n+m})$. (The phase factor $(-1)^{N+1}$ is introduced to simplify the final expressions.) Δ is the Vandermonde determinant ($n \geq 2$):

$$\Delta(x_1 \cdots, x_n) = \det[\Delta_{ij}] \ , \tag{3.79}$$

$$\Delta_{ij} = x_i^{n-j} \ . \tag{3.80}$$

A well known result is

$$\Delta(x_1 \cdots, x_n) = \prod_{i<j}^{n-1,n} (x_i - x_j) \ . \tag{3.81}$$

See for instance MacDonald or Fulton & Harris (MacDonald, 1979; Fulton & Harris, 1991) for properties of the Vandermonde determinant.

Proof

Depending on the (fixed) values of the (kinematical) p_i^+'s some poles are above and some are below the real axis. The integral is computed as $2\pi i$ times the sum of the residues. The residue of pole $p^- = H_i$ can be written as

$$(-1)^{i+1} \frac{\Delta(H_1, \cdots, H_{i-1}, H_{i+1}, \cdots, H_N)}{2^N (p_1^+ \cdots p_N^+) \Delta(H_1, \cdots, H_N)} \tag{3.82}$$

We can add a line and a column to the determinant in the numerator:

$$(-1)^{i+1}\begin{vmatrix} H_1^{N-2} & \cdots & H_1^2 & H_1 & 1 \\ H_2^{N-2} & \cdots & H_2^2 & H_2 & 1 \\ \cdot & & & & \cdot \\ H_{i-1}^{N-2} & \cdots & H_{i-1}^2 & H_{i-1} & 1 \\ H_{i+1}^{N-2} & \cdots & H_{i+1}^2 & H_{i+1} & 1 \\ \cdot & & & & \cdot \\ H_N^{N-2} & \cdots & H_N^2 & H_N & 1 \end{vmatrix} = (-1)^{N+1}\begin{vmatrix} H_1^{N-2} & \cdots & H_1^2 & H_1 & 1 & 0 \\ H_2^{N-2} & \cdots & H_2^2 & H_2 & 1 & 0 \\ \cdot & & & & \cdot & \cdot \\ H_{i-1}^{N-2} & \cdots & H_{i-1}^2 & H_{i-1} & 1 & 0 \\ H_i^{N-2} & \cdots & H_i^2 & H_i & 1 & 1 \\ H_{i+1}^{N-2} & \cdots & H_{i+1}^2 & H_{i+1} & 1 & 0 \\ \cdot & & & & \cdot & \cdot \\ H_N^{N-2} & \cdots & H_N^2 & H_N & 1 & 0 \end{vmatrix} \tag{3.83}$$

The final formula is obtained by adding determinants of type eq. (3.83) which amounts to just adding their last columns. This gives the result stated in the theorem.

Several loops

In the case of several loops we integrate loop by loop. We must use the residue theorem such that the order of integration does not change the result. In general, the momenta of the particles on the internal lines will be linear combinations of the integration variables, say $k_i = \sum_k \alpha_i^k p_k$, where k_i^μ is the four momentum on line i and p_k^μ is the integration variable. One has the freedom to choose the latter such that α_i^k is either $+1$, -1 or 0.

Theorem Multi-dimensional energy integration
An unambiguous expression is:

$$\int \mathrm{d}p_1^- \mathrm{d}p_2^- \cdots \mathrm{d}p_m^- \prod_{i=1}^{n} (\sum \alpha_i^k p_k^- + H_i)^{-1} =$$

$$(2\pi i)^m \sum_{\substack{\{j_1, j_2, \cdots, j_m\} \\ [\alpha^1 \cdots \alpha^k]_{j_1 \cdots j_k} \neq 0}} \frac{1}{[\alpha^1 \alpha^2 \cdots \alpha^m]_{j_1 \cdots j_m}} \prod_{i \neq j_r}^{n} \left(\frac{[\alpha^1 \alpha^2 \cdots \alpha^m H]_{j_1 \cdots j_m i}}{[\alpha^1 \alpha^2 \cdots \alpha^m]_{j_1 \cdots j_m}} \right)^{-1} . \tag{3.84}$$

The antisymmetrized product $[\alpha^1 \cdots \alpha^m]_{j_1 \cdots j_m}$ is the determinant of the matrix

$$(\alpha)_{j_1 \cdots j_m} \equiv \alpha = \begin{pmatrix} \alpha_{j_1}^1 & \cdots & \alpha_{j_m}^1 \\ \vdots & & \vdots \\ \alpha_{j_1}^m & \cdots & \alpha_{j_m}^m \end{pmatrix} \tag{3.85}$$

The inverse of the matrix α will be denoted by $\bar{\alpha}$. The poles $\{j_1, \cdots, j_m\}$ that are included in the sum have for all values of p_i^- the correct imaginary sign of H_j/α_j^i, because this sign is determined by the plus-components of the integration variables. Before we start to integrate we first determine inside which contours the different poles lie, then drop the $i\epsilon$-description. This is clearly an invariant formulation, so the order of integration can be altered.
Proof

An unambiguous way to define the integration is to shift the integration contour slightly into the complex plane and leave the poles on the real axis. The poles are determined by the following set of linear equations

$$\sum_i \alpha_k^i p_i^- + H_{j_k} = 0, \quad i,k = 1, \cdots m, \tag{3.86}$$

which have the solution

$$\bar{p}_i^- = -\sum_k \bar{\alpha}_i^k H_{j_k}, \tag{3.87}$$

$\bar{p}$ is the specific value for p which satisfy eq. (3.86). Next the multidimensional integral is written in terms of these new variables. The Jacobian of the transformation is $\det \bar{\alpha} = 1/\det \alpha = 1/[\alpha^1 \cdots \alpha^m]_{j_1 \cdots j_m}$. Subsequently, we apply the residue theorem to every $\bar{p}^-$-integration. We substitute the new variables, and find that the pole part of the integral factorizes:

$$\int \prod_{j=1}^{n} \mathrm{d}z_j \frac{f(z)}{(\alpha_1^j z_j - \gamma_1)\cdots(\alpha_m^j z_j - \gamma_m)} = \tag{3.88}$$

$$\det[\bar{\alpha}] \int \mathrm{d}y_1 \frac{1}{y_1 - \bar{\alpha}_1^j \gamma_j} \cdots \int \mathrm{d}y_m \frac{1}{y_m - \bar{\alpha}_m^j \gamma_j}\ f(\bar{\alpha} y). \tag{3.89}$$

We used the summation convention. Note that the integral is independent of the choice of integration variables.

This type of multi-dimensional complex integration is not related to topology, so the deformation of the contour might change the result. The torus obtained by closing the different contours depends on the choice of coordinates. To avoid ambiguities we take an algebraic view instead.

3.6.2 Recursion formula

The recursion formula is the basis of the proof of equivalence. It tells us how to take out of any Feynman diagram the building block of a l.c.t-ordered diagram: an energy denominator. This happens without changing the structure of the algebraic form of the reduced Feynman diagram, so we can apply this formula, a number of times (the recursion). The final result, obtained upon the last application of the recursion formula can immediately be evaluated. The final object is just a piece of a l.c.t.-ordered diagram (TOD): a product of energy denominators.

The recursion formula allows us to consecutively pull energy denominators out of $FD(\vec{H})$ in order to obtain a sum of TOD's.

Theorem The following identity is true for any m and n ($N = m + n$):

$$\frac{W_{m,n}(H_1, \cdots, H_m | H_{m+1}, \cdots, H_N)}{\Delta(H_1, \cdots, H_N)} = \frac{1}{H_1 - H_{m+1}} \times \tag{3.90}$$

$$\left(\frac{W_{(m-1),n}(H_2, \cdots, H_m | H_{m+1}, \cdots, H_N)}{\Delta(H_2, \cdots, H_N)} + \frac{W_{m,(n-1)}(H_1, \cdots, H_m | H_{m+2}, \cdots, H_N)}{\Delta(H_1, \cdots, H_m, H_{m+2}, \cdots, H_N)} \right)$$

Remark

The reduction step removes two poles, H_1 and H_{m+1}, and combines them into a single energy denominator, $H_1 - H_{m+1}$. The second factor of the r.h.s. of eq. (3.90) consists of two terms, both of which contain one pole less than the original form. The factor $(H_1 - H_{m+1})^{-1}$ is incorporated in the TOD. At the first stage, $W_{m,n}/\Delta$ is a structure that is directly related to a Feynman diagram. After taking steps in the reduction algorithm objects with the same structure are obtained, but these objects are not in the same way associated with (possibly different) Feynman diagrams. The last step in the algorithm is given by:

$$W_{1,n}(y|x_1,\cdots,x_n) = W_{n,1}(x_1,\cdots,x_n|y) = \Delta(x_1,\cdots,x_n) \tag{3.91}$$

First we prove the formula (3.90) and then we show how to carry out the reduction.
Proof

First express $W_{m,n}$ in terms of a determinant as in eq. (3.78). Then perform the usual manipulations with determinants: take linear combinations of rows or columns. If we subtract the first row from the rows 2 to m, the $m+1^{st}$ row from the other rows $\{m+2,\cdots,m+n\}$, and expand the determinant with respect to the last two columns, we obtain:

$$W_{m,n}(x_1,\cdots,x_m|y_1,\cdots,y_n) = (-1)^N \begin{vmatrix} x_2^K - x_1^K & \cdots & x_2 - x_1 \\ \vdots & & \vdots \\ x_m^K - x_1^K & \cdots & x_m - x_1 \\ y_2^K - y_1^K & \cdots & y_2 - y_1 \\ \vdots & & \vdots \\ y_n^K - y_1^K & \cdots & y_n - y_1 \end{vmatrix} \tag{3.92}$$

where $K = n+m-2 = N-2$. We can add a row and a column to the determinant to obtain:

$$\frac{(-1)^{m+1}}{x_1 - y_1} \begin{vmatrix} x_2^K - x_1^K & \cdots & x_2 - x_1 & 0 \\ \vdots & & \vdots & \vdots \\ x_m^K - x_1^K & \cdots & x_m - x_1 & 0 \\ x_1^K - y_1^K & \cdots & x_1 - y_1 & x_1 - y_1 \\ y_2^K - y_1^K & \cdots & y_2 - y_1 & 0 \\ \vdots & & \vdots & \vdots \\ y_n^K - y_1^K & \cdots & y_n - y_1 & 0 \end{vmatrix} \tag{3.93}$$

We split the determinant into two parts by adding and subtracting in the last column the column $(x_2 - x_1,\cdots,x_m - x_1,0,\cdots,0)$. Then we subtract the last column from the last but

one column in both determinants to obtain

$$\frac{(-1)^{m+1}}{x_1-y_1}\left(\begin{vmatrix} x_2^K-x_1^K & \cdot & 0 & x_2-x_1 \\ \vdots & & \vdots & \vdots \\ x_m^K-x_1^K & \cdot & 0 & x_m-x_1 \\ x_1^K-y_1^K & \cdot & 0 & x_1-y_1 \\ y_2^K-y_1^K & \cdot & y_2-y_1 & 0 \\ \vdots & & \vdots & \vdots \\ y_n^K-y_1^K & \cdot & y_n-y_1 & 0 \end{vmatrix} - \begin{vmatrix} x_2^K-x_1^K & \cdot & 0 & x_2-x_1 \\ \vdots & & \vdots & \vdots \\ x_m^K-x_1^K & \cdot & 0 & x_m-x_1 \\ x_1^K-y_1^K & \cdot & x_1-y_1 & 0 \\ y_2^K-y_1^K & \cdot & y_2-y_1 & 0 \\ \vdots & & \vdots & \vdots \\ y_n^K-y_1^K & \cdot & y_n-y_1 & 0 \end{vmatrix}\right) \tag{3.94}$$

We add the m-th row to the rows above it in the first determinant, and subtract it from the rows below it in the second determinant. The result is

$$\frac{(-1)^{m+1}}{x_1-y_1}\begin{vmatrix} x_2^K-y_1^K & \cdot & 0 & x_2-y_1 \\ \vdots & & \vdots & \vdots \\ x_m^K-y_1^K & \cdot & 0 & x_m-y_1 \\ x_1^K-y_1^K & \cdot & 0 & x_1-y_1 \\ y_2^K-y_1^K & \cdot & y_2-y_1 & 0 \\ \vdots & & \vdots & \vdots \\ y_n^K-y_1^K & \cdot & y_n-y_1 & 0 \end{vmatrix} + \frac{(-1)^{m}}{x_1-y_1}\begin{vmatrix} x_2^K-x_1^K & \cdot & 0 & x_2-x_1 \\ \vdots & & \vdots & \vdots \\ x_m^K-x_1^K & \cdot & 0 & x_m-x_1 \\ x_1^K-y_1^K & \cdot & x_1-y_1 & 0 \\ y_2^K-x_1^K & \cdot & y_2-x_1 & 0 \\ \vdots & & \vdots & \vdots \\ y_n^K-x_1^K & \cdot & y_n-x_1 & 0 \end{vmatrix} \tag{3.95}$$

Let $M = n+m-3$ and define for any k the symmetric function ϕ^{k-1} by the relation $x^k-y^k=(x-y)\phi^{k-1}(x,y)$. The rows contain one of the factors x_i-x_1, y_j-x_1, y_j-y_1 or x_i-x_1, that can be divided out. The product of these factors are written as the ratio of two Vandermonde determinants, to obtain from eq. (3.95):

$$\frac{(-1)^{m+1}}{x_1-y_1}\left(\frac{\Delta(x_1\cdot x_m,y_2\cdot y_n,y_1)}{\Delta(x_1\cdot x_m,y_2\ y_n)}\begin{vmatrix} \phi^M(x_2,y_1) & \cdot & 0 & 1 \\ \vdots & & \vdots & \vdots \\ \phi^M(x_m,y_1) & \cdot & 0 & 1 \\ \phi^M(x_1,y_1) & \cdot & 0 & 1 \\ \phi^M(y_2,y_1) & \cdot & 1 & 0 \\ \vdots & & \vdots & \vdots \\ \phi^M(y_n,y_1) & \cdot & 1 & 0 \end{vmatrix} + \frac{\Delta(x_2\cdot y_n,x_1)}{\Delta(x_2\cdot y_n)}\begin{vmatrix} \phi^M(x_2,x_1) & \cdot & 0 & 1 \\ \vdots & & \vdots & \vdots \\ \phi^M(x_m,x_1) & \cdot & 0 & 1 \\ \phi^M(y_1,x_1) & \cdot & 1 & 0 \\ \phi^M(y_2,x_1) & \cdot & 1 & 0 \\ \vdots & & \vdots & \vdots \\ \phi^M(y_n,x_1) & \cdot & 1 & 0 \end{vmatrix}\right) \tag{3.96}$$

The dependence of the first determinant on y_1 is only apparent. The same is true for the dependence on x_1 of the second determinant. We can easily see this through matrix multipli-

cation:

$$\begin{pmatrix} x_1^{n-2} & \cdot & x_1 & 1 & 1 \\ \vdots & & \vdots & \vdots & \vdots \\ x_m^{n-2} & \cdot & x_m & 1 & 1 \\ x_{m+1}^{n-2} & \cdot & x_{m+1} & 1 & 0 \\ \vdots & & \vdots & \vdots & \vdots \\ x_n^{n-2} & \cdot & x_n & 1 & 0 \end{pmatrix} \begin{pmatrix} 1 & 0 & \cdots & 0 & 0 \\ y & 1 & \ddots & \vdots & \vdots \\ \vdots & \ddots & \ddots & 0 & \vdots \\ y^{n-2} & \cdots & y & 1 & 0 \\ 0 & \cdots & 0 & 0 & 1 \end{pmatrix} = \begin{pmatrix} \phi^{n-2}(x_1,y) & \cdot & x_1+y & 1 & 1 \\ \vdots & & \vdots & \vdots & \vdots \\ \phi^{n-2}(x_m,y) & \cdot & x_m+y & 1 & 1 \\ \phi^{n-2}(x_{m+1},y) & \cdot & x_{m+1}+y & 1 & 0 \\ \vdots & & \vdots & \vdots & \vdots \\ \phi^{n-2}(x_n,y) & \cdot & x_n+y & 1 & 0 \end{pmatrix} \tag{3.97}$$

The determinant of the second matrix at the l.h.s. is 1, so the determinant of the first matrix at the l.h.s. is the same as the determinant of the matrix at the r.h.s.. Removing the y_1 dependence in the first determinant and the x_1 dependence in the second we get two familiar objects:

$$\frac{(-1)^n}{x_1-y_1}\left(\frac{-\Delta(x_1\cdot y_n)}{\Delta(x_1\cdot x_m, y_2\cdot y_n)}\begin{vmatrix} x_1^M & \cdot & x_1 & 0 & 1 \\ \vdots & & \vdots & \vdots & \vdots \\ x_m^M & \cdot & x_m & 0 & 1 \\ y_2^M & \cdot & y_2 & 1 & 0 \\ \vdots & & \vdots & \vdots & \vdots \\ y_n^M & \cdot & y_n & 1 & 0 \end{vmatrix} + \frac{\Delta(x_1\cdot y_n)}{\Delta(x_2\cdot y_n)}\begin{vmatrix} x_2^M & \cdot & x_2 & 0 & 1 \\ \vdots & & \vdots & \vdots & \vdots \\ x_m^M & \cdot & x_m & 0 & 1 \\ y_1^M & \cdot & y_1 & 1 & 0 \\ \vdots & & \vdots & \vdots & \vdots \\ y_n^M & \cdot & y_n & 1 & 0 \end{vmatrix}\right) \tag{3.98}$$

These determinants are nothing but W-functions, but now with less arguments than we started with. So we can write eq. (3.98) as follows

$$\frac{\Delta(x_1\cdots y_n)}{x_1-y_1}\left(\frac{W_{m,n-1}(x_1\cdots x_m|y_2\cdots y_n)}{\Delta(x_1\cdots x_m, y_2\cdots y_n)} + \frac{W_{m-1,n}(x_2\cdots x_m|y_1\cdots y_n)}{\Delta(x_2\cdots y_n)}\right) \tag{3.99}$$

If we divide the whole expression by $\Delta(x_1\cdots y_n)$ we get the reduction formula.

3.6.3 Reduction algorithm

We will now show that the application of the formula derived above gives us parts of l.c.t-ordered diagrams. First we need to specify the structure of a l.c.t.-ordered diagram.

Definition Loop connection tuple

The loop connection tuple $\vec{H} = (H_1, \cdots, H_n)$ is an ordered set of objects related to the propagator denominators $p_j^2 - m_j^2 + i\epsilon = 2p_j^+(p^- - H_j)$ or $H_j = p^- - p_j^- + \frac{p_{j\perp}^2+m_j^2}{2p_j^+}$. The ordering of the tuple corresponds to consecutive ordering of the internal lines in the corresponding loop in a Feynman diagram.

We will use the terminology of "lines" when we mean the corresponding momentum or energy, or state. There is some arbitrariness in the definition of the momenta in the loop, but in the objects of interest $H_i - H_j$ this arbitrariness is gone because they are invariant under a shift of the loop momentum ($p^\mu \to p^\mu + a^\mu$). The expression $H_i - H_j$ is the total incoming $\sum P_{ext}^-$ momentum minus the on-shell values of the minus-momenta of the internal lines $p_{i,on-shell}^- + p_{j,on-shell}^-$, calculated with the help of $p_{i,j}^+$ and $p_{i,j}^\perp$. (See also sect. 3.2.2.)

Definition Backward and forward

A line i of the loop connection tuple is going backward if the object H_i has a positive imaginary part and is going forward if it has negative imaginary part. Thus in the Feynman diagram above, eq. (3.78), $H_1, \cdots, H_m$ are going forward and $H_{m+1}, \cdots, H_N$ are going backward. The sign of the imaginary part is opposite to the sign of the on-shell energy of the particle, therefore this definition of backward and forward coincides with the causality condition: positive-energy particles go forward in l.c. time and negative-energy particles go backward in l.c. time.

Definition Early, late and trivial events

An early event is a vertex between a backward and a forward going line, a late event is a vertex between a forward and a backward going line, if one goes around the loop in the order corresponding to the connection tuple. All other vertices are trivial events.

There are equal numbers of early and late events.

Definition Flat loop diagrams

A flat loop diagram has one early (and thus one late) event.

Definition Crossed loop diagrams

A crossed loop has more than one early event.

Definition Skeleton graph

A skeleton graph is the tuple of signs of the objects H_i of a connection tuple. It is given by the mapping $\{H_1, H_2, \cdots, H_n\} \to \{\sigma(\mathbf{Im}H_1), \sigma(\mathbf{Im}H_2), \cdots, \sigma(\mathbf{Im}H_n)\}$. The function σ is the sign function.

For different external momenta in the Feynman graph we have a different set of skeleton graphs, and for each Feynman diagram there are a number of skeleton graphs. For each sector (associated with a specific number of poles above and below the real axis) of the loop momentum p^+ there is a skeleton graph, thus for a loop with n lines there are $n-1$ skeleton graphs.

The skeleton graph already tells us the general features of the l.c.t.-ordered diagrams which are contained in a Feynman diagram, because it tells us the direction of the internal lines. This is used as our guide how to take "time-slices" of the Feynman diagram. The direction of a line tells us in which order we can encounter events (vertices). Early and late events correspond to sign changes in the skeleton graph.

Definition Causally connected events

Two events are causally connected if they lie on the same loop and there are neither early nor late events lying in between.

So, two causally connected events are connected by parts of a loop that consist of lines that are either all forward or all backward.

Remark

Clearly, it makes sense to say that causally connected events are ordered in l.c. time. If we follow a loop in the direction given by the orientation defined by its connection tuple, then we will encounter forward and backward going lines. If two vertices are connected by a forward line, they are said to be ordered in l.c. time in the same way as they are ordered in the loop. Otherwise their order in l.c. time is the reverse of their order in the loop. This partial ordering, which is given by the skeleton graph, is obviously not complete. Only causally connected events are mutually ordered this way, but not with respect to other events.

Note that we don't make any statements here about reducible Feynman diagrams, which is a completely different story. Our causally unconnected parts connect up a later time, so they are parts of the same irreducible Feynman diagram.

Definition Simultaneous

Two parts of a skeleton graph are said to be *simultaneous* if they do not share events that are causally connected.

Remark

The flat box that we discussed in sect. 3.2 consisted of a late and an early vertex, connected by two distinct parts of the loop, one consisting of lines graded $+$, the other of lines graded $-$. The relative l.c.t.-ordering of the events on these two parts is not necessarily determined by the skeleton graph, but application of the reduction formula, eq. (3.90), produced immediately the two possible l.c.t. orderings. The diagrams found showed the expected energy denominators.

In situations where two simultaneous parts occur, the reduction formula does not provide immediately the l.c.t.-ordered diagrams. An example was given in sect. 3.2.1. From the point of view of l.c. time ordering, one expects diagrams to occur corresponding to all relative l.c.t. orderings of simultaneous parts. In momentum-energy language this means that diagrams with certain energy denominators should occur. Indeed, this is the content of the next theorem.

Theorem Simultaneous parts come in all combinations.

Remark

The proof of this theorem relies again on a recursion. First we suppose that we have two simultaneous parts, that are already ordered by themselves, but not mutually. Both parts correspond to sets of energy denominators, say $\{\alpha\}$ and $\{\beta\}$. So we have the two distinct TOD's $\Pi\alpha_i^{-1}$ and $\Pi\beta_j^{-1}$. In this language the content of the theorem can be written as $\{\{i_k, j_k\}_k | [\{i_k, j_k\} \neq \{i_{k+1}, j_{k+1}\}] \wedge [k < l \Rightarrow (i_k \leq i_l) \wedge (j_k \leq j_l)]\}$

$$\prod_{i=1}^{m} \alpha_i^{-1} \prod_{j=1}^{n} \beta_j^{-1} = \sum_{\text{all } i_k, j_k} \prod_{k=1}^{m+n} (\alpha_{i_k} + \beta_{j_k})^{-1}. \tag{3.100}$$

Proof

We apply the formula:

$$\prod_{i=1}^{m} \alpha_i^{-1} \prod_{j=1}^{n} \beta_j^{-1} = \frac{1}{\alpha_m + \beta_n} \times \left[\prod_{i=1}^{m-1} \alpha_i^{-1} \prod_{j=1}^{n} \beta_j^{-1} + \prod_{i=1}^{m} \alpha_i^{-1} \prod_{j=1}^{n-1} \beta_j^{-1} \right] \tag{3.101}$$

We can apply this algorithm recursively to obtain $\binom{n+m}{m}$ TOD's with energy denominators of the form $\sum \alpha_i + \sum \beta_j$. If the product consists of more than two TOD's we can apply this algorithm recursively, to two TOD's at a time, since it is associative.

The expressions obtained are composite energy denominators:

$$(P^-(\alpha) - H_0(\alpha)) + (P^-(\beta) - H_0(\beta)) = P^-(\alpha \cup \beta) - H_0(\alpha \cup \beta). \tag{3.102}$$

3.6.4 Reduction of Feynman diagrams

The previous sections were mainly concerned with algebraic identities. Now we turn to the general strategy of the reduction. The reduction algorithm for a flat loop is straightforward as we noted when we discussed simultaneous parts. The trivial vertices come in all orderings of vertices on the forward line ($\mathbf{Im}H < 0$) with respect to those on the backward line ($\mathbf{Im}H > 0$). The vertices on one line are already ordered with respect to each other by the skeleton graph.

Starting with the early event one can reduce the lines next to the early event. This algorithm ends and gives 2^{N-2} TOD's if the loop is flat for all skeleton graphs. For each skeleton graph there are $\binom{N-2}{m-1}$ TOD's.

Mapping

The mapping from a recursive algorithm to a time-ordered theory is straightforward for the flat loop. The order in which the poles H_i are removed in the reduction formula is the same as the time ordering. We refer to this reduction as time ordered reduction.

A flat Feynman diagram gives the topology of all TOD's contained in it and all combinations between trivial events appear respecting the causal order. Conservation of p^+-momentum determines whether a trivial vertex is an absorptive or emissive event. However, this is not a new element, because we have seen that a skeleton graph is determined by the external lines besides the value of the plus-component of the loop momentum. Of course, early events absorb external particles while late events emit them.

Because Feynman diagrams form the basis of our treatment of light-front field theory, the basic elements we are concerned with are the single particle propagators and the vertices derived from the underlying Lagrangian. The interaction $\mathcal{H}_{int}$ is derived from $\mathcal{L}_{int}$ with an additional phase-space factor $\left(\sqrt{2^N p_1^+ p_2^+ \cdots p_N^+}\right)^{-1}$ where the longitudinal momenta of all the lines from a vertex are included. A wave function must also be multiplied with the phase factor, as compared to the covariant wave function.

For the success of our reduction algorithm the details of $\mathcal{L}_{int}$ are of minor importance. The algebra is connected to plus-momentum flow in loops. The only internal lines in the diagram of interest are those in the loop, how momentum is extracted from and added to the loop is of less importance.

The most important feature of the reduction algorithm is the fact that it always starts from an early state with positive longitudinal momentum (there is always an early state as the result of momentum conservation), so we exclude "vacuum"-type diagrams.

First, reduction is performed on the skeleton graph starting from the early events, *i.e.*, removing lines directly connected to the early events. This can be followed by removing poles corresponding to consecutive pieces of the loop until a late vertex is reached. This is the point where $W_{m,n}/\Delta$ is reduced to a sum of terms of the form $W_{j,1}/\Delta'$ or $W_{1,k}/\Delta''$. Secondly, the simultaneous-parts theorem is applied to write all these terms as sums of terms containing true energy denominators

Because we could have started the reduction from the late vertices in stead of the early ones, we see that the algorithm can be written in different ways. The final result, however, is the same. The same is true, *mutatis mutandis*, for the application of the simultaneous-parts theorem.

So we peel off more and more of the Feynman diagram in a manner which is locally (for causally connected events) equal to time ordered reduction.

The relation of the results of the reduction process to l.c.t.-ordered diagrams in the crossed loop case is more complicated than in the case of a flat loop. The simple heuristic of cutting lines representing constant l.c. time surfaces leads to a more elaborate bookkeeping in the crossed-loop case. This is so, because only the global structure of the Feynman diagram determines which simultaneous parts are joined by early or late vertices. The general strategy proposed here is to start at an early vertex, use the reduction algorithm locally until a late

vertex is attained. This procedure is to be repeated until all late vertices have been processed. Next apply the simultaneous-parts theorem repeatedly.

Extension mapping

Multi-loop diagrams can be reduced one loop after another. The loop momenta that are not integrated over are kept fixed. The skeleton graph tells us again what is the general form of the time-ordered diagrams. Therefore, the skeleton graphs, associated with different finite domains in p^+-space need to be determined first.

Upon application of the reduction algorithm to the first loop, energy denominators occur that are combinations of two propagator poles. When the next loop is treated, some poles come from those energy denominators, while the others are due to propagator poles occurring in the part of the original Feynman diagram unaltered by the reduction so far. These different types of poles play the same role in the integration over the next variable. The pole is again the difference of the p^--flow and the on-shell energies from the poles and their associated lines in the Feynman diagram. The question which lines must be combined to generate energy denominators is related to the imaginary parts of the propagator poles and thus answered when the skeleton graph is determined. During the reduction process these combinations remain fixed.

The integration is invariant under coordinate transformations and reordering of the integrations. The mapping from a recursive algorithm to a l.c.t.-ordered approach is more complicated here than in the single-loop case, but in essence the same. The most complicated task is the construction of the skeleton graphs. After this job is done, the reduction algorithm is applied to one loop after another, and the interpretation of the result is the same as in the case of one loop.

Theorem Spectrum condition

The spectrum condition $p^+ \geq 0$ holds for all particles in the internal loops of the Feynman diagram.

Proof

The spectrum condition follows from two ingredients. First, at any vertex there is conservation of four-momentum, in particular plus-momentum. Secondly, lines with negative p^+, anti-particle lines, can be reinterpreted as particle lines with positive p^+ by reversing the direction of the four momentum on such lines. This reversal is in agreement with four-momentum conservation and l.c.t. ordering. This statement is not completely trivial; the time ordering must coincide with the p^+ flow through the diagram.

3.6.5 Methods of proof

In the sections above we have not given complete proofs for general cases. We restricted ourselves in writing down the rules along which a proof can proceed in each specific case. As proven above, each rule is an algebraic relation, such as eqs. (3.78), (3.90), and (3.100). The set of rules defines an algorithm (Bergstra & Klop, 1989), which reduces a specific diagram to the required time-ordered form. A rule is used to replace an expression by another expression at all places where the first expression is found. This process is defined iteratively and recursively. Such an algorithm is valid as proof when it stops at and only at the final form and this form is unique. This unique form is the complete set of time-ordered diagrams associated with

each Feynman diagram. Therefore it should only be possible to apply the rule at one of the subexpressions of the total expression at each stage of the calculation.

When a rule can be applied at different places at the same time we end up with different intermediate results and it will be hard to check whether these will lead to the same final answer. If the regions in which the rules can be applied are disconnected the problem of the simultaneous application is easily cured, since the application of both rules will lead to an unique answer independent of the order in which the rules are applied. When two rules can be applied to overlapping regions of the same expression we have a more serious problem. After applying one rule, the other rule cannot be applied anymore and we have two distinct intermediate results of which it will be hard to check whether they lead to the same final answer.

In our case we supplied each rule with a priority. We ordered the rules. If two rules can be applied at the same time the rule with the highest priority is applied first. Therefore the order in which the rules are applied is unique and the final answer is unique. Whether the final answer is correct can only be inferred from the correctness of the rules at each step of the calculation. As we are not able to show the equivalence between a Feynman diagram and some definite set of time-ordered diagrams, we must be satisfied with an indirect proof. That is, we conjecture that the local properties of the diagram uniquely determine its global properties. The local properties, such as the spectrum condition, are maintained by each step of the algorithm. For a number of examples this conjecture holds. For these examples it was simple to determine the complete set of time-ordered diagrams. It was found that these time-ordered diagrams coincided with the diagrams obtained using the algorithm.

3.7 Discussion

We have established the degree of equivalence between light-cone-time ordered perturbation theory and covariant perturbation theory for spin-0 and spin-1/2 particles. This effort might seem superfluous since the connection between ordinary time-ordered perturbation theory and covariant perturbation theory is well established (Feynman, 1949). One might be tempted to believe that the methods that work in the case of ordinary time-dependent perturbation theory apply to the l.c.t.-ordered theory too. This belief belongs to folklore. In practice the understanding of light-front field theory is growing only slowly. Basic results in covariant field theory were obtained in light-front field theory along a path through much trial and error. It took years to formulate a proper light-front version of the Schwinger-model (McCartor, 1988; Heinzl et al., 1991a) and to prove spontaneous symmetry breaking in the light-front version of ϕ^4 (Pinsky & van de Sande, 1994; Heinzl et al., 1992; Heinzl et al., 1991b; Robertson, 1993). The renormalization of light-front versions of known covariant, renormalizable field theories is still an unsolved problem (Perry, 1993; Perry, 1994b; Perry & Wilson, 1993; Głazek & Wilson, 1993). In general, approaches are followed that are specially tuned to the problems of light-front field theory. Therefore it turns out to be difficult to relate the solutions obtained to basic results in covariant field theory (Thorn, 1979; Mustaki et al., 1991).

In chapter 5 we present a method for renormalization which gives covariant results and a proper interpretation of the longitudinal singularities. That chapter forms the final part in the proof of equivalence between the light-front perturbation theory and the covariant perturbation theory.

4

A different approach to dimensional regularization

In this chapter we investigate dimensional regularization and the features which make it stand out against all other regularization schemes. If we want to use the useful features of dimensional regularization for time-ordered theories we will need to reformulate the scheme. The ordinary scheme depends heavily on the use of covariant perturbation theory, in the form of Feynman diagrams, and Feynman parametrization of the integrands. In the case of time-ordered theories we cannot use these techniques.

Dimensional regularization can be formulated such that integrands of divergent integrals are algebraically related to each other; associated with each integrand with an arbitrary degree of divergence there exists an integrand which is logarithmically divergent and has the same finite part. For the treatment of logarithmically divergent integrals different methods can be used. The pole subtraction in dimensional regularization actually deals only with these logarithmic divergences. However, the pole subtraction turns out not to be useful for time-ordered theories for the reasons given above. Logarithmic divergences are easy to cope with since different renormalization schemes will yield results that differ at most a constant.

The regularization method derived in this chapter has practical values. In time-ordered theories expressions tend to get out of control. The regularization derived is straightforward and can be implemented in a computer program which does algebraic manipulations. The integrals which need to be calculated numerically are finite and relatively well behaving. In this chapter we deal with the nucleon self-energy as an example.

4.1 Introduction

Dimensional regularization ('t Hooft & Veltman, 1972) is used routinely nowadays for manifestly covariant formulations of relativistic quantized field theories, notably gauge theories.

It is well known that the basic procedure of dimensional regularization is the continuation of integrals in dimension space. Divergencies which occur as poles at the physical dimension, are subtracted. Despite its popularity, dimensional regularization remains somewhat mysterious, since it is difficult to attach a physical meaning to a non-integer dimension space. The result

of writing divergent integrals in perturbation theory as functions of the space-time dimension d are expressions that have poles for integer values of d starting from the dimension of the loop space where the integral diverges logarithmically. In between those poles the integrals attain finite values, which is counterintuitive. One would expect an interpolating formula such that the degree of divergence rises monotonously when d increases from the value where the integrals diverge logarithmically.

If one examines the procedure of dimensional regularization in more detail, one finds that there are indeed infinities that do not occur as poles in d. Those are the surface terms which occur upon partial integration and are discarded. These parts are $pure\ numbers$. Removal of the surface terms is a purely algebraic procedure and based on dimensional analysis. The remaining poles in dimension space at each of the dimensions where the original integral is divergent, are the residual logarithmic divergences which cannot be treated using dimensional analysis. The actual regularization deals only with the subtraction of the latter divergences.

We introduce a procedure where this algebraic nature of the procedure of lowering the divergences to logarithmic ones comes about naturally and shows its close connection with dimensional analysis. Because our formalism differs in some respects from conventional dimensional regularization, the fact that the results of our method agree with those obtained using dimensional regularization, sheds some new light on the nature of dimensional regularization: is it an analytical or an algebraic procedure (de Wit & Smith, 1986)?

Our motivation is mainly practical. We wish to apply the results to Hamiltonian field theory. Although Hamiltonian field theory is more difficult and less elegant than the covariant approach, the physics is more transparent. Indeed, for the calculation of bound states, which goes beyond the realm of perturbation theory, the clear physical picture provided by the Hamiltonian method, is a handle to hold on to.

In particular we have in mind light-front field theory, but we will show below that our formalism can be used for ordinary time-ordered theories ("old-fashioned perturbation theory") as well. In these cases we cannot use the machinery designed for Feynman diagrams due to the presence of, $e.g.$, square roots (like $\sqrt{p^2+m^2}$) in ordinary time-ordered field theory, or hyperbolic forms (like $p^{-1} \pm p$) in light-cone time-ordered theory. We cannot use Feynman parametrization, Wick-rotation and the limited table of dimensionally regularized integrals.

Often, the behavior of integrals is argued on the basis of a dimensional analysis. In the case of manifestly covariant expressions, this analysis is based on the Euclidian forms of propagators after a Wick rotation has been performed. Our method has the novel property that it can be applied to expressions that are not manifestly covariant. This is of interest especially for light-front field theory where one separates longitudinal and transverse dimensions.

Nowadays, most authors are only interested in singularities of Green's functions in configuration space and their renormalizability. These singularities are independent of the masses occurring. As the expressions become simpler in massless theories, and results can be derived which cannot be obtained in massive theories, they use effective massless theories with the same high-energy behavior. We have the opposite interest; we would like to know the behavior in the physical range of the (effective) theory; in the range of the masses that occur. Therefore we need a method which can remove the divergences irrespectively of the (complicated) form of the integrands, and would also allow for numerical implementation. This method turns out to have a close relation to the BPHZ scheme (Hepp, 1966; Speer, 1967; Hahn & Zimmermann, 1968; Zimmermann, 1968; Zimmermann, 1969; Caswell & Kennedy, 1982), where also finite integrals are obtained. BPHZ became in disuse due to computational difficulties not

shared with dimensional regularization. We feel that our reformulation combines the elegance of dimensional regularization with the advantages of BPHZ.

For completeness we mention the work of Symanzik (Symanzik, 1981) who performed a related investigation of the divergences of field theories with boundaries, which can be applied to Schrödinger-like field theory where the boundaries act as initial and final time surfaces. Note that in standard time-ordered perturbation theory these surfaces are absent (see sect. 4.4).

Before the regularization described in this chapter can be applied to light-front field theory some additional investigations are required. This will be done in the next chapter.

The organization of this chapter is as follows. After a very brief section where we discuss our point of view on renormalization, section 4.3 describes our method, and in section 4.4 we reformulate it for time-ordered perturbation theory. The next section is devoted to overlapping divergences. The relation with dimensional regularization is described in section 4.6. A novel way to deal with the logarithmic divergences is given in section 4.7, illustrated with one example. We discuss the application to gauge theories in the next section. In section 4.9 we treat the nucleon self-energy, where we regularize separately the forward and backward diagram through local subtractions. Independently, the diagrams are non-covariant and give rise to different corrections to the off-shell propagator. The main part ends with some concluding remarks. Finally, some technical details are given in an appendix.

4.2 Renormalization

Renormalization is the procedure of subtracting divergent, hence meaningless, terms from a perturbative expansion, at the same time motivating this procedure by including the subtracted parts in an infinite rescaling of the parameters that occur in the theory. The physical values of the parameters are observed but turn out not to be the values which are related to the free theory: Interaction does not only create the possibility of scattering but also "dresses" free particles and "screens" the charges. This effect changes the charge and the mass by an infinite amount, but fortunately this is largely concentrated at the position of the bare particle. So we can redefine the bare particle as the bare particle which includes these infinite effects, at each order in perturbation theory.

Because these effects are infinite, they are hard to handle. The infinities occur in a perturbative expansion defined in terms of integrals over momentum space. In momentum space the idea of a local interaction is abstract, usually understood as a number times a polynomial in the momenta. This makes the subtraction principle also slightly abstract: What is an infinite number times a polynomial in terms of a divergent integral? Usually one introduces a regularization which makes the theory finite. The regularization depends on a parameter and the regularized expression can be separated into a finite part and a part that grows without bounds when the regularization is removed. The growing part must be, or converge[1] to, a local expression. This part is subtracted using a *regulator*. The success of a regularization depends largely on which properties (*e.g.*, covariance, gauge invariance) are invariant under regularization. Dimensional regularization turned out to be the most successful one ('t Hooft & Veltman, 1972), (Bollini & Giambiagi, 1972), (Leibbrandt, 1975), (Muta, 1987). It uses

[1]Some authors tend to attach some physical meaning to the convergence to a local expression. However, the convergence only exists within the mathematical framework of regularization and it is rather meaningless since it becomes multiplied with an infinite number.

analytical continuation in the dimension of the integral, and separates the divergent numbers associated with the local parts as a pole in dimension space.

A disadvantage of dimensional regularization is that it still needs regulators, and does not render the theory finite like BPHZ does. In BPHZ the integrands are made finite and the counterterms are automatically subtracted (Collins, 1984). The core of BPHZ is the Taylor expansion in the external momenta, such that the local parts associated with the polynomials in external momenta are found and subtracted, rendering the integrals finite.

Dimensional regularization has always been associated with Feynman diagrams and Feynman integrals; it does not simply allow the inclusion of wave functions and it does not work for time-ordered Hamiltonian theories. Especially for the use in Hamiltonian perturbation theory we want to create a happy marriage between BPHZ and dimensional regularization.

4.3 Dimensional analysis

In a perturbative expansion of field theory by means of Feynman rules only a limited number of objects occur in an arbitrary diagram. For these objects (*i.e.*, propagators, vertices) we can write down a *dimensional operator* of which the propagators are eigenfunctions with their dimension as eigenvalue. This operator is

$$D + \nabla. \tag{4.1}$$

D contains the external variables, masses and external momenta, and ∇ is a similar operator for loop momenta[2]. The explicit forms of these objects are:

$$D = \sum_i p_i^\mu \frac{\partial}{\partial p_i^\mu} + \sum_j m_j \frac{\partial}{\partial m_j}, \tag{4.2}$$

$$\nabla = \sum_{i=1}^{n} k_i^\mu \frac{\partial}{\partial k_i^\mu}. \tag{4.3}$$

The corresponding eigenvalues are given by the relations:

$$(D+\nabla)\frac{1}{p^2-m^2} = -2\frac{1}{p^2-m^2}, \tag{4.4}$$

$$(D+\nabla)\frac{\not{p}+m}{p^2-m^2} = -1\frac{\not{p}+m}{p^2-m^2}, \tag{4.5}$$

where p is a linear combination of the internal and external momenta.

Other objects, like vector-boson propagators and derivative couplings are also eigenfunctions of the dimensional operator, but we will consider the simple case of fermions and bosons without derivative couplings. The extension to derivative couplings is trivial. Any integrand or part of an integrand, $I_\mathcal{G}$, defining a Feynman amplitude, is an eigenfunction of the dimensional operator and the eigenvalue, $\Gamma_\mathcal{G}$, is obtained by simple power counting:

[2]Throughout this chapter we will use p for external momenta and k for loop momenta.

$$(D+\nabla)I_{\mathcal{G}} = \Gamma_{\mathcal{G}} I_{\mathcal{G}} = -(2 \text{ number of boson lines } + \text{ number of fermion lines }) I_{\mathcal{G}}. \quad (4.6)$$

Obviously, in d-dimensional space the integral is convergent only if $d + \Gamma_{\mathcal{G}} < 0$. We can also use partial integration to rewrite an integrand. The divergence of an integral is the leading behavior of the integrand as the loop momenta tend to infinity. The divergence depends on the dimension of the space. In dimensional regularization partial integration is used to extend the domain of convergence in dimension space of an integral. Then surface terms occur that satisfy the equation

$$\text{surface term } = 1 + \frac{1}{n_{\mathcal{G}}\ d}\nabla, \quad (4.7)$$

where $n_{\mathcal{G}}$ is the number of loops in the integrand $I_{\mathcal{G}}$, d is the dimension of the space. 't Hooft and Veltman ('t Hooft & Veltman, 1972) call this the *partial* k operation. Generally, the surface term of the sphere at infinity is neglected, although not all authors using dimensional regularization mention this. We will discuss the neglect of the surface term at some length in the section on dimensional regularization (sect. 4.6), and only say here that the physics should not depend on what happens at infinite values of the loop momenta. The dimensional operator and the partial k operation form the fundamental tools of this chapter.

If we set the surface term equal to zero and insert eq. (4.7) in eq. (4.6), then we obtain the degree of divergence $\delta_{\mathcal{G}}$ of $I_{\mathcal{G}}$:

$$DI_{\mathcal{G}} = \delta_{\mathcal{G}} I_{\mathcal{G}} \equiv (n_{\mathcal{G}} d + \Gamma_{\mathcal{G}}) I_{\mathcal{G}}. \quad (4.8)$$

Note that the l.h.s. is less divergent than the r.h.s. The equality sign only implies that the finite parts of the integrals are the same. It is possible to extend this equation in such a way that it includes different orders in perturbation theory (see sect. 4.11.1).

Formula (4.8) can also be applied to an arbitrary part of an integrand. Then only the momenta k corresponding to loops which are fully contained in such a part are treated as internal variables, all other momenta are treated as external variables. The degree of divergence depends on which part of the integrand is selected, and thus over which integration variables integration is performed. (We expect the reader to identify the proper divergent parts of a diagram. A detailed discussion of subdiagrams and divergences can be found in (Collins, 1984; Caswell & Kennedy, 1982).) For each part $\mathcal{G}'$ taken from a diagram $\mathcal{G}$, such that $\mathcal{G}' \subset \mathcal{G}$, the integrand $I_{\mathcal{G}}$ factorizes into two parts: $I_{\mathcal{G}} = I_{\mathcal{G}'} I_{\mathcal{G}\setminus\mathcal{G}'}$. The dimension is additive and the number of loops is exclusive additive:

$$n_{\mathcal{G}} d + \Gamma_{\mathcal{G}} = (n_{\mathcal{G}'} d + \Gamma_{\mathcal{G}'}) + (n_{\mathcal{G}\setminus\mathcal{G}'} d + \Gamma_{\mathcal{G}\setminus\mathcal{G}'}) + (n_{\mathcal{G}} - n_{\mathcal{G}\setminus\mathcal{G}'} - n_{\mathcal{G}'}) d \quad (4.9)$$

The last term contains the number of loops that are cut to separate $\mathcal{G}'$ from $\mathcal{G} \setminus \mathcal{G}'$. To find all the divergences in the general case is a difficult combinatorial problem. In order to prove renormalizability of a theory, it is necessary to deal with that problem. However, as long as the way to deal with divergences is straightforward, we will not need this machinery.

The integrand on the l.h.s. of eq. (4.8) has a lower degree of divergence than the integrand on the r.h.s. If one allows the space to have an arbitrary number of dimensions, eq. (4.8) is a simple way to obtain eqs. (13), (26) and (31) in ('t Hooft & Veltman, 1972). If the integral

is logarithmically divergent, $\delta = 0$ (or $\delta = n(d-4)$ if we have an arbitrary dimension), then eq. (4.8) is homogeneous, $DI = 0$. Higher order divergences can always be related to lower order divergences. Applying the D-operation twice does not decrease the divergence since the differentiation of the second D acts on the momenta occurring in the first D, keeping the degree the same. To decrease the divergence at every application of D we must place all momenta and masses to the left of all differentiations. We call this the *normal-ordered D-operation* which can be obtained in a relatively simple way from the ordinary D-operation. The definition is

$$\begin{aligned} :D^m: &\equiv D(D-1)\cdots(D-m+1) \\ &= \sum p_{i_1}^{\mu_1}\cdots p_{i_l}^{\mu_l} m_{j_{l+1}}\cdots m_{j_m} \frac{\partial^m}{\partial p_{i_1}^{\mu_1}\cdots\partial p_{i_l}^{\mu_l}\partial m_{j_{l+1}}\cdots\partial m_{j_m}} \ . \end{aligned} \tag{4.10}$$

The sum runs over all combinations of external momenta and masses. This immediately relates any divergent integral, with degree of divergence say δ, to a logarithmically divergent integral:

$$:D^s:I = \frac{\delta!}{(\delta-s)!}I, \tag{4.11}$$

$$:D^\delta:I = \delta! I, \tag{4.12}$$

$$:D^{\delta+1}:I = 0. \tag{4.13}$$

Similar formulae are obtained in dimensional regularization by continuing the dimension to non-integer values. Therefore the factorials are usually written as gamma functions. In our derivation we keep the dimension d fixed and integer.

The relations above relate expressions with different degrees of divergence. The terms with higher order divergence are equal to terms with lower order divergence up to *homogeneous terms* of the D-operations, which are polynomials in the external momenta and the masses, up to order δ. The polynomials are the local expressions mentioned before; they are subtracted in a renormalization prescription. The D-operation removes the divergences which are local and thus automatically regularizes the expression. If we succeed to remove the logarithmic divergences we have a renormalization prescription without regulators. We will discuss the logarithmic divergences in a later section (sect. 4.7). In a renormalizable theory the subtracted parts can be written as terms in the original Lagrangian with infinitely rescaled parameters, *e.g.*, masses and coupling constants. Which counterterms are necessary, and whether they are generated by the original Lagrangian, can be analyzed separately by standard dimensional analysis and has not much to do with the actual subtraction, apart from problems with anomalies.

As long as our operations act on integrands, we encounter local counterterms only. As soon as integrals are performed, we obtain nonlocal[3] expressions of the same degree as the counterterms. So if we subtract parts of the *integrand* we preserve locality. A similar procedure is followed in BPHZ renormalization. The D-operation should commute with the integration,

[3]The discussion of the locality of counterterms has always been rather formal, we are no exception. Locality and momentum space are on different sides of the same coin: one can look at one side at a time only.

therefore the homogeneous relation eq. (4.13), should hold for the amplitude. Indeed, we see that this is true for the ϕ^3 one-loop self-energy (see sect. 4.11.2):

$$D\left(\text{constant } -\sqrt{\frac{p^2-4m^2}{p^2}}\text{arctanh}\sqrt{\frac{p^2}{p^2-4m^2}}\right)=0, \tag{4.14}$$

which expresses the fact that the amplitude has the proper dimension.

As mentioned before one sees that the integration leads to non-local terms (non-polynomial expressions) which also vanish under differentiation, which shows some of the subtilities of locality. In the divergent integral the constant is infinite. Renormalization in this case means changing the constant: changing the infinite constant into a finite constant, and reabsorbing the infinite part in the definition of the Langrangian. A finite renormalization (oversubtraction) may change the value of the finite constant.

4.4 Time-ordered perturbation theory

Since the D-operation contains only external momenta it should commute with integrations in general. In the case of time-ordered diagrams (Heitler, 1954) or "old-fashioned perturbation theory" (Weinberg, 1966) or theories formulated in terms of Goldstone diagrams (Koltun & Eisenberg, 1988), we can derive the same relation. In diagrams occurring in time-ordered perturbation theory the loop momenta do not contain the energy variable, so we need to introduce a new operation in this case, that we call $\overline{\nabla}$, defined as:

$$\overline{\nabla}=\sum_j \vec{k}_j\frac{\partial}{\partial\vec{k}_j}, \tag{4.15}$$

which does not contain the energy-components of the loop momenta k_j. The operator partial k, eq. (4.7), also changes since now the dimension is one less than in the covariant case:

$$1=-\frac{1}{n\ (d-1)}\overline{\nabla}. \tag{4.16}$$

Again we set the surface term equal to zero.

If we take the integrand of the integral corresponding to an arbitrary time-ordered diagram, we see that indeed it is an eigenfunction of the dimensional operator $D+\overline{\nabla}$, because all the factors that appear in a time-ordered diagram are either linear or square roots of quadratic expressions (schematically):

$$\begin{aligned}(D+\overline{\nabla})&\frac{(\not{p}_1+m_1)\cdots(\not{p}_r+m_r)}{E_1\cdots E_m(p_1^0-E_{1_1}-E_{1_2})\cdots(p_s^0-E_{s_1}-E_{s_2})}\\ &=\overline{\Gamma}\frac{(\not{p}_1+m_1)\cdots(\not{p}_r+m_r)}{E_1\cdots E_m(p_1^0-E_{1_1}-E_{1_2})\cdots(p_s^0-E_{s_1}-E_{s_2})}.\end{aligned} \tag{4.17}$$

Where $\overline{\Gamma}$ is also given by simple counting arguments:

$$\overline{\Gamma}=-\#\text{lines } -\ \#\text{intermediate states } +\ \#\text{spin projections}. \tag{4.18}$$

The lines account for the phase-factors E_j^{-1}, the energy denominators $(p_j^0 - E_{j_1} \cdots E_{j_n})^{-1}$ are given by the intermediate states. If we now apply the partial $\vec{k}$ operation, eq. (4.16), we find for the time-ordered diagram the same degree δ as we would find for a covariant diagram that has the same topology, because the number of intermediate states equals the number of lines minus the number of loops. Thus:

$$DI_{\mathrm{time-ordered}} = \delta I_{\mathrm{time-ordered}}, \tag{4.19}$$

with the same merits as in the covariant case. One can obtain time-ordered diagrams from Feynman diagrams through integration over the intermediate energies, as we have seen in chapter 3. The residues obtained from contour integration satisfy the same relation, eq. (4.18), but the δ occurring is not the degree of divergence of each residue separately. Each residue restricts k to an on-shell value determined from $(p+k)^2 = m^2$, therefore the k^2 terms are of the same order of divergence as the $p \cdot k$ terms. The l.h.s. as well as the r.h.s. contain higher order divergences which are not lowered by the D-operation because the leading order terms in the denominator are $p \cdot k$ which are not altered by the D-operation:

$$D\frac{1}{p^2 + m^2 + p \cdot k} = -\frac{1}{p^2 + m^2 + p \cdot k} + \text{lower order terms} \tag{4.20}$$

The lower order terms tend to zero faster than $|p \cdot k|^{-1}$, which is the behavior of the leading order term. Only after recombining the residues in such a way that time-ordered diagrams emerge, these higher-order divergences cancel and the D-operation lowers the divergence. If we consider, for example, the scalar loop, we will see that this happens. The Feynman diagram is given by:

$$\int \mathrm{d}^4k \frac{1}{((p+k)^2 - m^2 + i\epsilon)(k^2 - m^2 + i\epsilon)}. \tag{4.21}$$

The residue of the pole at $k^0 = \sqrt{\vec{k}^2 + m^2}$ is

$$-2\pi i \int \mathrm{d}^3k \frac{1}{2\sqrt{\vec{k}^2 + m^2}\left(p^2 + 2p^0\sqrt{\vec{k}^2 + m^2} + 2\vec{p}\cdot\vec{k}\right)}, \tag{4.22}$$

which is clearly linearly divergent, but contains terms odd in $\vec{k}$. A similar expression can be obtained for the pole at $k^0 + p^0 = \sqrt{(\vec{k}+\vec{p})^2 + m^2}$. If we combine the two residues we will recover the two time-ordered diagrams with logarithmic divergences and the terms linear in $\vec{k}$ will have disappeared:

$$-2\pi i \int \mathrm{d}^3k \frac{1}{2\sqrt{\vec{k}^2 + m^2}\sqrt{(\vec{p}+\vec{k})^2 + m^2}\left(p^0 - \sqrt{\vec{k}^2 + m^2} - \sqrt{(\vec{p}+\vec{k})^2 + m^2}\right)} \tag{4.23}$$

and

$$-2\pi i \int \mathrm{d}^3k \frac{1}{2\sqrt{\vec{k}^2 + m^2}\sqrt{(\vec{p}+\vec{k})^2 + m^2}\left(p^0 + \sqrt{\vec{k}^2 + m^2} + \sqrt{(\vec{p}+\vec{k})^2 + m^2}\right)}. \tag{4.24}$$

In the case of light-cone time-ordered perturbation theory, where a light-like direction is used as "time" direction, this recombination does not occur and higher divergences remain. We analyzed renormalization of light-cone time-ordered perturbation theory in the next chapter.

In the spectator model (Gross, 1993) the same higher order divergences are present. In this model one of the lines of the Feynman diagram, with one loop, is set on-shell which is equivalent to the use the residue of one pole. The divergences do not cancel because the other poles are neglected in the spectator model.

4.5 Overlapping divergences and all that

Finding the proper counterterms for each specific diagram is a difficult problem. The problems are largely of a combinatorial nature and similar to the question of finding all the Feynman diagrams of a specific order. There are a number of authors who wrote down general formulae for counterterms (Hepp, 1966; Speer, 1967; Hahn & Zimmermann, 1968; Zimmermann, 1968; Zimmermann, 1969; Caswell & Kennedy, 1982), we will not do so. We only want to make apparent that we can reduce all the divergences to logarithmic divergences in the same way as we did in the simple case, and that this treatment does not essentially interfere with the presence of overlapping divergences or subdivergences. Our treatment is similar to the treatment of 't Hooft and Veltman, with the advantage that we do not have to discuss the nature of the regulators or whether non-polynomial parts cancel each other. To each part of a diagram we can apply the D-operation, with the stipulation that for some parts some loop momenta act as external momenta. We might have excluded parts of the integrand where these loop momenta also occur, and thus we cannot apply the partial k operation with respect to these loop momenta. The generalized D operation, which now includes those loop momenta external to the particular loop under consideration, will lower the degree of divergence of loop momenta to which we could apply the partial k operation, the degree of divergence in the other loop momenta stays the same. Picking different parts of the integrand, we can decrease all divergences to logarithmic ones.

As an example we will consider a diagram with two loops, momenta k and k', that occur in the same integrand (nested or overlapping):

$$I = I_1(k)I_2(k+k')I_3(k'), \tag{4.25}$$

with dimensions Γ_1, Γ_2 and Γ_3 respectively. On can, for instance, consider the two-loop diagram in fig. 3.11; lines 1 and 2 form I_1, the propagator of line 3 is I_2 and the lines 4 and 5 form I_3. If $\Gamma_1 + \Gamma_2 + d > 0$, and therefore the k integration divergent, we apply the operation $(\Gamma_1+\Gamma_2+d)!^{-1} : (D+\nabla')^{\Gamma_1+\Gamma_2+d} :$, which acts distributively on I_1 and I_2, to the integrand I_1I_2. This lowers the divergence in k. We can subsequently apply the operation $(\Gamma_2+\Gamma_3+d)!^{-1} : (D+\nabla)^{\Gamma_2+\Gamma_3+d} :$ to I_2I_3 and $I_2'I_3$; the two integrands obtained after the $D+\nabla'$ operation. The second operation lowers the divergence in k'. We finally apply $(\Gamma_1+\Gamma_2+\Gamma_3+2d)!^{-1} : D^{\Gamma_1+\Gamma_2+\Gamma_3+2d} :$ to the complete integrand $I_1I_2I_3$ if there are overall divergences. The reduction is done in more detail (and in another context) by 't Hooft and Veltman ('t Hooft & Veltman, 1972). The major difference with their treatment is the absence of regulators in our case. The prescription is only complete if it is supplemented with a regularization of logarithmic divergences, which we will carry out in a different section (sect. 4.7), since it is a sideline with respect to the dimensional analysis on which this lowering of divergences is based.

4.6 Dimensional regularization

To legalize in a mathematical sense the neglect of the surface term in the partial k operation we could include in the integrand a Gaussian weight:

$$I \to \hat{I} = \mathrm{e}^{-\mu k^2} I. \tag{4.26}$$

This will suppress the surface terms, and all the additional terms acquired by differentiating the weight will vanish afterwards in the limit $\mu \to 0$ and the usual results eqs. (4.11), (4.12) and (4.13) obtain. This is rather formal. We are looking for a way to relate divergent integrals to finite integrals times "poles in dimension space", a method similar to dimensional regularization. In dimensional regularization the integral can only become finite if the number of dimensions decreases. However, using less than four dimensions will interfere with the four dimensions of the external momenta. The partial k operation extends the domain on which the integral is defined and therefore it is central to dimensional regularization. We can mimic the non-integer dimension of dimensional regularization by adding a weight to the loop integral:

$$I \to \tilde{I} = (k^2)^{\frac{\epsilon}{2}} I. \tag{4.27}$$

If the divergence of the original integrand were δ, then the divergence of the integral $\tilde{I}$ is $\delta + \epsilon$. We find that the divergent integral equals a finite integral, which is an analytic function of ϵ, times ϵ^{-1}. This integral goes to infinity for $\tilde{I} \to I$:

$$\tilde{I} = \frac{1}{(\delta+\epsilon)(\delta+\epsilon-1)\cdots(\epsilon+1)} \frac{1}{\epsilon} : D^{\delta+1} : \tilde{I}, \tag{4.28}$$

This is similar to the case of dimensional regularization. To obtain the finite part we must find the term of order ϵ in the finite integral $: D^{\delta+1} : \tilde{I}$ which is:

$$\frac{1}{2} \ln k^2 : D^{\delta+1} : I, \tag{4.29}$$

since the only ϵ dependence[4] was in the weight and

$$(k^2)^{\frac{\epsilon}{2}} \sim 1 + \frac{\epsilon}{2} \ln k^2 + \mathcal{O}(\epsilon^2). \tag{4.30}$$

The integral over k is generally not invariant under a change of the loop momentum, as the position of the origin of the cut of $(k^2)^{\frac{\epsilon}{2}}$ plays a role. Integrals of the type eq. (4.29) are hard to evaluate.

The procedure described here has a resemblance to dimensional regularization, since dimensional regularization is largely based on one integral (Gradshteyn & Ryzhik, 1980):

$$\int_0^\infty \mathrm{d}k \frac{k^n}{(k^2+\alpha)^m} = \frac{1}{2} \frac{\Gamma(\frac{1}{2}(n+1)\Gamma(m-\frac{1}{2}(n+1))}{\Gamma(m)\alpha^{m-\frac{1}{2}(n+1)}}. \tag{4.31}$$

In order to use this formula, one introduces Feynman parametrization and the unique shift of the loop momentum such that the dot-product terms in the denominator vanish (Muta, 1987).

[4]The ϵ dependence in the factorials can be put in a finite renormalization similar to MS $\to \overline{\mathrm{MS}}$. The same is true for any angular integral.

This choice of the origin of the loop momenta turns out to be a good one: For $k = 0$ the denominator has it lowest value; if a threshold occurs, then the lower integration limit is always below this threshold. As a consequence, the physical content (imaginary part) of a diagram remains unchanged under dimensional regularization.

For our purposes (finite integrands without regulators), choosing a unique value for the integration variable is not a good way to proceed. Apart from difficulties with integrals one runs into a complicated discussion about the choice of integration variables and flow of the external momenta through the diagram (Wu, 1962). In our approach, every divergence is in an algebraic way related to a logarithmic divergence. In this respect it is equivalent to dimensional regularization. The regularization of the logarithmically divergent integrals should be made independent of the choice of integration variables. In sect. (4.7) we derive such a method.

4.6.1 Partial k

Many physicists, dealing with renormalization, must have dreamt, at one time or another, that *infinity* is just one point, that could be cut from the space they work in. Then the edges should be glued together. This procedure should make the theory finite and the compact version of the space should have the same symmetries as infinite space. Howerver, sheer topological complexity turns this dream into a nightmare.

Partial k preserves a bit of this idea. The surface term of the partial integration eq. (4.7) is at infinity and has the same order of divergence δ as the original integrand:

$$\int \mathrm{d}^d k I = \frac{1}{\delta} \int \mathrm{d}^d k D I + \int_{|k|=\infty} \mathrm{d}^{d-1}\Omega \; |k| I. \tag{4.32}$$

The first term on the r.h.s. has a lower divergence than the other terms. The leading order behavior is a function of the loop momentum k only, therefore one might suspect that the neglect of the surface term is precisely the omission of the meaningless divergent behavior at infinity. The surface term is a pure number since it belongs to the Ker of the D-operation. This motivates the use of the partial k operation. It remains unclear whether the shift in integration variables always leaves the finite part invariant[5]. By means of justification, we can refer to the results of dimensional regularization and some simple examples.

There is a stronger, but up-side-down, argument why this method should produce the correct answer: Assume a regularization that removes the divergent ultraviolet contributions and preserves the algebraic properties of the diagram. Then the two core formulae eq. (4.7) and eq. (4.8) are valid and our procedure is completely legitimate.

4.7 Regularization of logarithmic divergences

Although a number of schemes are available for regularization of logarithmic divergences, we will derive a different scheme which is closely related to the dimensional analysis introduced above. Logarithmic divergences constitute only a minor problem, different regularizations should differ

[5]The same is true for BPHZ.

only by a finite *constant*. Our starting point is the homogeneous equation (4.13):

$$\sum_{\text{all}} p_{i_1}^{\mu_1}\cdots p_{i_l}^{\mu_l} m_{i_{l+1}}\cdots m_{i_\delta}\left[\sum_j p_j^\mu \frac{\partial}{\partial p_j^\mu}+\sum_i m_i\frac{\partial}{\partial m_i}\right]\left\{\frac{\partial^\delta}{\partial p_{i_1}^{\mu_1}\cdots\partial p_{i_l}^{\mu_l}\partial m_{i_{l+1}}\cdots\partial m_{i_\delta}} I\right\}=0 \tag{4.33}$$

We can rewrite it as a differential operator $[\cdots]$ acting on the integrand, $I_0=\{\cdots\}$, of a logarithmically divergent integral, leading to the relation:

$$\sum_j p_j^\mu \frac{\partial}{\partial p_j^\mu} I_0 = -\sum_j m_j \frac{\partial}{\partial m_j} I_0 \tag{4.34}$$

The δ-divergent integral is differentiated δ times with respect to the external variables which yields I_0. The logarithmically divergent integrand I_0 contains δ loose indices which afterwards are contracted with the external variables to obtain the amplitude. We can relate the integrand to a convergent line integral:

$$\int \mathrm{d}^d k I_0(k,p) = -\int_{\mathcal{R}}^{p_j^\mu} \mathrm{d}p_j'^\mu \frac{1}{p_j'^\mu}\left(\int \mathrm{d}^d k \sum_j m_j \frac{\partial}{\partial m_j} I_0(k,p') + \text{constant}\right), \tag{4.35}$$

the integral on the l.h.s. is logarithmically divergent, but the integral on the r.h.s. is finite, and the lower integration limit $\mathcal{R}$ of the line integral determines the renormalization point (the freedom of finite renormalization). After the integration over k the constant must be fixed such that the amplitude disappears for $p_j'^\mu \to 0$. Since the inverse of a differential operator is not uniquely determined the line integral will introduce a spurious pole at $p_j'^\mu = 0$ if we do not subtract this part. This might be considered the fixing of the finite renormalization, which then is reintroduced by the line integral.

For the line integral we can choose a straight line from the renormalization point to the specific momenta we are considering. If we use the origin as renormalization point we can integrate over the fraction λ of the total momentum: $p_j'^\mu = \lambda p_j^\mu$ and the line integral is

$$\sum_i \int_{p_i'^\mu=0}^{p_i'^\mu=p_i^\mu} \frac{dp_i'^\mu}{p_i'^\mu} I(p_i') = \int_0^1 \frac{d\lambda}{\lambda} I(\lambda p_i). \tag{4.36}$$

Another renormalization point is given by a different lower limit in the line integral; if we choose as lower limit $\mu/|p|$, the scale will be set at $p^2=\mu^2$.

For this regularization we have separated the D operation in differentiations with respect to mass and with respect to momenta. One could imagine that a different separation would be more appropriate. For example, in the case of massless theories one could differentiate with respect to one external momentum variable and integrate with respect to another. Again we state that the different schemes can only differ by a constant as the result of the logarithmic divergence. The value of this constant is fixed by the choice of the lower integration limit. In section 4.11.3 we show that this regularization gives the same finite momentum dependent part as dimensional regularization.

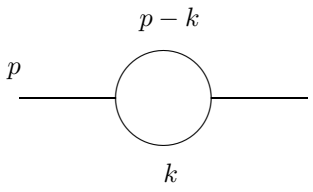

Figure 4.1: ϕ^3 self-energy loop.

4.7.1 An example: ϕ^3 self-energy

As an example of the reduction of a logarithmic divergence we will deal with the ϕ^3 one-loop self-energy diagram (see fig. 4.1), written in Feynman parameters (which are not essential but simplify the calculation):

$$\mathcal{F} = \frac{g^2}{32\pi^4}\int_0^1 \mathrm{d}x \int \mathrm{d}^4k \frac{1}{(k^2+x(1-x)p^2-m^2)^2}. \tag{4.37}$$

Differentiating with respect to the mass renders the integral finite. Note that the shift in integration variable does not interfere with the differentiation. Since the integral is finite we can perform a Wick-rotation, which accounts for an additional factor i:

$$m\frac{\partial}{\partial m}\mathcal{F} = \frac{ig^2\Omega_4}{32\pi^4}\int_0^1 \mathrm{d}x \frac{m^2}{(x(1-x)p^2-m^2)}, \tag{4.38}$$

$\Omega_4 = 2\pi^2$ is the surface area of the four-dimensional unit sphere. After we have subtracted from the integrand its value at $p=0$, we can perform the line integral. The correct imaginary part follows from the small negative imaginary part of the mass. The line integral should also respect this pole structure, therefore $\mathbf{Im}\ p^2 > 0$ for $p^2 > 0$. Thus we find with the help of eq. (4.33):

$$\mathcal{F} = -\frac{ig^2}{16\pi^2}\int_0^1 \mathrm{d}x \int_0^{p^\mu} \mathrm{d}p'^\mu \frac{p'_\mu x(1-x)}{(x(1-x)p'^2-m^2)} = -\frac{ig^2}{32\pi^2}\int_0^1 \mathrm{d}x \ln\left[\frac{m^2-x(1-x)p^2}{m^2}\right], \tag{4.39}$$

which leads to the correct amplitude eq. (4.14), see also sect. 4.11.2. The finite renormalization is fixed here such that the amplitude $\mathcal{F}$ vanishes[6] for $p^2 = 0$.

4.8 Gauge theories

In gauge theories some of the gauge symmetry is preserved at the quantum level. The Ward-Takahashi identities, and their generalizations for non-abelian theories, the Slavnov-Taylor

[6] This has nothing to do with the $p' = 0$ subtraction earlier, which removed the spurious pole.

identities, reflect current conservation on the level of Feynman amplitudes. If the proper choice of loop variables is made, the Ward-Takahashi identities are exact relations among integrands of self-energy diagrams and vertex functions of the same order. A gauge-invariant regularization should preserve these relations.

In order to show that our regularization scheme satisfies the Ward-Takahashi identities we need to prove a number of features of our scheme. First, the answer should not depend on the choice of integration variables. Second, all the operations we perform must be linear. If all operations are linear, they will preserve the algebraic relations. Third, we can choose the renormalization points of the different diagrams such that they are consistent with the Ward-Takahashi identities. If we have proven the first one, the second and third features will be technical details. However, these details clarify our approach to regularization.

If we change the integration variables, the integrals will change only by surface terms at infinity of finite integrals, which are automatically zero. Take an arbitrary integrand $I(p,k)$. Redefining the loop momentum k means that we shift it by a finite amount proportional to the external momenta: $I'(p,k) = I(p,k+\alpha p)$, where α is some real number. I' is algebraically a different expression, but I and I' differ only a total divergence since the differentiation with respect to the second argument equals a differentiation by the loop momentum:

$$DI(\cdot,k+\alpha p) \equiv p^\mu \frac{\partial}{\partial p^\mu} I(\cdot,k+\alpha p) = \alpha p^\mu \frac{\partial}{\partial k^\mu} I(\cdot,k+\alpha p). \tag{4.40}$$

If we integrate over the component of k in the direction of p, this term will only give surface contributions.

A surface contribution is not necessarily zero, since the integrals are divergent. However, if we make the integrals finite through the D operation we generate surface terms which are zero since they belong to finite integrals:

$$\int \mathrm{d}k^1 \cdots \mathrm{d}k^{n-1} \mathrm{d}k^n \frac{\partial}{\partial k^n} I(k^1,\cdots,k^{n-1},k^n) =$$

$$\int \mathrm{d}k^1 \cdots \mathrm{d}k^{n-1} \left(I(k^1,\cdots,k^{n-1},L) - I(k^1,\cdots,k^{n-1},-L) \right). \tag{4.41}$$

In the case that the original integral is logarithmically divergent, $I \sim (k^n)^{-n}$, the integral eq. (4.41) vanishes. The only surviving part is the part which is only differentiated with respect to the first coordinate. Any additional contributions due to the shift in integration variable vanishes. Because of the close connection with dimensional regularization we already expected this result.

Rather than insisting on a particular renormalization scheme, we want to argue that one can consistently choose the renormalization points, i.e., the value for which the amplitude vanishes. We have seen that the algebraic part of reducing the degree of divergence to a logarithmic one is straightforward. The treatment of the logarithmic divergence remains an issue. In practice this means that we are free to choose an additive constant for each amplitude we calculate. This is the finite renormalization. To insure gauge invariance different constants must be chosen consistently. Consider, for example, the electron self-energy and the vertex function. The Ward-Takahashi identity:

$$\Sigma(p) - \Sigma(p+q) = q_\mu \Lambda^\mu(p,p+q) \tag{4.42}$$

is the result of a similar relation among the integrands (the bold-face quantities):

$$\mathbf{\Sigma}(p,k) - \mathbf{\Sigma}(p+q,k) = q_\mu \mathbf{\Lambda}^\mu(p, p+q, k). \tag{4.43}$$

The one-loop self-energy correction, $\mathbf{\Sigma}$, is linearly divergent, hence the vertex correction is logarithmically divergent. A straightforward calculation gives

$$Dq_\mu \mathbf{\Lambda}^\mu = q_\mu (D-1)\mathbf{\Lambda}^\mu. \tag{4.44}$$

With a renormalization scale, μ, for the electron self-energy:

$$\Sigma(\mu^2) = 0, \tag{4.45}$$

the condition for the vertex correction follows from eq. (4.42):

$$q_\nu \Lambda^\nu(\mu^2, \mu^2) = 0, \tag{4.46}$$

which freezes the freedom we had for the renormalization of the vertex function.

Since our regularization scheme uses a line integral from a particular point in p, q space we fix uniquely the point where the amplitude vanishes. Lorentz invariance ensures that the amplitude vanishes for all values that are related to this point by transformation of the coordinate frame.

4.9 An application: nucleon self-energy

Most models for nucleon-meson dynamics start with a nucleon as an elementary field (Bethe & de Hoffmann, 1955). This reduces the phenomenological input of the model to the choice of an interaction Lagrangian. The predictive power of such a model is determined by the proper choice of elementary processes (diagrams). The natural treatment of the nucleon spin is one of the advantages of this approach. The price paid for this parameter-free approach are infinities due to the local interactions of the elementary fields. This problem is twofold; under renormalization we acquire higher order meson-meson interactions (Weinberg, 1967), and one needs to remove the infinities. At this point some authors (Lepage & Brodsky, 1980; Thies, 1985; Achtzehnter & Wilets, 1988; Jaroszewicz & Brodsky, 1991) argue that because the nucleons and mesons are composite particles, phenomenological form factors need to be introduced. These form factors render the integrals occurring in the Feynman diagrams convergent. Apparently, two steps are combined in this way: the theory is made finite and corrections owing to the composite nature of the particles are introduced. The question remains what are the true corrections due to the compositeness; how well is the nucleon described by an elementary nucleon surrounded by a virtual meson cloud. Another problem with the nucleon as an elementary field is the possibility to create nucleon−anti-nucleon intermediate states from a meson. If we think of the nucleon as a bound state of three quarks we realize that it is hard to create three quark−anti-quark pairs from a single meson, so such processes should be suppressed. It is difficult to determine beforehand which processes will be dominant, but one suspects low energy states to contribute the most. However, one knows that the high-energy states give an infinite (local) contribution.

Our method of regularization enables us to pursue the idea of the nucleon as an elementary field and separate the nucleon states (forward diagrams) from the two-nucleon−one-anti-nucleon states (pair diagrams) and see how much each contribute to the amplitude after the

Figure 4.2: (a) The forward diagram; (b) the backward, or Z, diagram.

amplitude is made finite through local subtractions. It turns out that the forward process is dominant but the pair-creation process is not negligible. Details depend on the type of interaction.

For low energies, as in nucleon bound states, we suspect the main contribution from temporary presence of a pion. The effective size of the nucleon is determined by the mass of the pion. The pion couples to the nucleon by pseudoscalar coupling:

$$\mathcal{L}_{\rm int} = ig\phi\bar{\psi}\gamma^5\psi. \tag{4.47}$$

In the center-of-momentum frame of the incoming nucleon the correction has the form:

$$\Gamma\Sigma(p^0)_{n\pi}\Gamma = \frac{-g^2}{32\pi^3}\sum_{\alpha=1,2}\int \mathrm{d}^3k \frac{\Gamma|\chi^\alpha(\vec{k})\rangle\langle\chi^\alpha(\vec{k})|\Gamma}{E_N E_\pi(p^0 - E_N - E_\pi)}, \tag{4.48}$$

with $E_N = \sqrt{\vec{k}^2 + m_N^2}$ and $E_\pi = \sqrt{\vec{k}^2 + m_\pi^2}$. For the local theory eq. (4.47) $\Gamma = \gamma^5$, but if one introduces dimensional constants to include in Γ a nonlocal form factor we can still treat this integral with our method. We use a slightly different definition than the standard definition of Σ because we excluded the vertices from the definition of the self-energy.

The integral eq. (4.48) is linearly divergent and non-covariant since we only include the particle state $|N\pi\rangle$ and not the two-particle one anti-particle state $|NN\bar{N}\pi\rangle$ (see fig 4.2). Therefore it might be possible that apart from the divergent local subtractions we subtract non-local terms that cancel in a covariant calculation against similar terms with the opposite sign from the $|NN\bar{N}\pi\rangle$-sector. However, these terms are local in time as the result of causality, and therefore already incorporated in the arbitrariness of the definition of the causal propagator (Bogoliubov & Shirkov, 1959). "Backward" and "forward" refer to the space-time formulation of field theory, these two processes are space-time separated and can only overlap for $t = 0$. The subtraction is covariant.

We can separate the finite perturbative expansion into three different parts: Zeroth, first and second order terms in an expansion in terms of $(p^0 - E_N - E_\pi)$, with weight functions which make all diagrams finite (see eq. (4.50)). The weight functions are due to the local subtractions only, but contain some of the typical scales of the problem.

The subtractions are made on-shell, such that the mass of the nucleon is not altered by the perturbative correction.

Figure 4.3: The different contributions to the nucleon self-energy. The vertical scale is in $g^2/(8\pi^2)$.

The spin-projection of the nucleon is independent of the spinor-basis[7]:

$$\sum_{\alpha=1,2} |\chi^\alpha(\vec{k})\rangle\langle\chi^\alpha(\vec{k})| = \gamma^0 E_N + \not{\vec{k}} + m, \tag{4.49}$$

$\vec{k}$ is odd and will remain so under regularization, therefore the term $\not{\vec{k}}$ can be dropped. We use the regularization described in Sect. 4.7. Then we obtain an integral with a finite integrand, given by:

$$\Sigma(p^0)_{finite} = \frac{-g^2}{32\pi^3} \int \mathrm{d}^3k \left\{ \sum_{j=0}^{2} \frac{(A_j\gamma^0 E_N + B_j m)}{E_N E_\pi (p^0 - E_N - E_\pi)^j} + \frac{C_0\gamma^0 + D_0}{E_N E_\pi} \ln[p^0 - E_N - E_\pi] \right\} \tag{4.50}$$

The weight functions A, B, C and D are smooth functions of $\vec{k}^2$ and linear functions of p^0. One cannot combine the p^0 dependence in numerator and denominator to a Laurent expansion in $(p^0 - E_N - E_\pi)$ without introducing divergences in the separate terms. We calculated numerically the forward diagram eq. (4.48) and the Z-graph with the $|NN\bar{N}\pi\rangle$-state and found that they add up to the covariant answer.

The total truncated amplitude Σ has four parts that were separately calculated:

$$\Sigma(p^0)_{cov} = \gamma^0\Sigma(p^0)^{vec}_{N\pi} + \Sigma(p^0)^{scal}_{N\pi} + \gamma^0\Sigma(p^0)^{vec}_{N\bar{N}N\pi} + \Sigma(p^0)^{scal}_{N\bar{N}N\pi}, \tag{4.51}$$

[7]Again the slashed momentum is part of a Lorentz invariant: $\not{\vec{k}} = -(\gamma^1 k^1 + \gamma^2 k^2 + \gamma^3 k^3)$.

which are plotted in fig. 2. The meson mass is set to 0.147 m_N. The signs of the corrections to the off-shell nucleon mass due to pseudoscalar coupling to the pion ($\Gamma = \gamma^5$) follow from these results through:

$$\gamma^5\gamma^0\gamma^5 = -\gamma^0, \qquad \gamma^5\gamma^5 = 1. \tag{4.52}$$

4.10 Conclusions

We have defined a method of regularizing diagrams without regulators, and without reference to the general proof of renormalization. The formulae obtained as intermediate results are the same as those of dimensional regularization although they are derived in a different context. In this way we avoided the discussion and treatment of regulators which complicates the procedure of renormalization and moves the attention away from the physical part of the theory to the meaningless, divergent expressions.

We have not proven renormalizability of some specific theories, but from our method one can infer by simple power counting which counterterms are subtracted for the diagrams that occur. The counterterms belong to the Ker of the differential operator D, that is central to our method. The differential operator needed to relate a general divergent diagram to a logarithmically divergent diagram follows from power counting. The remaining logarithmic divergences are treated in a way resembling dispersion methods, but we realize that at this stage many different methods of regularizations can be applied without difficulties.

Although different renormalization schemes are related to each other in a formal way, it is generally not possible to relate them rigorously. We borrowed some of the elements of dimensional regularization, and have the same results at intermediate stages in the calculation. However, for our specific needs we altered some of the methods. The method described in this chapter shares some of the merits with dimensional regularization. It also allows us to apply it in other cases, like light-front Hamiltonian field theory. Our focus is largely on the latter matter, but we feel that the discussion in this chapter has it own merits and should not become blurred by a technical discussion of light-front field theory.

4.11 Covariant calculations

4.11.1 Generalized dimensional operator

It is possible to derive the general behavior of a Greens function G independent of the order in the coupling constant, with a striking simplicity:

$$\left(\rho g\frac{\partial}{\partial g} + D\right) G(\sigma_f, \sigma_b) = \left(4 - 3\sigma_b - \frac{5}{2}\sigma_f\right) G(\sigma_f, \sigma_b). \tag{4.53}$$

The Greens function G has σ_f external fermion lines and σ_b external boson lines. The constant ρ is given by the number of lines that couple to the elementary, bare, vertex with coupling constant g:

$$\rho = \frac{3}{2}\#\text{fermion lines } + \#\text{boson lines } - 4 \tag{4.54}$$

Proof

The derivation consists of some straightforward algebra in the spirit of Lee (Lee, 1976) in combination with eq. (4.8). The ingredients are the formulae below:

$$\begin{aligned} \#\text{lines} &= \frac{1}{2}(\chi_f+\chi_b)\#\text{vertices}+\frac{1}{2}(\sigma_f+\sigma_b), && (4.55)\\ \#\text{loops} &= \#\text{lines}-(\sigma_f+\sigma_b)+1-\#\text{vertices}, && (4.56)\\ (D-4\#\text{loops})I &= -\left(\frac{1}{2}(\sigma_f+2\sigma_b)+\frac{1}{2}(\chi_f+2\chi_b)\#\text{vertices}\right)I, && (4.57)\end{aligned}$$

I is the integrand defining Γ, χ_f and χ_b are the number of fermion and boson lines resp. attached to a vertex. The relation that holds for the integrand also holds for the integral since it contains only external variables.

4.11.2 ϕ^3 self-energy

We will calculate the finite part of the ϕ^3 one-loop self-energy diagram (fig. 4.1). In the case of dimensional regularization we need to multiply the integral with a constant μ that has the dimension of a mass, to maintain the correct dimension of the integral.

$$\begin{aligned} \mathcal{F} &= \frac{g^2\mu^\epsilon}{2(2\pi)^{4-\epsilon}}\int \mathrm{d}^{4-\epsilon}k\frac{1}{[(p-k)^2-m^2][k^2-m^2]} && (4.58)\\ &= \frac{g^2\mu^\epsilon}{2(2\pi)^{4-\epsilon}}\int_0^1 \mathrm{d}x\int \mathrm{d}^{4-\epsilon}k\frac{1}{(k^2+x(1-x)p^2-m^2)^2}. && (4.59)\end{aligned}$$

We perform a Wick-rotation of the loop momentum, which gives an additional factor i, and integrate over the loop momenta. With the use of eq. (4.31) we can calculate the integral over k. Then we obtain:

$$\mathcal{F}=\frac{i\pi^2g^2}{2(2\pi)^{4-\epsilon}}\int_0^1 \mathrm{d}x\,\Gamma\left(2-\frac{1}{2}\epsilon\right)\Gamma\left(\frac{1}{2}\epsilon\right)\left(\frac{m^2-x(1-x)p^2}{\mu^2}\right)^{-\frac{\epsilon}{2}}. \qquad (4.60)$$

In the neighborhood of $\epsilon=0$, the integral has a pole, the pole of the second gamma function, as well as some finite pieces (behaving as ϵ^0). However, the finite pieces lead to a finite integral, that is constant so we do not worry about them. These parts can be absorbed in the arbitrary constant μ. Also the angular integral will give some finite pieces; without calculating them we add all these parts as finite renormalizations to the pole part, $2\epsilon^{-1}$, of the second gamma function. We seek the part of order ϵ in the remainder of the integrand that cancels the pole in the gamma function and gives us the p-dependent finite part:

$$\left(\frac{m^2-x(1-x)p^2}{\mu^2}\right)^{-\frac{\epsilon}{2}}\sim 1-\frac{\epsilon}{2}\ln\left(\frac{m^2-x(1-x)p^2}{\mu^2}\right)+\mathcal{O}(\epsilon^2), \qquad (4.61)$$

which gives the correct finite part eq. (4.14)

$$\mathcal{F} = \frac{ig^2}{16\pi^2}\left(1 - \frac{1}{2}\ln\left(\frac{m^2}{\mu^2}\right) - \sqrt{\frac{p^2-4m^2}{p^2}}\operatorname{arctanh}\sqrt{\frac{p^2}{p^2-4m^2}}\right). \tag{4.62}$$

The finite renormalization is given by the arbitrary constant μ. In the kinematical region given by:

$$\sqrt{\frac{p^2}{p^2-4m^2}} > 1, \tag{4.63}$$

the arctanh has an imaginary part since we are not on the principal branch of the arctanh. Taking into account this imaginary part gives indeed the proper breakup amplitude.

4.11.3 Comparison between finite results

In this section we will show that our regularization scheme for logarithmic divergences leads to the same finite parts as the dimensional regularization does. An arbitrary logarithmically divergent integral can be written, after Feynman parametrization, as:

$$\mathcal{I} = \int_0^\infty \mathrm{d}k^2 \frac{k^{2n}}{(k^2 + \alpha_{ij}p_i^\mu p_{j\mu} + \alpha_j m_j^2)^{n+1}}, \tag{4.64}$$

where α_{ij} and α_j are functions of the Feynman parameters only. Repeated indices are summed over. Differentiating with respect to the masses, as described in section 4.7, and subsequently integrating over k^2 yields:

$$m_j\frac{\partial}{\partial m_j}\mathcal{I} = \frac{-2\alpha_j m_j^2}{\alpha_{ij}p_i^\mu p_{j\mu} + \alpha_j m_j^2}. \tag{4.65}$$

We subtract the value at $p_j^\mu = 0$ for all μ and j:

$$m_j\frac{\partial}{\partial m_j}\mathcal{I}(p) - m_j\frac{\partial}{\partial m_j}\mathcal{I}(p=0) = \frac{2\alpha_{ij}p_i^\mu p_{j\mu}}{\alpha_{ij}p_i^\mu p_{j\mu} + \alpha_j m_j^2}. \tag{4.66}$$

The line integral, eq. (4.36), along a straight line from the origin in $4N$ dimensional space to the point $(p_1^0, \cdots, p_1^3, \cdots, p_N^0, \cdots, p_N^3)$ is a one dimensional integral over the scalar parameter λ ($\lambda \in [0,1]$). This yields:

$$\mathcal{I}_\mathrm{r} = \int_{\lambda_\mathrm{r}}^1 \mathrm{d}(\alpha_{ij}p_i^\mu p_{j\mu}\lambda^2)\frac{1}{\alpha_{ij}p_i^\mu p_{j\mu}\lambda^2 + \alpha_j m_j^2}. \tag{4.67}$$

If the amplitude should vanish for a particular value of $\alpha_{ij}p_i^\mu p_{j\mu}$ (e.g., $\alpha_{ij}p_i^\mu p_{j\mu} = \mu^2$), we can choose λ_r accordingly:

$$\mathcal{I}_\mathrm{r} = -\ln\left[\frac{\alpha_{ij}p_i^\mu p_{j\mu} + \alpha_j m_j^2}{\mu^2 + \alpha_j m_j^2}\right]. \tag{4.68}$$

Dimensional regularization would yield exactly the same finite momentum dependent part. One sees that $\sum p_j^\mu \partial_{p_j^\mu} I_\mathrm{r}$ yields eq. (4.66).

5

Renormalization of light-front Hamiltonian field theory

The renormalization of light-front Hamiltonian field theory is more or less an open question. For some cases it has been shown that the same finite results can be obtained as in covariant field theory. Often a special reference frame is chosen, and the counterterms have non-covariant forms. At least a much more difficult technique is needed to obtain these results. The additional singularities that occur in light-front perturbation theory are to blame for most of the confusion.

Covariant field theory has difficulties of a similar nature. Covariance is often preimposed to derive the finite parts and the counterterms associated with a Feynman diagram. We have seen in the chapter on dimensional regularization that parts of the divergent diagrams are subtracted without associating counterterms to them; counterterms correspond only to the remaining logarithmic divergence.

In light-front perturbation theory these higher order divergences are not so easily discarded. They are intertwined with the different structures that occur in a time-ordered diagram. In the case of a manifestly covariant Lagrangian we know that the sum of all time-ordered diagrams should add up to a covariant result. In this chapter we show that we can separate the different structures and recover the covariant finite part and the proper counterterms. We do not need an elaborate machinery to obtain these results. The proper regularization automatically separates the different terms. The use of non-covariant gauges requires some additional investigations.

With the dimensional analysis designed in the previous chapter we show that the divergences and singularities we encounter all belong to either of the two classes; they are the proper covariant divergences or they are of a higher order and cannot be associated with a proper Lorentz structure.

5.1 Introduction

Due to the apparent breaking of manifest covariance in light-cone time-ordered perturbation theory people tend to treat the singularities and divergences in the longitudinal direction separately from the divergences in the perpendicular direction (Perry & Wilson, 1993; Głazek &

Wilson, 1993; Wilson et al., 1994; Perry, 1994b). This separation makes it hard to recover the covariant result in lowest order perturbation theory (Mustaki et al., 1991; Brodsky et al., 1973). Especially the longitudinal singularities are hard to interpret and lead to the belief that (confining) potentials occur owing to renormalization of light-front field theory (Perry, 1994a).

Our approach is closest related to the work of Brodsky, Roskies and Suaya (BRS) (Brodsky et al., 1973), who apply a subtraction method, the alternating denominators, to a large number of diagrams in QED, establishing the anomalous magnetic moment of the electron up to the fifth order in the infinite momentum frame. However, we have a different aim. First of all we work strictly with light-front momenta, we do not take the infinite momentum limit. BRS need part of the backward diagrams for fermions, which violate the spectrum condition, to cancel the longitudinal singularities. This stands in close relation with the use of the infinite momentum frame limit which regulates part of the divergences. So it is clear that BRS regulate the diagrams first and take the infinite momentum frame limit afterwards. Therefore it is difficult to identify, in their final results, the contribution of divergent diagrams. This stands in contrast with our approach in which the l.c.t-ordered diagrams, obeying the spectrum condition, are identified first and regularized afterwards, if necessary. Secondly, they find a different power counting, than we do, due to the fact that they consider only on-shell diagrams.[1] Furthermore they do not treat diagrams with multiple vector particles such as the fermion-loop vacuum polarization. Vacuum polarization is the real test-case for regularization and renormalization. Although transversality of the vacuum polarization, ($\Pi^{\mu\nu}(p) = (p^2 g^{\mu\nu} - p^\mu p^\nu)\Pi(p^2)$), should follow from the Ward-Takahashi identity, it is often used in calculations without further ado, also by BRS and in many of the covariant calculations. Thirdly, the locality of the counterterms is another issue which requires some attention. Since the time-ordered formalism is not manifestly covariant it is also not manifestly local. In our scheme the counterterms are local in time, and due to the formal covariance of the divergent amplitudes (see chap. 3) and the covariance of the finite amplitudes we deduce that the counterterms are also fully local. To show that the finite amplitudes are covariant we calculate the amplitudes with arbitrary off-shell momenta, and we show that they only depend on Lorentz invariant objects.

We introduce a regularization scheme which maintains the symmetries of the theory such that the total amplitude is covariant order by order. We remove in our scheme the lowest orders in a Taylor expansion of the amplitude, which can be reabsorbed in counterterms to the original Lagrangian. The regularization also removes the longitudinal singularities without extra effort. This strengthens our belief that the instantaneous terms in low order diagrams are artifacts of the light-front formulation of perturbation theory and hence meaningless. They might be considered to be local structures since they occur at finite order in the Taylor expansion, but they do not have the proper dimension to act as such.

The regularization scheme of subtracting low order terms in the Taylor expansion (Hepp, 1966; Hahn & Zimmermann, 1968; Zimmermann, 1968; Zimmermann, 1969; Caswell & Kennedy, 1982) might sound old-fashioned, but it has advantages over most other regularization schemes. First, it preserves covariance, and secondly, it is fully local. Thirdly, it is a linear operation and can be applied to separate parts independently, and fourth, it gives finite integrands and allows for numerical implementation. Some of the problems that occur in manifestly covariant field theory, by means of Feynman diagrams, are not present in light-cone time-ordered perturbation theory with this regularization, since the external energy flow

[1] On-shell diagrams can only be used for the scattering of free particles. If particles are localized, off-shell in a bound state it requires knowledge of the off-shell scattering amplitudes.

through the diagram is fixed from the start. The freedom to choose the flow of external momenta is the origin of most problems in the regularization of Feynman diagrams. The problem of the regularization procedure we propose is the separation of different orders of divergence that occur in amplitudes with a nontrivial tensor-structure. The separation in each energy-denominator of internal and external coordinates, which is one of the advantages of light-front dynamics, turns out to solve this problem easily.

The dimensional analysis of each term in the light-cone time-ordered perturbative expansion tells us that they separately have the proper dimensions and that the same subtractions must be made as in the covariant case apart from the subtractions that, due to their tensorial structure, correspond to "negative powers" in the Taylor expansion. These terms are low order remnants of the instantaneous interactions, which are the implementation of constraints in Hamiltonian perturbation theory. We consider these negative terms to be meaningless, and they automatically vanish if the proper divergences are subtracted from the diagram.

5.2 Dimensional analysis

In this section we restate some of the results already obtained in chapter 4, and apply the methods developed there to specific examples in light-cone time-ordered perturbation theory. The starting point for dimensional analysis is the construction of an operator that has the "building blocks" of the perturbative expansion as its eigenfunctions with the "dimensions" of those building blocks as eigenvalues. For light-front field theory this dimensional operator is:

$$\overline{\nabla} + D; \tag{5.1}$$

$\overline{\nabla}$ contains the internal variables k_i and D the external variables p_j:

$$\overline{\nabla} = \sum_i k_i^+ \frac{\partial}{\partial k_i^+} + \vec{k}_{i\perp} \cdot \frac{\partial}{\partial \vec{k}_{i\perp}} \tag{5.2}$$

$$D = \sum_i m_i \frac{\partial}{\partial m_i} + \sum_j p_j^\mu \frac{\partial}{\partial p_j^\mu}. \tag{5.3}$$

The dimensional operator acting on a light-cone time-ordered diagram which contains l energy denominators, s fermion propagators and $n-s$ boson propagators, returns the dimension of the diagram (schematically):

$$(\overline{\nabla} + D)\frac{(\not{q}_1 + m_1)\cdots(\not{q}_s + m_s)}{q_1^+ \cdots q_n^+ [p_1^- - H_1]\cdots[p_l^- - H_l]} = (s - l - n)\frac{(\not{q}_1 + m_1)\cdots(\not{q}_s + m_s)}{q_1^+ \cdots q_n^+ [p_1^- - H_1]\cdots[p_l^- - H_l]}. \tag{5.4}$$

The momenta q_i are combinations of the internal (k) and the external momenta (p). The s spinor projections ($\not{q}_i + m_i$) have an on-shell minus component: $q_i^- = (q_{\perp i}^2 + m_i^2)/(2q_i^+)$. The l energy denominators contain the difference between the total incoming p^--momentum and the sum of all the on-shell energies of the particles present in an intermediate state j, which are given by:

$$H_j = \sum_{r \in j} \frac{q_{r\perp}^2 + m_r^2}{2q_r^+}. \tag{5.5}$$

If we include all the appropriate external lines in the intermediate states the energy flow through each state is the same and $p_i^- = p_j^-$. With the help of partial integration ('t Hooft & Veltman, 1972), and chapter 4, we can relate integrands with higher order divergences to integrands with lower order divergences, which forms the basis of dimensional regularization.

There are two major differences between the covariant approach and "old-fashioned" perturbation theory (Weinberg, 1966). First, in light-cone time-ordered diagrams the longitudinal integration extends over a finite domain only, therefore partial integration will lead to additional surface terms which renders a naive application of partial integration useless. Secondly, light-cone time-ordered diagrams contain singularities which can not be associated with objects with the proper dimension as obtained in naive power counting.

Although partial integration leads to surface terms, each time-ordered diagram that corresponds to a single Feynman diagram, appears to have the same dimension as the covariant amplitude. The same equation that provides us with the dimension of the full covariant amplitude, also gives the dimension of the time-ordered diagrams (see chap. 4):

$$D\mathcal{F}(p) = \delta\mathcal{F}(p). \tag{5.6}$$

$\mathcal{F}$ is an amplitude or a part of a amplitude. The surface terms from the partial integration are cancelled by the surface terms obtained by commuting the D-operation with the integral:

$$\int_{p_1^+}^{p_2^+} \mathrm{d}k^+\mathrm{d}^2k_\perp DI(k^+,\vec{k}_\perp) = D\int_{p_1^+}^{p_2^+} \mathrm{d}k^+\mathrm{d}^2k_\perp I - \int \mathrm{d}^2k_\perp(p_2^+ I(p_2^+,\vec{k}_\perp) - p_1^+ I(p_1^+,\vec{k}_\perp)). \tag{5.7}$$

In many cases the surface terms are infinite so this is a formal relation. The surface terms spoil many of the algebraic relations that exist in the standard cases (chap. 4). Therefore we have invented a method which does not generate these surface terms and removes the end-point singularities.

5.2.1 Transverse dimensional analysis

Often, power counting in the longitudinal and in the perpendicular directions are separated. Although we wish to deal in our regularization scheme with all directions in the same way, the separation of dimensions gives some insight in the spin dependence of the degree of divergence. We apply the ideas of ordinary dimensional analysis to a general time-ordered diagram, eq. (5.4). To do so, we introduce two dummy variables ξ and η, which are set to unity afterwards, and are used to determine the dimension of the spin structure:

$$\gamma^+ \rightarrow \xi\gamma^+, \tag{5.8}$$

$$\gamma^- \rightarrow \eta\gamma^-. \tag{5.9}$$

Also the transverse parts of gauge propagators must be multiplied with the same appropriate factors depending on the number of free $-$ and $+$ (upper)-indices. We can define a transverse dimensional operator:

$$\overline{\nabla}_{\mathrm{T}} + D_{\mathrm{T}}, \tag{5.10}$$

as follows:

$$\overline{\nabla}_{\rm T} = \sum_i \vec{k}_{i\perp} \cdot \frac{\partial}{\partial \vec{k}_{i\perp}}, \tag{5.11}$$

$$D_{\rm T} = \sum_i m_i \frac{\partial}{\partial m_i} + 2\sum_j p_j^- \frac{\partial}{\partial p_j^-} + \sum_j \vec{p}_{j\perp} \cdot \frac{\partial}{\partial \vec{p}_{j\perp}} - \xi \frac{\partial}{\partial \xi} + \eta \frac{\partial}{\partial \eta}. \tag{5.12}$$

The external longitudinal momentum, p^+, is absent because the internal longitudinal momentum is absent in the transverse dimension of an integrand. An arbitrary time-ordered diagram will contain different eigenfunctions of the transverse dimensional operator. Note that the dimension in the minus direction is twice the dimension in the perpendicular direction. Applying this operator to the time-ordered diagram above, eq. (5.4), gives us the following transverse dimension:

$$\Gamma_{\rm T} = s - 2l - n^+ + n^-, \tag{5.13}$$

where $n^+(n^-)$ is the number of free $+(-)$ indices. s and l are defined below eq. 5.4. This relation allows us to use dimensional regularization ('t Hooft & Veltman, 1972), (Mustaki et al., 1991) for the perpendicular dimensions, since we can use partial integration and obtain the integrand identity:

$$D_{\rm T} I = (\Gamma_{\rm T} + 2L) I. \tag{5.14}$$

Here, L is the number of loops. However, if there are longitudinal singularities present in the integrand, these would interfere with the perpendicular dimensional regularization. Equation (5.14) has a straightforward relation with the covariant dimension, eq. (5.6): $(\Gamma_{\rm T} + 2L) = \delta + n^- - n^+$. It is easy to check that if only covariant objects $\not{p}, p^2, p^\mu p^\nu, etc.$ occur in the amplitude the two relations are equivalent.

The transverse dimension is our guideline for subtraction. Our regularization scheme is covariant, so if we subtract terms which remove the transverse divergence they automatically remove the associated longitudinal singularity. The longitudinal singularities are more complicated as guideline since they are more difficult to interpret, and a diagram can have a transverse logarithmic divergence without longitudinal singularities.

From eq. (5.13) we see that we need to separate different divergences if we treat an amplitude with nontrivial tensor structure. We will demonstrate this separation in several examples.

5.2.2 Longitudinal dimensional analysis

Using the ordinary dimensional analysis and the transverse dimensional analysis we can derive the appropriate longitudinal operator. Since $D = D_{\rm L} + D_{\rm T}$ it follows that the longitudinal operator:

$$\overline{\nabla}_{\rm L} + D_{\rm L}, \tag{5.15}$$

has the following definitions:

$$\overline{\nabla}_{\rm L} = \sum_i k_i^+ \cdot \frac{\partial}{\partial k_i^+}, \tag{5.16}$$

$$D_{\rm L} = -\sum_j p_j^- \frac{\partial}{\partial p_j^-} + \sum_j p_j^+ \frac{\partial}{\partial p_j^+} + \xi \frac{\partial}{\partial \xi} - \eta \frac{\partial}{\partial \eta}. \tag{5.17}$$

The dimension it returns compensates for the inclusion of spin and the exclusion of the longitudinal direction in the transverse dimensional analysis.

$$(\overline{\nabla}_{\rm L} + D_{\rm L})I(p,k) = (l - n + n^+ - n^-)I(p,k). \tag{5.18}$$

Note that the number $n - l = L$, the number of loops in the diagram.

5.3 Minus regularization

After the discussion of dimensional properties of light-cone time-ordered diagrams we propose a straightforward regularization for them, which we call "minus regularization". We differentiate the diagram with respect to the external light-front energy p^- until the integral exists, and we can integrate over the internal variables $k^+, \vec{k}_\perp$. Afterwards we integrate the integral again over the external light-front energy as often as we have differentiated the integrand (symbolically):

$$\int_0^{p^+} {\rm d}k^+ \int {\rm d}^2k_\perp I(p,k) \doteq \left(\int_{\frac{p_\perp^2}{2p^+}}^{p^-} {\rm d}p'^- \right)^n \int_0^{p^+} {\rm d}k^+ \int {\rm d}^2k_\perp \left(\frac{\partial}{\partial p^-} \right)^n I(k,p) = \mathcal{F}(p) - P(p). \tag{5.19}$$

$P(p)$ is a polynomial in p^-, which equals the n-th order Taylor-expansion of the amplitude $\mathcal{F}$. The lower limit of the integration is the renormalization point, for which we have chosen $p^2 = 0$. One should take care that the renormalization point is below any production thresholds, otherwise the subtracted part $P(p)$ is not real and unitarity is violated. This procedure removes from the amplitude the lowest order terms in the Taylor expansion of the amplitude around the renormalization point:

$$\begin{aligned} \mathcal{F}(p) &= a_0 + a_1 \left(p^- - \frac{p_\perp^2}{2p^+} \right) + a_2 \left(p^- - \frac{p_\perp^2}{2p^+} \right)^2 + \cdots + \mathcal{O}\left(\left(p^- - \frac{p_\perp^2}{2p^+} \right)^n \right) \\ &= P(p) + \mathcal{O}\left(\left(p^- - \frac{p_\perp^2}{2p^+} \right)^n \right). \end{aligned} \tag{5.20}$$

Since we differentiate only with respect to the external energy, p^-, the masses act as internal variables. This has some consequences for the ease in which gauge invariance is ensured, and is the largest difference between our scheme and dimensional regularization. Thus the first $n - 1$ derivatives of the amplitude, with respect to p^-, vanish if they are subjected to our regularization, eq. (5.19). Different time-ordered diagrams can be subjected to this procedure separately and added together afterwards since the differentiations and integrations are linear operations and can be applied to each terms separately, if the renormalization point is chosen the same for the separate pieces. One should only take care that the instantaneous diagrams are added to the diagrams with ordinary singularities, in order to avoid unnecessary differentiations. In chapter 3 we have seen that longitudinal singularities are the result of contributions of the semicircle in the contour integration. If one performs the contour integration with caution there are no singularities. Here we will see that the singularities are terms in the Taylor expansion that do not correspond to a Lorentz structure. They vanish under renormalization where the power counting correspond to the counting of powers in p^-.

In the case of scalar amplitudes there are no extra powers in p^- apart from the covariant divergence, and the subtraction similar to the covariant subtraction is the full story. The number of differentiations needed equals the order of divergence of the amplitude. In the case of spinors or vector-bosons the amplitude has an internal structure and mixes different orders in p^-, thus different numbers of differentiations are needed to remove the divergence of different parts of the integrand. If we consider the truncated electron self-energy we know the general structure from covariance (de Wit & Smith, 1986):

$$\Sigma(p) = \not{p} f(p^2) + m g(p^2), \tag{5.21}$$

but we see that this structure mixes different orders in p^-:

$$\Sigma(p) = \frac{\gamma^+}{2p^+} p^2 f(p^2) + \left(\frac{\gamma^+ p_\perp^2}{2p^+} + \gamma^- p^+ - \vec{\gamma}_\perp \cdot \vec{p}_\perp \right) f(p^2) + m g(p^2). \tag{5.22}$$

Renormalization in this case means: $f(p^2) \to f(p^2) - f(0)$ and $g(p^2) \to g(p^2) - g(0)$. Part of the integrand should be differentiated twice, and the rest of the integrand should be differentiated only once to remove the divergence. For the amplitude this separation is straightforward, but for the integrand it is more elaborate. In general the longitudinal momenta k^+ and p^+ are our guide. We will show this for different examples in separate sections below.

The truncated vacuum polarization contains even more orders in p^- (de Wit & Smith, 1986):

$$\Pi^{\mu\nu}(p) = (g^{\mu\nu} p^2 - p^\mu p^\nu) \Pi(p^2). \tag{5.23}$$

In this case renormalization means $\Pi(p^2) \to \Pi(p^2) - \Pi(0)$. If we look at the tensor $p^\mu p^\nu$ we see three different orders in p^-:

$$\begin{aligned}
\begin{pmatrix} p^-p^- & p^-p^+ & p^-p^1 & p^-p^2 \\ p^+p^- & p^+p^+ & p^+p^1 & p^+p^2 \\ p^1p^- & p^1p^+ & p^1p^1 & p^1p^2 \\ p^2p^- & p^2p^+ & p^2p^1 & p^2p^2 \end{pmatrix} &= p^4 \begin{pmatrix} \frac{1}{(2p^+)^2} & 0 & 0 & 0 \\ 0 & 0 & 0 & 0 \\ 0 & 0 & 0 & 0 \\ 0 & 0 & 0 & 0 \end{pmatrix} \\
&+ p^2 \begin{pmatrix} \frac{2p_\perp^2}{(2p^+)^2} & \frac{p^+}{2p^+} & \frac{p^1}{2p^+} & \frac{p^2}{2p^+} \\ \frac{p^+}{2p^+} & 0 & 0 & 0 \\ \frac{p^1}{2p^+} & 0 & 0 & 0 \\ \frac{p^2}{2p^+} & 0 & 0 & 0 \end{pmatrix} \\
&+ \begin{pmatrix} \frac{p_\perp^4}{(2p^+)^2} & \frac{p^+p_\perp^2}{2p^+} & \frac{p^1p_\perp^2}{2p^+} & \frac{p^2p_\perp^2}{2p^+} \\ \frac{p^+p_\perp^2}{2p^+} & p^+p^+ & p^+p^1 & p^+p^2 \\ \frac{p^1p_\perp^2}{2p^+} & p^1p^+ & p^1p^1 & p^1p^2 \\ \frac{p^2p_\perp^2}{2p^+} & p^2p^+ & p^2p^1 & p^2p^2 \end{pmatrix}.
\end{aligned} \tag{5.24}$$

For the amplitude this separation is again straightforward, but in terms of integrands it is more complicated. First we introduce internal variables as is done in front-form dynamics (Dirac, 1949; Leutwyler & Stern, 1978; Lev, 1993). These coordinates have the advantage that the

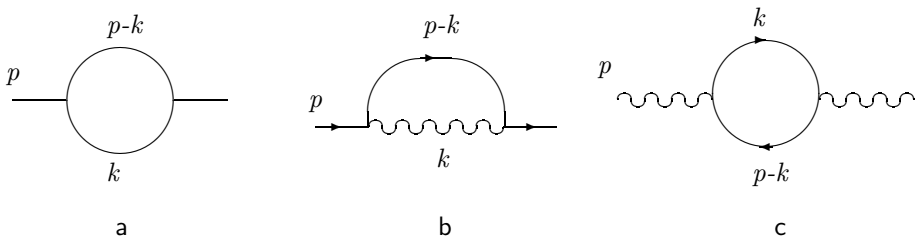

Figure 5.1: (a) the scalar loop; (b) the fermion self-energy; (c) the vacuum polarization.

integrand changes in a trivial way under a Lorentz-transformation of the external momenta. We can therefore separate the different structures and determine their appropriate degree of divergence. These terms are differentiated according to their divergence. For example, in eq. (5.24) we have three orders. To subtract "$\Pi(0)$" from the vacuum polarization the first term should be differentiated three times, the second term two times and the last one only once.

Both in the electron self-energy and in the vacuum polarization there are instantaneous terms in a light-front perturbative expansion, but these do not contribute to the amplitude; they are removed by the regularization procedure. They are independent of p^- (or in some cases linear functions of p^-) and therefore drop under differentiations. The only assumption we made to introduce our regularization procedure was covariance of the amplitude. The fact that different diagrams together make up the complete covariant amplitude does not bother us since differentiation and integration are linear operations.
The instantaneous parts and other longitudinal singularities are considered meaningless in this procedure, they correspond to the "negative order" Taylor expansion. For the fermion self-energy, for example, this term is:

$$\frac{\gamma^+(p^- - \frac{p_\perp^2}{2p^+})}{p^2} \int \mathrm{d}k^+ \mathrm{d}^2k_\perp \frac{p^+}{2(p^+ - k^+)k^+}. \tag{5.25}$$

There are no rigorous methods to determine the integration limits in this case. The precise form of the integrand depends on the implementation of the instantaneous terms (see chap. 3). These instantaneous terms drop automatically in our regularization procedure. We do not associate counterterms with these parts. It is a strange artifact of light-front field theory that these negative orders exist; It is the result of the linearity in p^2 of p^-. These terms can also be removed by removing the negative orders of the Taylor expansion (Bergère & Zuber, 1974) in k^+ around the singularities in the time-ordered diagrams, which frees one of the combinatorial job to combine the time-ordered singularities with the instantaneous parts as done in the "blink" procedure (see chap. 3).

5.3.1 Scalar loop

As a first, completely explicit, example we consider the light-front time-ordered diagram for the scalar loop with two propagators, fig. 5.1(a):

$$\mathcal{F}(p) = \int_0^{p^+} \frac{\mathrm{d}k^+\mathrm{d}^2k_\perp}{4k^+(p^+-k^+)} \quad \frac{1}{p^- - \frac{k_\perp^2+m^2}{2k^+} - \frac{(p_\perp-k_\perp)^2+m^2}{2(p^+-k^+)}}. \tag{5.26}$$

The integration limits are those of the longitudinal integration in k^+; the perpendicular integration $k_\perp = (k^1, k^2)$ extends over the whole space R^2. Throughout this chapter we do not include the coupling constants and the additional factors ($2\pi i$, symmetry factors, -1 for fermion loops) to keep the formulae as simple as possible. After differentiating the integrand once with respect to p^- we can integrate over the internal variables $(k^+, \vec{k}_\perp)$, with the result:

$$\frac{\partial\mathcal{F}}{\partial p^-} = \frac{\pi p^+}{p^2} - \frac{4\pi m^2 p^+}{p^4}\sqrt{\frac{p^2}{p^2-4m^2}}\ \mathrm{arctanh}\sqrt{\frac{p^2}{p^2-4m^2}}. \tag{5.27}$$

The finite part of the amplitude is obtained by integrating over p^-:

$$\mathcal{F}_r(p) = \mathcal{F}(p^2) - \mathcal{F}(0) = \int_{\frac{p_\perp^2}{2p^+}}^{p^-} \mathrm{d}p'^- \frac{\partial\mathcal{F}(p')}{\partial p'^-} = -\pi + \pi\sqrt{\frac{p^2-4m^2}{p^2}}\mathrm{arctanh}\sqrt{\frac{p^2}{p^2-4m^2}}. \tag{5.28}$$

The expressions simplify if we introduce the variables $x = k^+/p^+$, $y = x - \frac{1}{2}$, $\xi = \sqrt{\frac{p^2}{p^2-4m^2}}$ and $\mathrm{d}\xi = -(4m^2p^+/\sqrt{p^2(p^2-4m^2)^3})\mathrm{d}p^-$. The proper imaginary part is obtained if we take into account that the mass has a small negative imaginary part, and we are not on the principal branch for the arctanh for $p^2 > 4m^2$.

5.3.2 Fermion self-energy

The time-ordered diagram for the truncated fermion self-energy in the Feynman gauge is given by, fig. 5.1(b):

$$\Sigma(p) = \int_0^{p^+} \frac{\mathrm{d}k^+\mathrm{d}^2k_\perp}{4k^+(p^+-k^+)} \quad \frac{\gamma_\mu(\not{p}-\not{k}+m)\gamma^\mu}{p^- - \frac{k_\perp^2}{2k^+} - \frac{(p_\perp-k_\perp)^2+m^2}{2(p^+-k^+)}}. \tag{5.29}$$

The instantaneous term is included in the integrand therefore the spinor projection is defined as:

$$\not{p}-\not{k}+m = \gamma^+(p^- - \frac{k_\perp^2}{2k^+}) + \gamma^-(p^+-k^+) - \vec{\gamma}_\perp\cdot(\vec{p}_\perp - \vec{k}_\perp) + m, \tag{5.30}$$

without the instantaneous part the final result would be the same. Note also that there is a longitudinal singularity for $k^+ \to 0$. As we have seen, the self-energy mixes different orders

of p^-. We separate the different parts of the integrand by going to internal and external light-front variables:

$$k^+ = xp^+ \tag{5.31}$$
$$\vec{k}_\perp = x\vec{p}_\perp + \vec{q}_\perp. \tag{5.32}$$

This separates the different orders of divergence:

$$\not{p} - \not{k} + m = \gamma^+ \left(p^- - \frac{k_\perp^2}{2k^+} - (1-x)\frac{p_\perp^2}{2p^+} \right) + \vec{\gamma}_\perp \cdot \vec{q}_\perp + \left[(1-x)\not{\bar{p}} + m \right]. \tag{5.33}$$

The last term contains the fraction$(1-x)$ of external momenta flowing through the fermion line. The fraction x is measured in terms of longitudinal momentum p^+. The barred quantity $\bar{p}$ has an energy component such that $\bar{p}^2$ vanished at the renormalization point: $\bar{p}^2 = 0$, therefore: $\bar{p}^- = \frac{p_\perp^2}{2p^+}$. The first term is differentiated twice with respect to p^-, the last term is differentiated only once. The middle term can be made finite with differentiations, but being odd, it does not contribute. All integrals are then finite, and we can integrate over the internal variables $x, \vec{q}_\perp$. Afterwards we integrate the first term twice over p^- and the last term once and obtain the finite part of the covariant amplitude:

$$\begin{aligned} \Sigma_r(p) = \Sigma(p) - \Sigma(0) &= -4\pi \not{p} \left(-\frac{1}{16} - \frac{m^2}{8p^2} + \left(\frac{1}{8} - \frac{m^4}{8p^4} \right) \ln \left[\frac{m^2 - p^2}{m^2} \right] \right) \\ &+ 8\pi m \left(-\frac{1}{4} + \left(\frac{1}{4} - \frac{m^2}{4p^2} \right) \ln \left[\frac{m^2 - p^2}{m^2} \right] \right). \end{aligned} \tag{5.34}$$

5.3.3 Vacuum polarization

The light-cone time-ordered diagram for the vacuum polarization in QED is given by, fig. 5.1(c):

$$\Pi^{\mu\nu}(p) = \int_0^{p^+} \frac{\mathrm{d}k^+ \mathrm{d}^2 k_\perp}{4k^+(p^+ - k^+)} \; \frac{\mathrm{Tr}[\gamma^\mu(\not{p}_1 + m)\gamma^\nu(\not{p}_2 + m)]}{p^- - \frac{k_\perp^2 + m^2}{2k^+} - \frac{(p_\perp - k_\perp)^2 + m^2}{2(p^+ - k^+)}}, \tag{5.35}$$

without instantaneous parts. Before we proceed, we introduce again internal and external variables which facilitates the separation of the different orders, counting powers of $q_\perp$:

$$k^+ = xp^+, \tag{5.36}$$
$$\vec{k}_\perp = x\vec{p}_\perp + \vec{q}_\perp, \tag{5.37}$$
$$p_1^\mu = x\bar{p}^\mu + q_\perp^\mu + g^{\mu+} \left(\frac{p_\perp \cdot q_\perp}{p^+} + \frac{q_\perp^2 + m^2}{2p^+ x} \right), \tag{5.38}$$
$$p_2^\nu = (x-1)\bar{p}^\nu + q_\perp^\nu + g^{\nu+} \left(\frac{p_\perp \cdot q_\perp}{p^+} + \frac{q_\perp^2 + m^2}{2p^+(x-1)} \right). \tag{5.39}$$

The barred p-momentum has the minus component: $\bar{p}^- = \frac{p_\perp^2}{2p^+}$. It is part of the lowest order in the Taylor expansion around $p^2 = 0$, see eq. (5.24). To remove all the divergences, the

integrand should be differentiated three times. We will follow a different procedure. Because the separation of the different degrees of divergence makes the calculation lengthy and complicated, we will use a method which boils down to the same subtraction, but allows us to see which terms are removed where and when, while differentiations acts as an almost black box. Upon differentiation terms are removed without a clear view on the algebraic structure of these terms. Since the only p^- dependence is in the denominator we can see which terms would drop under differentiation. These are the constant, linear and quadratic terms in an analytical expansion (around $p^2 = 0$) of the denominator:

$$I = \frac{1}{2p^+(x(1-x)p^2 - m^2 - q_\perp^2)} = -\frac{1}{2p^+(m^2+q_\perp^2)} \sum_{j=0}^{\infty} \left(\frac{x(1-x)p^2}{m^2+q_\perp^2} \right)^j . \tag{5.40}$$

We see that the removal of the constant term is equivalent to multiplying the integrand by a factor $x(1-x)p^2/(m^2+q_\perp^2)$:

$$\mathcal{F}_r(p^2) \equiv \mathcal{F}(p^2) - \mathcal{F}(0) = \int_0^1 \mathrm{d}x \mathrm{d}^2q \left(\frac{x(1-x)p^2}{m^2+q_\perp^2} \right) I. \tag{5.41}$$

Apparently, the procedure of differentiation followed by integration with respect to the variable p^- is equivalent to the calculation of certain moments of the variable $x(1-x)p^2/(m^2+q_\perp^2)$. Note also that in this (covariant) calculation the singularities in the longitudinal direction are lowered at the same time as the divergences in the perpendicular direction. This an even more easy way to calculate the scalar loop (sect. 5.3.1). At each differentiation or calculation of a higher moment, the divergence in the perpendicular directions is lowered by two. The symmetries are maintained under differentiation and subtraction: rotational symmetry in the $\vec{q}_\perp$-plane, and the symmetry with respect to the interchange of x and $1-x$. The calculation of a higher moment is equivalent to subtracting certain low-order terms in a Taylor expansion. (See also the section on counterterms sect. 5.5). For the minus components of the four-vectors, eqs. (5.38, 5.39), we can do this immediately:

$$p_1^\mu = x\bar{p}^\mu + q_\perp^\mu + g^{\mu+}\left(\frac{p_\perp \cdot q_\perp}{p^+} - \frac{(x-1)p^2}{2p^+} \right) \tag{5.42}$$

$$p_2^\nu = (x-1)\bar{p}^\nu + q_\perp^\nu + g^{\nu+}\left(\frac{p_\perp \cdot q_\perp}{p^+} - \frac{xp^2}{2p^+} \right). \tag{5.43}$$

We separate the different terms by performing the trace:

$$4T = \mathrm{Tr}[\gamma^\mu(\not{p}_1 + m)\gamma^\nu(\not{p}_2 + m)] = 4(g^{\mu\nu}(m^2 - p_1 \cdot p_2) + p_1^\mu p_2^\nu + p_2^\mu p_1^\nu). \tag{5.44}$$

Owing to the rotational symmetry of the denominator, terms in the integrand with $(q_x)^2$ will lead to the same answer as those with $\frac{1}{2}q_\perp^2$. If we use this symmetry the trace yields:

$$\begin{aligned} T &= 2x(x-1)\bar{p}^\mu\bar{p}^\nu + g^{\mu\nu}\left(\frac{q_\perp^2 + m^2}{2x(1-x)} - q_\perp^2 \right) \\ &+ \frac{g^{+\nu}\bar{p}^\mu q_\perp^2}{p^+} + \frac{g^{+\mu}\bar{p}^\nu q_\perp^2}{p^+} \end{aligned}$$

$$+ \quad (2x(1-x)-1)\left(\frac{g^{+\nu}\bar{p}^{\mu}p^2}{2p^+}+\frac{g^{+\mu}\bar{p}^{\nu}p^2}{2p^+}\right)$$
$$+ \quad 2x(x-1)g^{+\mu}g^{+\nu}\frac{p^4}{(2p^+)^2}. \tag{5.45}$$

For the terms without $q_\perp^2$-dependence we calculate the first moment, for those with $q_\perp^2$ dependence we calculate the second moment. The m^2 terms are treated in the same manner as the $q_\perp^2$ terms since in a Taylor expansion in p^2 the mass acts as an internal variable. Here we see that the mass is treated as internal variable. The integrals give us the finite part of the vacuum polarization:

$$\Pi_r^{\mu\nu}(p) = (g^{\mu\nu}p^2 - p^\mu p^\nu)[\Pi(p^2)-\Pi(0)] = (g^{\mu\nu}p^2 - p^\mu p^\nu)\left(\frac{\pi}{18}+\frac{2m^2+p^2}{3p^2}\mathcal{F}_r\right). \tag{5.46}$$

5.4 Ward-Takahashi and vertex corrections

In the self-energy diagrams there is only one external momentum and the fraction of the longitudinal loop momentum plays the role of a Feynman parameter. In the case of one-loop three- and four-point functions there is still only one longitudinal momentum, but in a Feynman parametrization there would occur more Feynman parameters. In our regularization scheme, where we differentiate with respect to the external momenta we acquired additional freedom, since we can choose with respect to which external momenta we differentiate. If a diagram is only logarithmically divergent, one differentiation is enough and we would have fixed the value of the amplitude for one external momentum while the others run freely. This choice is a freedom we have.

The remnant of current conservation, the Ward-Takahashi identities (Ward, 1950), (Takahashi, 1957), fixes this freedom for gauge theories. It tells us how to do our differentiation and integration in order to keep the result gauge invariant. In the covariant case the Ward-Takahashi identities can be formulated as identities among integrands (de Wit & Smith, 1986). If we start with a self-energy diagram of a specific order and momentum p, the vertex function of the same order can be obtained by attaching a photon line, with momentum q, to the self-energy diagram at all possible fermion lines in the (truncated) diagram such that the outgoing momentum is $p+q$. If we now apply the identity

$$\frac{\not{p}+m}{p^2-m^2}-\frac{\not{p}+\not{q}+m}{(p+q)^2-m^2} = \frac{\not{p}+m}{p^2-m^2}\not{q}\frac{\not{p}+\not{q}+m}{(p+q)^2-m^2}, \tag{5.47}$$

to all the diagrams at the places where the photon line is attached, we see that we end up with the difference of the (truncated) self-energy diagrams with momenta p and $p+q$. Sometimes we must shift the internal momenta to make this apparent; closed fermion loops in the diagram do not contribute. If we have chosen a proper regularization, this relation among the integrands should lead to the same relation among the integrals:

$$q^\mu\Gamma_\mu^{(n)}(p,p+q) = \Sigma^{(n)}(p)-\Sigma^{(n)}(p+q). \tag{5.48}$$

Similar relations can be established among the integrands of time-ordered diagrams. If our regularization procedure does not destroy this relation we automatically satisfy the Ward-Takahashi identities. Therefore we should differentiate the integrands only with respect to p^-,

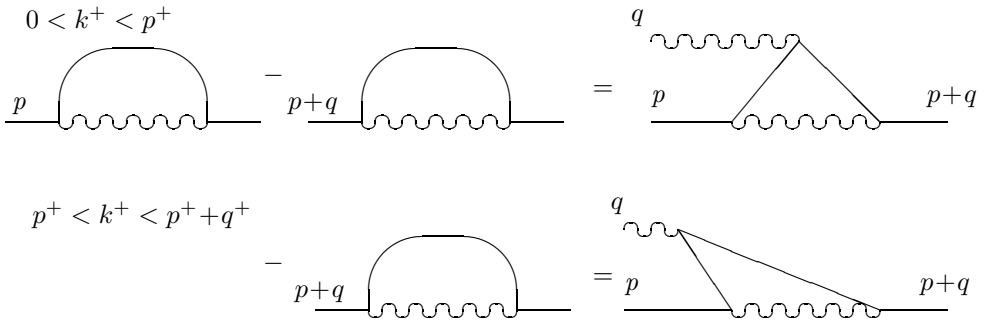

Figure 5.2: The Ward-Takahashi identities can be satisfied for each of the time-ordered diagrams, in their appropriate physical sectors, but only after inclusion of the instantaneous parts.

not q^-. This is nothing special since Ward derived the $q \to 0$ limit of the Ward-Takahashi identity in a similar way (Ward, 1950). There are no problems with the shift of coordinates here, since the minus momenta are fixed in a time-ordered diagram. The one loop vertex correction is related to the fermion self-energy diagrams in the Feynman gauge, see fig. (5.2). One should take proper care to include the instantaneous parts of all the diagrams ($0 < k^+ < p^+$):

$$\frac{\gamma^\mu\gamma^+\gamma_\mu}{2(p^+-k^+)} + \frac{\gamma^\mu(\gamma^+\frac{(p_\perp-k_\perp)^2+m^2}{2(p^+-k^+)} + \vec{\gamma}\cdot(\vec{p}-\vec{k})+m)\gamma_\mu}{4(p^+-k^+)k^+(p^- - \frac{(p_\perp-k_\perp)^2+m^2}{2(p^+-k^+)} - \frac{k_\perp^2}{2k^+})} \tag{5.49}$$

$$-\frac{\gamma^\mu\gamma^+\gamma_\mu}{2(p^++q^+-k^+)} - \frac{\gamma^\mu(\gamma^+\frac{(p_\perp+q_\perp-k_\perp)^2+m^2}{2(p^++q^+-k^+)} + \vec{\gamma}\cdot(\vec{p}+\vec{q}-\vec{k})+m)\gamma_\mu}{4(p^++q^+-k^+)k^+(p^-+q^- - \frac{(p_\perp+q_\perp-k_\perp)^2+m^2}{2(p^++q^+-k^+)} - \frac{k_\perp^2}{2k^+})}$$

$$= \gamma^\mu\left(\frac{\gamma^+}{2(p^+-k^+)} + \frac{(\gamma^+\frac{(p_\perp-k_\perp)^2+m^2}{2(p^+-k^+)} + \vec{\gamma}\cdot(\vec{p}-\vec{k})+m)}{4(p^+-k^+)(p^- - \frac{(p_\perp-k_\perp)^2+m^2}{2(p^+-k^+)} - \frac{k_\perp^2}{2k^+})}\right)\times$$

$$\not{q}\left(\frac{\gamma^+}{2(p^++q^+-k^+)} + \frac{(\gamma^+\frac{(p_\perp+q_\perp-k_\perp)^2+m^2}{2(p^++q^+-k^+)} + \vec{\gamma}\cdot(\vec{p}+\vec{q}-\vec{k})+m)}{4(p^++q^+-k^+)k^+(p^-+q^- - \frac{(p_\perp+q_\perp-k_\perp)^2+m^2}{2(p^++q^+-k^+)} - \frac{k_\perp^2}{2k^+})}\right)\gamma_\mu$$

If $p^+ + q^+ > k^+ > p^+$, only the integrand of the self-energy diagram with the momentum $p+q$ contributes to the integrand identity:

$$-\frac{\gamma^\mu(\gamma^+\frac{(p_\perp+q_\perp-k_\perp)^2+m^2}{2(p^++q^+-k^+)} + \vec{\gamma}\cdot(\vec{p}+\vec{q}-\vec{k})+m)\gamma_\mu}{4(p^++q^+-k^+)k^+(p^-+q^- - \frac{(p_\perp+q_\perp-k_\perp)^2+m^2}{2(p^++q^+-k^+)} - \frac{k_\perp^2}{2k^+})} = \tag{5.50}$$

$$\gamma^\mu\left(\frac{-\gamma^+}{2(p^+-k^+)} + \frac{(-\gamma^+(\frac{(k_\perp-p_\perp)^2+m^2}{2(k^+-p^+)} + \vec{\gamma}\cdot(\vec{p}-\vec{k})+m)}{2(p^+-k^+)(q^- - \frac{(k_\perp-p_\perp)^2+m^2}{2(k^+-p^+)} - \frac{(p_\perp+q_\perp-k_\perp)^2+m^2}{2(p^++q^+-k^+)})}\right)\times$$

$$\not{q}\left(\frac{(\gamma^+\frac{(p_\perp+q_\perp-k_\perp)^2+m^2}{2(p^++q^+-k^+)}+\vec{\gamma}\cdot(\vec{p}+\vec{q}-\vec{k})+m)}{4(p^++q^+-k^+)k^+(p^-+q^--\frac{(p_\perp+q_\perp-k_\perp)^2+m^2}{2(p^++q^+-k^+)}-\frac{k_\perp^2}{2k^+})}\right)\gamma_\mu$$

In order to see how the regularization of the electron self-energy fixes the regularization of the vertex function we can best look at the truncated amplitudes, see eq. (5.22):

$$q_\mu\Gamma^\mu_r(p,p+q)=\Sigma_r(p)-\Sigma_r(p+q). \tag{5.51}$$

We want to separate in the integrand of the vertex function the parts which give rise to different electron self-energies. If we separate the differentiation with respect to p^- in two pieces:

$$\frac{\partial}{\partial p^-}=\left(\frac{\partial}{\partial p^-}-\frac{\partial}{\partial q^-}\right)+\frac{\partial}{\partial q^-}, \tag{5.52}$$

the separate terms in the r.h.s. of eq. (5.51) vanish under the different terms in the differentiation eq. (5.52). The lower integration limit of each term is now determined by the self-energy renormalization $\Sigma_r(0)=0$. Also note that we do not have the same difficulties with the flow of external momenta through the diagram as in the covariant case, for in time-ordered diagrams the external energy variable is fixed in each diagram (Wu, 1962), (Mills & Yang, 1966).

The differentiation and integration with respect to the two variables, eq. (5.52), lead precisely to the counterterms already obtained in the fermion self-energy diagram. Both act only on a single energy denominator of the two denominators in the first order correction in the vertex function. The subtracted part for each is the value of the integrand at $p^2=0$ and $(p+q)^2=0$, respectively. Hence the Ward-Takahashi identity is satisfied. Note the special role played by the plus-component of the vertex correction Γ^+, since it does not commute with the differentiations:

$$\left(\frac{\partial}{\partial p^-}-\frac{\partial}{\partial q^-}\right)q_\mu\Gamma^\mu = q_\mu\left[\left(\frac{\partial}{\partial p^-}-\frac{\partial}{\partial q^-}\right)\Gamma^\mu-\frac{g^{-\mu}}{q^-}\Gamma^+\right] \tag{5.53}$$

$$\frac{\partial}{\partial q^-}q_\mu\Gamma^\mu = q_\mu\left[\frac{\partial}{\partial q^-}\Gamma^\mu+\frac{g^{-\mu}}{q^-}\Gamma^+\right] \tag{5.54}$$

The first term must be integrated over incoming momentum, p, from the point where $p^2=0$, the second over the outgoing momentum $p+q$. To remove the divergences of the vertex correction, in a gauge invariant way, we should not only use different renormalization points for the separate denominators, but we should also subtract and add a factor Γ^+/q^-.

5.5 Counterterms

In the section on the vacuum polarization we introduced a moment formula to subtract the lower order contributions of the integrand. This allows us to express the counterterms in terms of integrals. After regularizing the diagrams, the infinite parts which are subtracted from the diagrams, are added to the original Lagrangean to cancel against the counterterms(Muta, 1987),(Collins, 1984). The counterterms are infinite constants times expressions present in the initial Langrangian. They arose in the diagrams we considered in earlier sections; respectively ϕ^3 self-energy ($C_1\phi^2$), fermion self-energy ($C_2\bar{\psi}m\psi$, $C_3\bar{\psi}\not{p}\psi$) and vacuum polarization

($C_4 F_{\mu\nu}F^{\mu\nu}$). These infinite numbers can be written in our regularization scheme as integrals over internal coordinates.

$$C_1 = -\int_0^1 \mathrm{d}x\mathrm{d}^2q_\perp \frac{1}{2(m^2+q_\perp^2)}, \tag{5.55}$$

$$C_2 = -2\int_0^1 \mathrm{d}x\mathrm{d}^2q_\perp \frac{1}{(xm^2+q_\perp^2)}, \tag{5.56}$$

$$C_3 = \int_0^1 \mathrm{d}x\mathrm{d}^2q_\perp \frac{1-x}{(xm^2+q_\perp^2)}, \tag{5.57}$$

$$C_4 = -\int_0^1 \mathrm{d}x\mathrm{d}^2q_\perp \frac{2x(1-x)}{(m^2+q_\perp^2)}. \tag{5.58}$$

Note also the (integrable) infrared singularity in the electron self-energy for $(x \to 0, q_\perp \to 0)$, which would cause complications for on-shell renormalization(Jauch & Rohrlich, 1955). Besides these terms we have counterterms which are specifically associated with the singularities of the instantaneous contributions. We saw that these contributions dropped automatically in our regularization procedure. These terms need no special treatment in our scheme. We maintain here that these contributions are meaningless and do not contain any physics.

5.6 Conclusions

We have dealt with the divergences and singularities in light-front Hamiltonian field theory that are the result of local divergences. For these divergences we have defined a renormalization of light-cone time-ordered perturbation theory. We have recovered the covariant amplitude with light-cone time-ordered diagrams for the scalar two-propagator loop, the electron self-energy and the vacuum polarization. Our method defines the regularization of the vertex correction if we wish to satisfy the Ward-Takahashi identities. Ambiguities as the result of the longitudinal singularities vanish.

Only after one has a proper method to remove all the local divergences one can deal with infrared divergences, long-range effects and the strong-coupling regime. Often these two separate parts are intertwined in the discussions on the renormalization of light-front field theory, as the result of a lack of proper interpretation and method to deal with the local divergences. We hope that our way to deal with the local part of the theory will shed some light on the true nonperturbative content of light-front field theory. The parts that are subtracted are infinite local terms. They have no scale, therefore we avoided the use of renormalization group methods because there is no sensible way to approach a point nor an infinite constant. Although some of the local structures look like potentials (infrared divergences) we have seen that these can be accounted for in the proper way as local terms or discarded as artifacts.

6

The relativistic Hamiltonian in the bound-state problem

In the earlier chapters we were concerned with formal aspects of light-front Hamiltonian field theory. We argued our case from the perspective of field theory. Covariant field theory was often the starting point of our investigation to ensure covariance of our results and to resolve ambiguities.

In this chapter we will derive a relativistic Hamiltonian. This Hamiltonian contains phase-space factors which are usually not present in the local Hamiltonian. However, they are necessary to obtain results equivalent to the covariant ones. In different Hamiltonian approaches some of these phase-space factors appear in different places; in wave-function normalization, in form factors and in scattering phase spaces. All these phase-space factors can be replaced consistently, in our formulation, by the phase-space factors in the interaction part of the Hamiltonian. The states, on which this Hamiltonian acts, are normalized to unity, similar to the quantum mechanical normalization. The presence of different Fock components, with different numbers of particles, in one state is the major difference between field theory and the quantum mechanical theory. Particle number is not conserved in field theory and consequently components with different number of particles mix in the true eigenstates of field theory. The phase-space factors are the logical consequences of the introduction of an equal time-plane in covariant field theory which is a nonrelativistic concept which singles out the time direction in space time. Because of these additional phase-space factors of the integrals occurring in the perturbative expansion, the convergence is better than the usual convergence in the nonrelativistic cases.

The Hamiltonian is the evolution operator of the states and will therefore lead to a Schrödinger equation. Because of causality the Schrödinger equation is a first order differential equation in time. Only the positive energy states evolve forward in time and there is no ambiguity about the sign of the energy as there would be in the Klein-Gordon equation. Again we will show that stationary perturbation theory will lead to results equivalent to the covariant results derived with Feynman perturbation theory.

Ultimately we are interested in the bound state; we want to describe a system where the lowest Fock components of the eigenstate contains two or more particles. In perturbation theory such a bound state can only arise if an infinite number of interactions are summed.

Furthermore, the bound state poses many, more or less, fundamental problems.

The earth and the moon mysteriously revolve around each other. They constantly change their relative velocity and their relative position. The earth and the moon form a bound system. If one introduces a potential, their movements will be described and predicted. With the simple phenomenological input of a potential it is possible to describe many features of bound states, such as the energy spectrum and the charge radius. However, a potential does not tell us the nature of the interaction between the constituents, or its origin. We do not know what makes the constituents stay together. The potential signifies a missing energy as a function of relative position. The potential is a classical concept that seems to have survived the "quantum-revolution."

The potential transports momentum and energy from one constituent of the bound system to another. However, since the introduction of quantum mechanics it is assumed that something that carries momentum and energy must be a particle which can be observed independently. The change in momenta of the constituents is the result of the emission or absorption of a particle. This is generally a virtual particle that does not have enough energy to live for a long time. Otherwise the particle will be emitted from the bound state. Although it seemed at first as if the constituents were free and had no reason to stay close to another, the undetected presence of the virtual interacting particles changes this picture drastically. However, the virtual particles usually go undetected.

The virtual particle cloud which binds the constituents replaces the classical potential. However, as it turns out, it is very hard to make this picture quantitative and one generally tries to replace actual knowledge of the virtual cloud by a potential which should have the same effect as the virtual cloud. This potential can either be a potential in the classical sense or the kernel of the Bethe-Salpeter equation, which sums some contributions of particle exchanges in a region forbidden for scattering. After all, if particles are bound, they cannot move freely; they are off-shell. If only a finite number of particles are exchanged the constituents have no reason to stay bound. After the last exchange the constituents move outward freely, or the constituents cannot exist since there is not enough total energy in the system.

The creation and annihilation of particles is described within quantum field theory, which is a local, dynamical theory. Local means that particles are created at a specific point in space where the source is located at that time. Dynamical means that we consider time-dependent processes such as the creation of a particle at one time and annihilation at another. Although this theory has been very successful for the description of scattering processes, it is clear that it is not so useful for the description of bound states. First, a bound state is a stationary state which is only indirectly described by the summing over processes and the averaging over time of a dynamical theory. Secondly, in a local theory the global properties, such as the relative position of the constituents, are only available as indirect information; the theory does not use the relative position as a variable to describe the system. However, after the dynamics is solved we can also determine the relative position and other global properties of the bound state, while in a potential picture many properties of the bound state can be inferred from the potential without performing any calculation.

The picture that arises is similar to the picture of chemical binding. Two hydrogen atoms bind into a hydrogen molecule because it is favorable to have an overlap between the wave functions of their respective electrons. The interference between the wave functions push the wave function outward or inward depending on the interaction and the wave functions. The electron wave function plays the role of the virtual cloud in field theory. In quantum field

theory the constituents share the virtual cloud which is energetically more favorable than to have separate virtual clouds. The one-boson-exchange diagram approximation to the potential can be seen as the first order interference term between the virtual clouds. The potential is not a fundamental property of a particle but the net effect of the interference between two clouds and can only be the result of two or more particles in each other's vicinity.

The virtual clouds, which surround particles, are the wings of a hummingbird. The wings move too fast to be seen: however, they do make the bird move. We will study properties of the virtual cloud in this chapter. Higher Fock states are well described by the tree diagrams which constitute the lowest order approximation in coupling constant of the higher Fock state given the lowest Fock state, or constituent part.

The virtual cloud is smeared with respect to the constituent state. This result is not trivial, but follows from estimates of the tree diagrams. This nontriviality is enhanced due to the dependence of the higher Fock state content on the frame or the time direction. In field theory particle creation and annihilation are intertwined with Poincaré invariance.

In this chapter we will start with the concept of an equal-time plane in covariant field theory which is necessary to define a state. We will write down the Hamiltonian for a general field theory, both for the ordinary instant time variable and the light-cone time variable, and make some remarks about the connection with covariant field theory. In the next section the Schrödinger equation is derived with a Coulomb potential as the lowest order approximation to scalar quantum electrodynamics.

We discuss the next-to-leading-order corrections to this result. More generally, it can be shown that if one solves the Hamiltonian eigenvalue equation truncated to a specific number of particles one generates all diagrams with at most this number of particles in each intermediate state.

The next section is devoted to higher Fock states, in the light-front formalism, in a strongly coupling field theory. We will show that combinatorics, virtuality and kinematics determine the occupation of the higher Fock states. The distribution of longitudinal momenta is determined largely by the higher Fock state occupations of the bound state. The presence of transverse variables does not influence the results significantly which shows the peculiar mixing of particle creation and annihilation, and covariance.

6.1 Time evolution in the space-time approach

The standard, covariant, formulation of scattering is the space-time formulation. It is based on the pioneering work of Feynman who treated the spatial and the time direction on equal footing (Feynman, 1949). The manifestly covariant amplitudes, which result from these calculations, can be related to scattering amplitudes through the inclusion of noncovariant phase-space factors. Central to this approach is the causal, or Feynman, propagator,

$$\langle 0|\mathcal{T}\phi(y)\phi^\dagger(x)|0\rangle = D(y-x). \tag{6.1}$$

Feynman noted that, while particle numbers are not conserved, the charge is conserved. Particle and anti-particle, with opposite charge, can annihilate each other. If one follows the local current, one will move forward and backward in time. The causal propagator reflects this aspect. The time-ordering operator $\mathcal{T}$ picks out the forward evolution of the particle and the backward motion of the anti-particle. Depending on the sign of the time component of $y-x$

either mode can evolve freely. This can be seen from the momentum representation of the causal propagator (sec. 2.5):

$$D(\vec{x},t)=\frac{1}{(2\pi)^3}\int \mathrm{d}^3k\left(\theta(t)\frac{\mathrm{e}^{-i\sqrt{k^2+m^2}t+i\vec{k}\cdot\vec{x}}}{2\sqrt{k^2+m^2}}+\theta(-t)\frac{\mathrm{e}^{+i\sqrt{k^2+m^2}t-i\vec{k}\cdot\vec{x}}}{2\sqrt{k^2+m^2}}\right). \tag{6.2}$$

If the particle interacts at different space-time points and evolves freely between those points we can use the causal propagator irrespectively whether points along the route are chronologically ordered. The causal propagator ensures current conservation and the proper dynamics. Instead of the charge we can follow the energy flow for the same argumentation. However, we miss the intuitive picture charge conservation supplies us with.

In quantum field theory the interaction is a product of fields. The field operators annihilate and create particles at a specific space-time point. However, this cannot be interpreted in a strict sense. If we separate the initial and the final point by a surface and annihilate and create the particle when the particle passes this surface, the propagation will not be the same as the direct propagation from the initial point to the final point. Even in the specific case where the surface is the equal-time surface in between the initial point and the final point the ergodic property does not hold, and the causal propagator does not describe the *evolution* of the fields:

$$D(x_2-x_1)\neq\int \mathrm{d}^3x D(\vec{x}_2-\vec{x},t_2-\tau)D(\vec{x}-\vec{x}_1,\tau-t_1). \tag{6.3}$$

The ergodic property means that the propagators are elements of a semi-group which is additive in the time parameter. On the basis of covariance we could deduce that this relation could not hold. An equal-time surface is a nonrelativistic object; integration over all points on that surface gives a frame-dependent result. A phase-space factor, $\sqrt{\vec{k}^2+m^2}$, which is nonlocal in configuration space, restores covariance:

$$D(x_2-x_1)=\int \mathrm{d}^3x D(\vec{x}_2-\vec{x},t_2-\tau)\ 2\sqrt{\vec{k}^2+m^2}\ D(\vec{x}-\vec{x}_1,\tau-t_1), \tag{6.4}$$

as can be seen from the momentum representation of the propagator, eq. (6.2). A formulation in terms of the free evolution, where one can evolve the fields from one equal-time surface to the next without inclusion of phase-space factors requires that we allocate these factors in the interaction part of the field theory, such that we can use normed fields and a norm-conserving propagation. This is possible, as we will see below. The evolution of the fields is the evolution of the positive energy components, since causality restricts the forward evolution to the positive energy components ($t>0$):

$$e^{-iH_0(s)t}=\int\frac{\mathrm{d}^3k}{(2\pi)^3}\mathrm{e}^{-i\sqrt{\vec{k}^2+m^2}t-i\vec{k}\cdot\vec{x}}=2i\partial_t D=\frac{im^2t}{4\pi s}H_2(m\sqrt{s}), \tag{6.5}$$

where s is the square of the invariant length: $s=t^2-\vec{x}^2$. This propagator is more singular (Symanzik, 1981) than the causal propagator; however, it reduces to a local function for $t\to 0$ such that for $\vec{x}\neq 0$ the function vanishes. The classical relativistic dynamics was determined by a second order differential equation in time, with field values and the time derivative of field

values as initial conditions on an equal time surface. Due to causality only one initial condition is necessary. Given the field, the time derivative of the field is fixed at the initial surface, $t = 0$:

$$\phi|_{t=0} = g(\vec{x}), \tag{6.6}$$

$$\partial_t \phi|_{t=0} = -i\sqrt{\vec{k}^2 + m^2}\; g(\vec{x}). \tag{6.7}$$

The local field variables lead to nonlocal boundary conditions due to the implementation of the second boundary condition as the result of causality.

We are primarily interested in a quantum mechanical formulation of field theory. Therefore we define a state, $|\psi\rangle$, which describes the correlation of all the particles present at one time, t. If this state is an eigenstate, the evolution will only be a change in phase:

$$|\psi(\vec{x}_1, \cdots, \vec{x}_n; t)\rangle = \mathrm{e}^{-iEt}|\psi(\vec{x}_1, \cdots, \vec{x}_n; t = 0)\rangle. \tag{6.8}$$

The evolution of an arbitrary state is governed by the Schrödinger equation. The Schrödinger equation can be deduced from Feynman's space-time approach by taking a thin time slice, Δt, of a Feynman diagram. $|\psi\rangle$ contains the fields at this time slice. The fields evolve freely between t and $t + \Delta t$, except when an interaction occurs. The likelyhood of an interaction is proportional with Δt, and therefore small for short times. The relativistic evolution of a state is given by:

$$|\psi(\vec{x}, t+\Delta t)\rangle = \int \prod \frac{\mathrm{d}^3 k}{(2\pi)^3} \prod \mathrm{d}^3 x' \mathrm{e}^{-i\sum_j \omega_j \Delta t - i\vec{k}\cdot(\vec{x}'-\vec{x})} \left(1 + \frac{\Delta t \mathcal{L}_{\mathrm{int}}}{\prod \sqrt{2\omega_j}}\right) |\psi(\vec{x}', t)\rangle, \tag{6.9}$$

where $\omega_j = \sqrt{\vec{k}_j^2 + m_j^2}$, the on-shell energy of a particle with momentum $\vec{k}_j$ and mass m_j, occurring in the phase-space factors. In the limit for $\Delta t \to 0$ this reduces to

$$\frac{\partial}{\partial t}|\psi(\vec{x}_1, \cdots, \vec{x}_n, t)\rangle = \left(-i\sum_j \omega_j + \frac{\mathcal{L}_{\mathrm{int}}}{\prod \sqrt{2\omega_j}}\right) |\psi(\vec{x}_1, \cdots, \vec{x}_n, t)\rangle, \tag{6.10}$$

which we call the relativistic Schrödinger equation. An arbitrary state, $|\psi_t\rangle$, is given by the fields on an equal-time surface which does not contain an interaction. We see that the relativistic Hamiltonian, H, which is generally assumed to be local has additional phase-space factors. In a Hamiltonian approach the local interaction Lagrangian leads to a nonlocal interaction Hamiltonian:

$$H_{\mathrm{int}} = \frac{i\mathcal{L}_{\mathrm{int}}}{\prod_{j=1}^{v} \sqrt{2\omega_j}}, \tag{6.11}$$

where the phase-space factor contains the energies for all the lines attached to a vertex, hence, for all the field operators in the interaction.

6.1.1 Time-ordered perturbation theory from the space-time approach

From the Feynman diagrams in configuration space one can derive the time-ordered diagrams. First one has to multiply the amplitude with a phase rotation, $\mathrm{e}^{iE\tau}$, due to free evolution

to bring the state in the Heisenberg representation. Secondly one has to integrate over the intermediate time between two successive vertices allowing all possible times between zero and infinity. This integration gives rise to the energy denominators:

$$|\psi(\vec{x},t=0)\rangle = \frac{\mathcal{L}_{\rm int}}{\prod\sqrt{2\omega_j}}\int_0^\infty \mathrm{d}\tau \mathrm{e}^{iE\tau}\int\prod\frac{\mathrm{d}^3k}{(2\pi)^3}\prod\mathrm{d}^3x'\mathrm{e}^{-i\sum_j\omega_j\tau-i\vec{k}\cdot(\vec{x}'-\vec{x})}|\psi(\vec{x}',\tau)\rangle. \tag{6.12}$$

This process has to be repeated until all the intermediate times are integrated out. The different terms in the interaction give rise to different time-ordered diagrams. In the time-ordered diagram each intermediate state is associated with an energy denominator, $(E-\sum\omega)^{-1}$, and each line with a phase-space factor, $(2\omega)^{-1}$.

6.2 Hamiltonian field theory

Central to most Hamiltonian approaches is the determination of eigenvalues, and eigenstates of the Hamiltonian. With the eigensystem, i.e., eigenvalues and eigenstates, measurable aspects of the physical system can de determined.

In most cases it is difficult to determine the eigensystem. Instead one uses the eigensystem of a Hamiltonian which one can use as a basis and treat the difference, V, between this free Hamiltonian, H_0, and the original Hamiltonian, $H=H_0+V$, as a perturbation in which one can expand the eigensystem.

The eigenstate $|\psi\rangle$ with eigenvalue E can be determined from the eigenstate $|\phi^{(0)}\rangle$ with the same eigenvalue, E, of the free Hamiltonian:

$$|\psi\rangle = \sum_{n=0}^{\infty}\left(\frac{1}{E-H_0}V\right)^n|\phi^{(0)}\rangle, \tag{6.13}$$

with: $(E-H_0)|\phi^{(0)}\rangle=0$. This eigenstate expansion, central to the Lippman-Schwinger equation (Lippmann & Schwinger, 1950) has led a life of its own. One considers different terms in the expansion to correspond to different "processes". However, in stationary perturbation theory no process occurs. The time-ordered perturbation theory has no time-dependence. However, we can relate the different free states, which are parts of a true eigenstate, to outcomes of scattering experiments, which are described with processes in Feynman's perturbation theory, which is a dynamical theory.

The proper Hamiltonian interpretation of the scattering matrix, S, is the projection of free in-and out-states onto the eigenstates of the perturbed Hamiltonian, and this for each energy separately:

$$S_{\alpha\beta}(E) = \langle\phi^{(0)}_\alpha(E)|\psi^+(E)\rangle\langle\psi^+(E)|\psi^-(E)\rangle\langle\psi^-(E)|\phi^{(0)}_\beta(E)\rangle. \tag{6.14}$$

where ψ^- and ψ^+ are the in- and out-states of the perturbed system in the interaction representation. Ordinarily the S matrix is defined as $S_{\alpha\beta}=\langle\psi^+_\alpha(E)|\psi^-_\beta(E)\rangle$ (Weinberg, 1995). (See also the discussion in (Bogoliubov & Shirkov, 1959).) However, it is assumed that the interacting states reduce to the free states in the Heisenberg representation for long times. In the case of bound states and self-interaction this cannot be true. Therefore the projection onto the Heisenberg states is necessary to recover the degrees of freedom, such as momenta

and polarizations, with which the system is described. The explicit dependence on the energy reflects the adiabatic connection between free and interacting states.

The problems one may have with this formulation reflect many of the formal problems of scattering theory. Formally, the different free states are components of a true eigenstate. Therefore, starting in one free state, the system oscillates to other free states. In scattering theory the oscillations are averaged over due to the long time between the initial and final state. The occupations, in terms of the free states basis, of the perturbed eigenstate remain.

The essential difference between the quantum mechanical state and the field theoretical states is that particle number is conserved in the first state, whereas it is not the field state. Different Fock states are combined in one eigenstate. It is like saying that a hydrogen atom consists of a combination of: the atom; a proton and an electron; a proton, an electron and a photon; a proton, an electron and two photons; a proton, two electrons and a positron, etc. Generally, we are not used to treating these different states as quantum mechanical degrees of freedom of one physical object.

In practice, we will write the state in terms of eigenstates of the free Hamiltonian, which is characterized by the momentum distributions of the particles:

$$|\psi\rangle = \sum_{n=0}^{\infty} |\phi_n(k_1 \cdots k_n)\rangle, \tag{6.15}$$

where ϕ_n is a combination of wave functions which contains n particles. A state is a sum of different Fock states, each with a specific number of particles; each particle has its own wave function, for which we use the plane wave with momentum k_j here. This state is normed nonrelativistically similar to the quantum mechanical state:

$$\langle\psi|\psi\rangle = \sum_{j=0}^{\infty} \int \prod_{n=1}^{j} \mathrm{d}^3 k_n \langle\phi_j(k_1 \cdots k_j)|\phi_j(k_1 \cdots k_j)\rangle = 1. \tag{6.16}$$

Therefore the results will be directly related to scattering experiments, and projection operators can be expressed in the sum over states. An exclusive measurement generally picks, projects, out one of the Fock states, ϕ_n. Therefore, we will only indirectly notice the relative strength of the different Fock states. For practical purposes we use normed Fock states different from the Fock state occupations of an eigenstate, ϕ_n:

$$\langle k'_1 \cdots k'_n | k_1 \cdots k_n \rangle \;=\; \langle k'|k\rangle \;= \delta^{3n}(k'-k). \tag{6.17}$$

These states have only a formal meaning, since a plane wave is not normed; they are not even functions in momentum space. The expansion of the eigenstate in free states can be expressed as operations on the free states Fock basis, such as eq. (6.13). Consider a local interaction, V, which creates an additional particle with momentum k_{n+1} on the particle with initial momentum k'_n. To describe a local interaction we use configuration space, while the energy denominator, $(E - H_0)^{-1}$, is defined in momentum space. Therefore we flip between the two representations of states in each term in the expansion on the states:

$$\langle k|V|k'\rangle \;=\; \langle k|r\rangle \langle r_1 \cdots r_{n+1}|G\delta^3(r_{n+1} - r'_n) \prod_{j=1}^{n} \delta^3(r_j - r'_j)|r'_1 \cdots r'_n\rangle \langle r'|k'\rangle \;, \tag{6.18}$$

where G is the nonrelativistic coupling constant. The plane waves are not normalizable[1], however, we will use the norm-preserving Fourier transform. In that case we are able to extend the meaning of our formulae beyond their original scope, and maintain the proper unitary normalizations:

$$\tilde{f}(x) = [\mathcal{F}f](x) = \frac{1}{\sqrt{2\pi}} \int \mathrm{d}k \; \mathrm{e}^{-ikx} f(k). \tag{6.19}$$

Expanding eq. (6.18) in plane waves, we find:

$$\langle k| \frac{1}{E - H_0} V |k'\rangle \;=\; \frac{G\delta^3(k'_n - k_n - k_{n+1}) \prod_{j=1}^{n-1} \delta^3(k_j - k'_j)}{\sqrt{2\pi}^{\,3}(E - \sum_{j=1}^{n+1} \omega_{k_j})}. \tag{6.20}$$

The momentum conserving delta functions tell us how the momenta thread through the diagram. In the previous section we have seen that the interaction in the Hamiltonian formulation has additional phase-space factors, which alter the matrix elements, and change the dimension of the coupling constant from nonrelativistic, G, to relativistic, g:

$$\langle k| \frac{1}{E - H_0} V_r |k'\rangle \;=\; \frac{g\delta^3(k'_n - k_n - k_{n+1}) \prod_{j=1}^{n-1} \delta^3(k_j - k'_j)}{\sqrt{2\pi}^{\,3} \sqrt{8\omega_{k'_n}\omega_{k_n}\omega_{k_{n+1}}}\,(E - \sum_{j=1}^{n+1} \omega_{k_j})} \tag{6.21}$$

The state is normed nonrelativistically; therefore the higher Fock states are suppressed by additional powers of the mass. Given the local Hamiltonian, $H = H_0 + V$, the associated, nonlocal, operators are given by:

$$\begin{aligned} V_r &= |k\rangle \frac{V}{\prod \sqrt{2\omega}} \langle k'| \;, \\ H_0 &= |k\rangle \left(\sum_j \sqrt{\vec{k}_j + m_j^2} \right) \langle k| \;, \end{aligned} \tag{6.22}$$

where V is the original local operator associated with the local Lagrangian density. Similarly, we find for the light-front Hamiltonian the operator representations:

$$\begin{aligned} V_r &= |k\rangle \frac{V}{\prod \sqrt{2k^+}} \langle k'| \;, \\ H_0 &= |k\rangle \left(\sum_j \frac{\vec{k}_{j\perp}^{\,2} + m_j^2}{2k_j^+} \right) \langle k| \;. \end{aligned} \tag{6.23}$$

However, in this case the connection between the configuration-space representation and the momentum-space representation is blurred due to the spectrum condition, $k^+ > 0$, that is

[1] Note the significance of this formulation; the particle has a local coordinate although its position might be smeared. The quantum processes are local and cause divergences in the amplitude. The finite part can be calculated afterwards and depends on the smearing of the position. Although it is my belief that it should be possible to formulate the theory without these intermediate divergences, the present formulation of local field theory does not seem to allow for such a formulation.

peculiar for the light-front case. Therefore we cannot assign a proper meaning to the representation transformation $\langle k^+, \vec{k}_\perp | x^-, \vec{x}_\perp \rangle$, since the delta function in the local interaction cannot be represented by functions on $k^+ > 0$ (Schlieder & Seiler, 1972). Therefore it is not possible to make sense in a simple way of the transform between the two representations (Leutwyler & Stern, 1978). However, we know that the relations above hold, due to our investigations in the third chapter.

The major difference between the equal-time Hamiltonian and the light-front Hamiltonian is in the coupling to the different Fock sectors. In the relativistic theory the relativistic invariance intertwines with the Fock state content; the particle numbers of a given system depend on the frame in which it is observed. Due to the spectrum condition the vacuum fluctuations decouple from the Hamiltonian. The spectrum condition requires that each particle, with positive p^+ momentum, must have received this momentum from another particle already present, while in the equal time formulation, particles can be created back-to-back from the vacuum if charge and spin are conserved in the process. This can be easily seen from a field theory with only three-point vertices, where we expanded the basis for the Hamiltonian in particle numbers. While the band diagonal structure of the equal-time Hamiltonian is five entries wide,

$$H_{\rm et} = \begin{pmatrix} H_0 & V & & V & & & & & \\ V & H_0 & V & & V & & & & \\ & V & H_0 & V & & V & & & \\ V & & V & H_0 & V & & V & & \\ & V & & V & H_0 & V & & V & \\ & & V & & V & H_0 & V & & \ddots \\ & & & V & & V & H_0 & V & \\ & & & & V & & V & H_0 & \ddots \\ & & & & & \ddots & & \ddots & \ddots \end{pmatrix}, \tag{6.24}$$

where $V = g(2\pi)^{-\frac{3}{2}} \prod(\sqrt{2\omega})^{-1}$ and $H_0 = \sum \omega$, the light-front Hamiltonian is only tridiagonal:

$$H_{\rm lf} = \begin{pmatrix} H_0 & V & & & & & & & \\ V & H_0 & V & & & & & & \\ & V & H_0 & V & & & & & \\ & & V & H_0 & V & & & & \\ & & & V & H_0 & V & & & \\ & & & & V & H_0 & V & & \\ & & & & & V & H_0 & V & \\ & & & & & & V & H_0 & \ddots \\ & & & & & & & \ddots & \ddots \end{pmatrix} \tag{6.25}$$

where $V = g(2\pi)^{-\frac{3}{2}} \prod(\sqrt{2k^+})^{-1}$ and $H_0 = \sum(k_\perp^2 + m^2)/(2k^+)$. Therefore, the computational advantage is large, since each entry in the matrix is an infinite dimensional space of the n-particle wave functions. Note also that the diagonal entries grow with the particle number, which suppresses the higher Fock states in the low-lying energy eigenstates, due to the virtuality of these higher Fock states.

Moreover, in deep-inelastic scattering there are advantages related to the specific differences in Fock-state contents due to the choice of time direction. In deep-inelastic scattering the true, or laboratory, time direction goes to the light-cone time and the frame-dependent Fock states will be more and more alike the outgoing states for higher and higher energies (Kogut & Susskind, 1973).

6.3 The relativistic Coulomb potential

In order to check the usefulness of the results above we investigate the bound-state equation of scalar electrodynamics. The lowest relevant Fock-state, ϕ_2, consists of two particles with opposite charge, e, which move back-to-back: $\vec{k}_1 = \vec{k}$ and $\vec{k}_2 = -\vec{k}$. We cut the Fock basis in such a way that we only allow for one extra massless particle. We can solve the eigenvalue equation for the three-particle state, which leads to an integral equation for the two-particle state, ϕ_2:

$$(E - 2\omega_k)\,\phi_2(k) = \frac{e^2}{(2\pi)^3\omega_k}\int \frac{\mathrm{d}^3k'}{4\omega_{k'}|k-k'|}\frac{\phi_2(k') - \phi_2(k)}{(E - \omega_k - \omega_{k'} - |k-k'|)}\ , \tag{6.26}$$

where the kernel of the integral equation represents two exchange diagrams and two divergent self-energy diagrams (see fig. 6.1). If the coupling, e/m, is weak [2], it will follow that $E_b \ll |\vec{k}| \ll m$, and the two-body equation will reduce to the Schrödinger equation with a Coulomb potential,

$$\left(E_b + \frac{k^2}{m}\right)\phi_2(k) = \frac{e^2}{4(2\pi)^3m^2}\int \mathrm{d}^3k'\frac{1}{|k-k'|^2}\phi_2(k')\ , \tag{6.27}$$

f the self-energy is also neglected. The binding energy $E_b = 2m - E$. The Fourier transform of the Coulomb potential is given by (Gel'fand & Shilov, 1964):

$$\frac{1}{\sqrt{2\pi}^3}\int \mathrm{d}^3k\mathrm{e}^{i\vec{k}\cdot\vec{r}}\frac{1}{r} = \sqrt{\frac{2}{\pi}}\ \frac{1}{|k|^2}\ . \tag{6.28}$$

As we expect the differences between the nonrelativistic Coulomb potential and our kernel to be the largest for s-waves we project on $l = 0$, which gives us the one-dimensional integral equation:

$$(E - 2\omega_k + \Sigma)\,\phi_2(k) = \frac{-e^2}{4(2\pi)^2|k|\omega_k}\int_0^\infty \frac{k'\mathrm{d}k'}{\omega_{k'}}\ln\left[\frac{-E + \omega_k + \omega_{k'} + |k+k'|}{-E + \omega_k + \omega_{k'} + |k-k'|}\right]\phi_2(k')\ . \tag{6.29}$$

The presence of the eigenvalue in the kernel of the integral equation should not surprise us. We eliminated the three-particle sector in order to obtain an effective two-body equation. The eigenvalue appears to regulate the infrared singularity of the Coulomb potential; if the two particles are bound the state has an energy below the production threshold, away from the singularity.

[2] Our scalar dimensionful relativistic coupling e is related to the electromagnetic coupling in Gauss units, e_{Gauss}, by: $e^2/(16\pi m^2) = e^2_{\mathrm{Gauss}}$

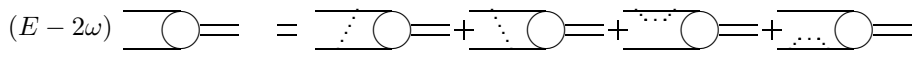

Figure 6.1: The diagrammatic representation of the bound-state equation with one massless exchange particle.

The self-energy, Σ, is divergent:

$$\Sigma = \frac{e^2}{(2\pi)^3}\int \frac{\mathrm{d}^3k'}{4\omega_k\omega_{k'}|k-k'|}\frac{1}{(E-\omega_k-\omega_{k'}-|k-k'|)} \;\rightarrow\; \infty\,. \tag{6.30}$$

However, the finite part goes like: $\Sigma \sim e^2/m^2(E_b+\vec{k}^2/m)\ln(E_b/m+\vec{k}^2/m^2)$, which is small in the weak coupling limit.

6.3.1 Numerical results

We calculated the spectra corresponding to the non-relativistic Coulomb potential and the effective relativistic two-body potential numerically. In order to estimate the effects of including the energy dependence and using relativistic kinematics separately, we repeated our calculations for three approximations: one with relativistic kinematics only, another with non-relativistic kinematics, but including the energy dependence, the third one with the full effective two-body kernel but still without the self-energy term. The corresponding kernels for the integral equations are:

$$K(k,k')_{\mathrm{non-rel,\,E\,indep}} = \ln\left[\frac{|k+k'|}{|k-k'|}\right], \tag{6.31}$$

$$K(k,k')_{\mathrm{rel,\,E\,indep}} = \frac{m^2}{\omega_{k'}\omega_k}\ln\left[\frac{|k+k'|}{|k-k'|}\right], \tag{6.32}$$

$$K(k,k')_{\mathrm{non-rel,\,E\,dep}} = \ln\left[\frac{E_b+|k+k'|}{E_b+|k-k'|}\right], \tag{6.33}$$

$$K(k,k')_{\mathrm{rel,\,E\,dep}} = \frac{m^2}{\omega_{k'}\omega_k}\ln\left[\frac{-E+\omega_k+\omega_{k'}+|k+k'|}{-E+\omega_k+\omega_{k'}+|k-k'|}\right]. \tag{6.34}$$

In order to be ale to include the self-energy we had to renormalize it. We subtracted the value of the self-energy for $E=2\omega_k$ such that it vanishes if the constituents share enough energy that both can be on-shell. The integral can be performed analytically:

$$\int_0^\infty \frac{k'\mathrm{d}k'}{\omega_{k'}}\ln\left[\frac{-E+\omega_k+\omega_{k'}+|k+k'|}{-E+\omega_k+\omega_{k'}+|k-k'|}\right]_{\mathrm{subtracted}} = \tag{6.35}$$

$$m^2\ln[m]\left(\frac{1}{-E+k+\omega}-\frac{1}{k-\omega}\right)-\frac{m^2}{2}\ln[k+\omega]\left(\frac{2\omega}{m^2}+\frac{2\omega-2E}{E(E-2\omega)+m^2}\right)$$
$$+\frac{1}{2}\ln[-E+2\omega](-E+2\omega)\left(1+\frac{m^2}{(-E-k+\omega)(k+\omega)}\right)$$

$$-\frac{1}{2}\ln\left[-E+k+\omega+\frac{m^2}{k+\omega}\right](-E+2k+2\omega)\left(1+\frac{m^2}{(-E+k+\omega)(k+\omega)}\right).$$

We can make an expansion of the self-energy, including the phase-factor ω_k, in k and find:

$$\Sigma \sim -\frac{e^2}{16\pi^2 m^2}\frac{m(E-2m)}{(E-m)^2}\left(m-E-E\ln\left[\frac{2m-E}{m}\right]\right)+ \tag{6.36}$$

$$k^2\frac{e^2}{16\pi^2 m^2}\left(\frac{E^3-E^2m+8Em^2-2m^3}{6m(E-m)^3}+\frac{E^2(E^2-4Em+5m^2)}{2m(E-m)^4}\ln\left[\frac{2m-E}{m}\right]\right)+\mathcal{O}(k^3).$$

If we expand in the binding energy, E_b, we find that for small and large values of E_b the self-energy give large corrections to the integral equation:

$$\Sigma \sim -\frac{e^2}{16\pi^2 m^2}E_b\left(1+2\ln\left[\frac{E_b}{m}\right]\right)+\frac{e^2}{16\pi^2 m^2}\frac{k^2}{m}\left(3+2\ln\left[\frac{E_b}{m}\right]\right). \tag{6.37}$$

The formula shows in the nonrelativistic approximation the major effects of the self-energy; an attractive energy shift and scaling of the kinetic energy. For the cases we have examined the net effect is a lowering of the energy eigenvalues. The self-energy vanishes for $E_b \to 0$ and $k \to 0$ due to our on-shell renormalization; however, for small values of E_b and k the contributions are still considerable, and the expansion, eq. (6.37), will be inappropriate. The results for a rather weak interaction are given in table 6.1. The colomns denoted by "non-rel, E indep" ... "rel, E dep" correspond to the kernels given in eqs. (6.31) ... (6.34) resp. In these calculations the self-energy was neglected. The last column in table 6.1 gives the spectrum for the complete model: kernel (6.34), self-energy included.

Table 6.1: Spectra for five versions of the Coulomb interaction. The mass is $m = 2.0$ and the charge is $e_{\mathrm{Gauss}} = 0.1$. The first five eigenvalues are calculated using a 10-dimensional basis. All energies must be multiplied with 10^{-4}

n	non-rel E indep	rel E indep	non-rel E dep	rel E dep	rel Σ incl
1	-0.500000	-0.499734	-0.482806	-0.434737	-0.5548556
2	-0.125000	-0.124900	-0.120705	-0.098501	-0.1325679
3	-0.055556	-0.054483	-0.053623	-0.038999	-0.0538246
4	-0.031250	-0.031187	-0.030142	-0.018783	-0.0266230
5	-0.020000	-0.019992	-0.019274	-0.009359	-0.0143953

The effects of relativistic kinematics and the energy dependence of the effective interaction become more pronounced for a stronger interaction. Therefore we also calculated the case where the coupling constant e_{Gauss} has the value 0.5. The results are given in table 6.2, which is organized in the same way as table 6.1. Both sets of results are also shown in figure 6.2.

It is clear from the two tables that the effects of relativistic kinematics, the energy-dependence of the effective interaction and the self-energy become more pronounced as the strength of the interaction is increased.

The effect of using relativistic kinematics is well known and easily understood, so we shall not discuss it here. Including the energy dependence is more interesting.We see that it is repulsive and that it changes the binding energy for the strong coupling case by ≈ 30 %. The reason for this repulsion is understood by comparing eqs. (6.31) and (6.33). The appearance of E_b, which is greater than zero, in the argument of the logarithm removes the singularity in the forward direction. The latter reflects the infinite range of the non-relativistic Coulomb potential. So its removal changes the behavior of the potential at large distances from r^{-1} to r^{-2}.

Table 6.2: Spectra for five versions of the Coulomb interaction. The mass is $m = 2.0$ and the charge is $e_{\rm Gauss} = 0.5$. The first five eigenvalues are calculated using a 10-dimensional basis.

n	non-rel E indep	rel E indep	non-rel E dep	rel E dep	rel Σ incl
1	-0.031250	-0.029539	-0.021833	-0.014631558	-0.1060710
2	-0.007813	-0.007546	-0.005497	-0.003463290	-0.0690461
3	-0.003472	-0.003384	-0.002445	-0.001399581	-0.0625281
4	-0.001953	-0.001912	-0.001375	-0.000684237	-0.0611915
5	-0.001250	-0.001227	-0.000880	-0.000360291	-0.0603675

For strong coupling, the self-energy dominates. To our knowledge, this has not been noticed earlier. However, Levine *et al.* (Levine et al., 1967) calculating the phase-shifts of the ϕ^3 theory, using the ladder approximation in the Bethe-Salpeter equation, find also large effects from the self-energy contributions. In the realistic case, where the spins of the fermions are included, the self-energy is smaller for the upper components of the spinors, where cancelations occur. This was illustrated before where we calculated the nucleon self-energy. (See sect. 4.9) So we may expect that the large differences between the non-relativistic Coulomb spectrum and the spectrum calculated using our effective two-body equation will be reduced in the realistic case.

6.3.2 Beyond three-particle states

In perturbation theory the Hamiltonian for the two-and three-body states leads to the ladder equation in the time-ordered theory, with the proper phase-space factors and self-energy corrections. These diagrams are the only possible ones in the two and three-particle sector. If we include higher Fock states, we will automatically generate all the appropriate self-energy and exchange diagrams for the kernel of the integral equation. This can be seen if one inverts the relations in the eigenvalue equation, $E\psi = H\psi$, between the $n+1$ particle state and the n particle state:

$$V\phi_n = -H_0\phi_{n+1} + K_{n+2}\phi_{n+1} \quad \Rightarrow \quad \phi_{n+1} = -\frac{1}{H_0}\sum_{j=0}^{\infty}\left(K_{n+2}\frac{1}{H_0}\right)^j V\phi_n = K_{n+1}\phi_n. \tag{6.38}$$

Figure 6.2: The lefthand spectrum visualizes the results of table 6.1. The righthand one corresponds with table 6.2.

The kernel, K_{n+2}, of the equation for the $n+1$ particle state is summed to infinite order to obtain the kernel, K_{n+1}, of the n particle state. If there are other methods to deal with the truncated Fock space, one will see that these methods incorporates the standard integral equations with (multiple) exchange diagrams.

6.4 Higher Fock states in the light-front formalism

In the previous sections we defined the relativistic Schrödinger equation, and applied this equation in the weak coupling limit to derive the relativistic version of the Schrödinger equation with a Coulomb potential. If the coupling is stronger these approximations cannot be made and the picture of the bound state will change drastically. First, the binding energy is in the range of the masses, relativistic effects, and effects such as recoil and energies carried by the exchanged particles, become important. Secondly, if a stronger binding occurs more exchange particles will be present at the same time, and the "potential" would arise from coherent processes of emission of several virtual particles. However, the simple potential picture corresponds to the instantaneous emission of one field quantum. This simple picture will be unrealistic.

Little is known about these generalized potentials, apart from the quantized version of the classical asymptotic Coulomb field first studied by Dirac (Dirac, 1974), and some indirect knowledge due to the studies of coherent states in quantum mechanics.

The Hamiltonian approach is well-suited for the study of strongly interacting theories. In this section we will study these aspects for massive ϕ^3 theory. The actual theory is not so important at this level since the major contributions to the higher Fock states are due to the trees where the type of theory only results in additional combinatorial factors. Although we are considering strongly interacting theories, we will use perturbation theory. Quantum field theory is only a formal theory without additional assumptions which make it calculable. In order to implement quantum corrections one has to start with an unperturbed ground state. Generally, this ground state is the free vacuum. Apart from the Higgs mechanism very little is known about implementation of other ground states in a full calculation.[3] Our results legitimate this starting point, because, as we will see, the kinematical factors will outweigh the coupling constant for the higher Fock states and suppress these eventually. The content of the higher Fock states determines the true nonperturbative content of the theory which is dynamically generated.

This section will illustrate some of the ideas of a quantum mechanical approach to field theory. We aim to invoke an intuitive picture where a stationary state makes sense and the calculations have a more direct interpretation in known objects. This requires the introduction of a state which is the superposition of different Fock states. A constituent can be ssen as the sum of one particle in the lowest Fock state and virtual states with more particles which couple to this particle. Interaction is not so much a matter of coupling, as it is a matter of correlation between the different constituents.

The weak coupling approximation is used in many cases, even in cases where the coupling constant is rather large (Wilson et al., 1994). In this section we will investigate how kinematics, combinatorics and virtuality of states play a role in the occupation of the higher Fock states, and how this influences the results of deep-inelastic scattering experiments. The weak coupling limit can be related to the occupation of the higher Fock states; if the population of a higher

[3] One might also ask oneself how to define an S matrix with a background field.

Fock state is much less than the lower state:

$$\cdots \gg \phi_j \gg \phi_{j+1} \gg \phi_{j+2} \gg \cdots \ , \tag{6.39}$$

we can argue that the wave functions and occupation of the higher Fock states is dominated by the tree-level results. This is the case in a weakly coupled theory, which means that different Fock states are coupled weakly. We will make this discussion more quantitative in this section. As a first approximation to each Fock state we consider the tree level result. In order to do so we have to assume some wave function for the lowest (or lower) Fock states. The bound state, a composite particle, is approximated by an elementary particle which couples to the constituents below the production threshold where the constituents can be on-shell. So we consider the n particle Fock states generated from the same trunk; the "elementary" bound state.

This approximation of the lowest Fock state gives reasonable results. A bound state with small binding energy, compared to the masses, has a wave function dominated by the low momenta, while a strongly bound system is dominated by the higher momenta, as determined by the phase spaces. Moreover, if the bound state has a total momentum different from zero, the tree diagram will account for the lowest order correction due to the Lorentz contraction of the wave function. This can easily be shown.

Lepage and Brodsky found that the lowest Fock states dominate[4] the cross section in exclusive hard scattering (Lepage & Brodsky, 1980). The higher Fock components are suppressed because of small wave function overlap. In exclusive processes in QCD this corresponds to one-gluon-exchange between the constituents which dominates the high-momentum tail of the wave functions. In this section we examine the bound state, where the higher Fock components cannot be discarded a priori, as we are interested in the wave function for all values of the momentum.

As said before, at tree level the higher Fock states, ϕ_n, are determined by kinematics, combinatorics and virtuality. We will use the light-front formalism since then the kinematics and the virtualities are determined largely by the longitudinal momenta; the transverse momenta play a minor role. At tree level, the results are equivalent to the covariant results, apart from the phase-space factors of the outgoing particles which depend on the time direction.

The number of diagrams for an n particle Fock state grows extremely rapidly. In ϕ^3 theory one finds that

$$\text{the number of trees is } \left(\frac{n!(n-1)!}{2^{n-1}}\right) \ . \tag{6.40}$$

However, the contribution of each tree decreases with j and n in

$$\phi_{j+n}(E) = \left(\sum_{\text{all}} \text{tree}\right) \phi_j(E), \tag{6.41}$$

which is nothing else but eq. (6.13) where the interaction V only increases the number of particles. The kinematical domain in the longitudinal momenta, $k_j^+ = x_j P^+$, is bound by the spectrum condition: $x_j > 0$ and $\sum x_j = 1$. P^+ is the total longitudinal momentum in the system. We can examine the properties of the wave functions at the boundaries of this domain.

[4]This is a gauge-dependent statement, and a priori only true in $A^+ = 0$ gauge.

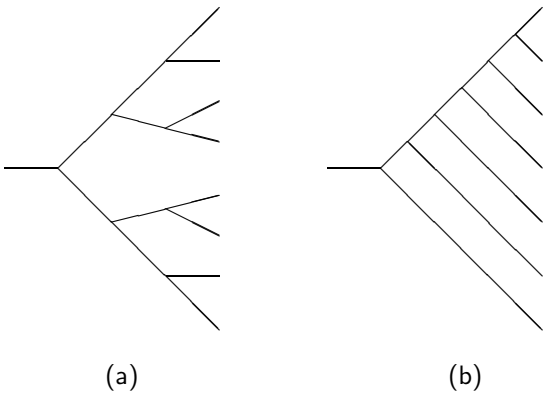

Figure 6.3: (a) The fully branched tree, (b) the one branch tree.

One can easily show that at the faces of the boundary of the kinematical domain the wave functions vanish, while in the corners integrable singularities occur, which are to leading order:

$$|\phi_n(x,\cdots,x,x_{j+1}\cdots,x_n)\rangle \underset{x\to 0}{\sim} x^{-\frac{1}{2}j+2}, \tag{6.42}$$

where $(x_i \neq 0)$. Numerical studies show that ϕ_n can be approximated in most of the kinematical domain by a constant function of the longitudinal momentum fraction, x_j. This can be used to study the influence of kinematics on the different Fock states. The boundaries influence the distributions of longitudinal momenta only little. This will be shown later.

A constant wave function is an uncorrelated wave function. In order to study the dynamics of binding one has to include correlation, which is essential for binding. At the moment we are not concerned with the precise mechanism of binding.

Trees with different topologies contribute differently to the wave function. The largest contribution is from the fully branched tree, while the one-branch tree contributes the least (see fig. 6.3). In order to estimate the wave function, ϕ_n, we assume the wave function to be constant and the largest contribution to the tree diagrams to arise when the longitudinal momenta are equally distributed.[5] The large contribution of the fully branched tree to the wave function legitimates this assumption. In the fully branched tree the momenta are equally distributed in the lines. The center of the kinematical domain of the virtual state ensures that for each intermediate state in the tree the largest contribution is due to the center of this kinematical domain as well, since the momentum of each intermediate line is fixed by the momenta of the final lines of the virtual state. So for the wave function ϕ_n we assume that

[5]This leading contribution is quite opposite to the leading contributions in deep-inelastic scattering, where the momentum flow favors the one-branch tree, which give rise to the ladder diagram. This shows that deep-inelastic scattering surveys the corners of the kinematical domain, which are not essential to the binding mechanism in strong-coupling theories.

each particle carries longitudinal momentum $n^{-1}P^+$. Then, for each new branch in the tree we get a phase-space factor, $n/(2P^+)$, and an energy denominator; $2P^+(n^2m^2)^{-1}$. The initial energy is neglected since it cannot compete with the virtuality, which grows like n^2. We neglect the correlation between the transverse momenta, sum all the trees and find an approximation for the n particle state.[6] A slight adjustment gives the result practical value:

$$\phi_n = \frac{\Gamma(n) g^{n-1} \sqrt{2\pi}^{3(1-n)}}{[m^2 + (q_1^\perp)^2][(m^2 + (q_1^\perp)^2 + (q_2^\perp)^2] \cdots [m^2 + (q_1^\perp) \cdots (q_{n-1}^\perp)^2]}. \tag{6.43}$$

Strictly speaking an additional factor $j+1$ would occur for each of the masses in the denominator, where j is the number of transverse momenta in that particular factor in the denominator. However, one cannot perform the integrations in that case, and that formula would have little practical value. Later we will estimate the error due to our adjustment.

Any additional effects due to boundaries, correlation, etc. will be of the order of some constant to the nth power, which can be incorporated in a change in the coupling constant. $\Gamma(n)$ is the combinatorial factor signifying the number of ways branches can grow on the tree. Because of the slight change, we have underestimated the masses in each of the denominators. We take the wave function constant in the longitudinal momenta. In the full calculation the wave function peaks slightly in the middle of the kinematical domain for lower Fock states, while it peaks at the boundary for the higher Fock states. This peaking is the result of the phase-space factors which will dominate for high virtualities, while for the low Fock states the energy denominators determine the overall feature of the wave function. Similar results were found in a phase-space analysis by Kuti and Weisskopf (Kuti & Weisskopf, 1971).

We find

$$\langle \phi_n | \phi_n \rangle = \frac{g^{2(n-1)}}{2^{3(n-1)} \pi^{2(n-1)} \Gamma(n) m^{2(n-1)}}, \tag{6.44}$$

using the Dirichlet integral (Whittaker & Watson, 1927):

$$\int \mathrm{d}x_1 \cdots \mathrm{d}x_n f(x_1 + \cdots + x_n) x_1^{\alpha_1 - 1} \cdots x_n^{\alpha_n - 1} = \frac{\Gamma(\alpha_1) \cdots \Gamma(\alpha_n)}{\Gamma(\alpha_1 + \cdots + \alpha_n)} \int_0^1 \mathrm{d}\tau \; f(\tau) \tau^{\sum \alpha - 1}, \tag{6.45}$$

where $x_j > 0$ and $\sum x_j < 1$, and also:

$$\int \frac{\mathrm{d}^2 q_1^\perp \mathrm{d}^2 q_2^\perp \cdots \mathrm{d}^2 q_{n-1}^\perp}{[m^2 + (q_1^\perp)^2]^2 [(m^2 + (q_1^\perp)^2 + (q_2^\perp)^2]^2 \cdots [m^2 + (q_1^\perp)^2 \cdots (q_{n-1}^\perp)^2]^2} = \frac{(\pi)^{n-1}}{\Gamma(n) m^{2(n-1)}}. \tag{6.46}$$

[6] I'm obliged to comment on the pathology of ϕ^3 theory (Baym, 1959). We are interested in the momentum flow through the trees and the contributions of different trees, therefore we neglected spin and other stuffings of the diagrams, and ended up with a theory which is considered "sick". If one considers the constant field mode, $\vec{k} = 0$, one can add an arbitrary background field: $\phi(\vec{k} = 0) \to \phi(\vec{k} = 0) + a$ which lowers the energy. The theory has no ground state. In high orders of perturbation theory one should feel the consequences of this feature. We will see that the wave function grows factorially with the number of particles for $\phi(\vec{k} = 0)$. However, the occupation probability remains finite since the region around $\vec{k} = 0$ becomes smaller and smaller in the phase space of more and more particles. Moreover, since we are considering a state with a definite longitudinal momentum there is no direct coupling to the vacuum, and our results are not influenced by the instability of the vacuum.

Given the wave functions, ϕ_n, we can calculate the distribution of the momenta. The self-energy has to be renormalized, since the expectation value of $(q^\perp)^2$ is infinite. However, we can neglect the infinite contribution of $(q_1^\perp)^2$ which is the same for each tree and retain the finite part:

$$\begin{aligned}\langle\phi_n|\frac{1}{n}\sum_{j=1}^{n}\delta(x-x_j)|\phi_n\rangle &= (n-1)(1-x)^{n-2}\langle\phi_n|\phi_n\rangle \\ \langle\phi_n|\frac{1}{n-2}\sum_{j=2}^{n-1}(q_j^\perp)^2|\phi_n\rangle &= m^2\langle\phi_n|\phi_n\rangle \end{aligned} \tag{6.47}$$

Since we underestimated the masses in each denominator it is possible that the expectation value of the transverse momentum square has a logarithmic dependence on the particle number:

$$\langle\phi_n|\frac{1}{n-2}\sum_{j=2}^{n-1}(q_j^\perp)^2|\phi_n\rangle \sim m^2\langle\phi_n|\phi_n\rangle\ln n\ . \tag{6.48}$$

The longitudinal momentum is contracted at $x=0$, which constitutes a smearing of the wave function along the associated light-like direction in configuration space. The smearing of the longitudinal space variable is not compensated by a contraction in the transverse direction, and the higher Fock states are extended in configuration space with respect to the lowest Fock state. This result is not obvious and might depend on the precise choice of theory. Commonly this smearing is assumed to occur, in analogy with the potential picture, where the exchanged particles generate a cloud around the constituents and thus account for the spread of the higher Fock state. However, there is little ground for this assumption. It might well be that the precise dynamics of binding depends on the spread of the higher Fock states. In one case these higher Fock states might form the background field through which the constituents move; in another case the constituents can be screened by the higher Fock states and only generate an effective charge.

We can elaborate on the distribution of longitudinal momenta. The gross behavior of the distribution, away from the end points, is dominated by the particle number. If we introduce the uncorrelated one-particle wave function, x_j^α, which pushes the distribution to the end points for $\alpha<0$ and inward for $\alpha>0$, we will find that the general behavior changes only slightly ($\alpha\sim 0$):

$$\begin{aligned}&\int \mathrm{d}x_1\cdots\mathrm{d}x_{n-1}(1-x_1\cdots-x_{n-1})^\alpha x_1^\alpha\cdots x_{n-1}^\alpha &=& \\ &\frac{\Gamma(1+\alpha)^{n-1}}{\Gamma((n-1)(\alpha+1))}\int_0^1 \mathrm{d}\tau(1-\tau)^\alpha\tau^{(n-1)(\alpha+1)-1} &=& \frac{\Gamma(1+\alpha)^n}{\Gamma(n(\alpha+1))}\ ,\end{aligned} \tag{6.49}$$

while the end point, ($x\to 0$), behavior can change considerably:

$$\int \mathrm{d}x_1\cdots\mathrm{d}x_{n-1}\delta(x-x_j)(1-x_1\cdots-x_{n-1})^\alpha x_1^\alpha\cdots x_{n-1}^\alpha = \frac{\Gamma(1+\alpha)^{n-1}x^\alpha(1-x)^{(n-1)(\alpha+1)-1}}{\Gamma((n-1)(\alpha+1))}\ . \tag{6.50}$$

The latter integral is calculated by scaling the momenta: $x_i \to (1-x)x_i'$. The integration over x_j results in the Dirichlet integral over the reamining variables. The correction to lower Fock states can be approximated with a larger value of α ($\alpha \sim \frac{1}{2}$) than the value of α ($\alpha \sim 0$) for higher Fock states (Kuti & Weisskopf, 1971).

The tree diagrams were our first estimate to the Fock state contents of a given bound state. Corrections to these results are radiative corrections with additional closed loops. Expanding in the maximal number of particles and the number of additional loops, we find the first correction to the bound state energy in the form of the expectation value of $E - H_0$,

$$\Sigma_{irr}^{(1)} = \langle\psi|(E - H_0)|\psi\rangle \ , \tag{6.51}$$

which would be the same result as in field theory if we calculated ψ exactly from the different trees. All the loops are due to contracting the bra and the ket. Additional loops would correspond to higher order corrections of lower Fock states. However, we are concerned with the general behavior for high Fock states. The higher Fock states are influenced less by the (finite part of the) radiative corrections. Note that the infinite part affects all states alike by changes in masses and coupling constants. Since these states are highly virtual, the actual energy of the trunk has little influence on the finite result. If we use the following trick:

$$\phi_n(E') = \frac{1}{E' - H_0} V \frac{1}{E - H_0} V \cdots V \frac{1}{E - H_0} V |\phi_1\rangle, \tag{6.52}$$

and expand this expression in powers of E'/H_0, we will find the finite part of the radiative corrections to the lowest order:

$$\Sigma_{irr}^{(1)} = \int_0^E \mathrm{d}E' \langle\psi(E')|\psi(E')\rangle \sim E + \sum_{j=2}^{\infty} \frac{E^2}{j^2 m^2} \langle\phi_j|\phi_j\rangle \ . \tag{6.53}$$

Similarly, we find that the radiative corrections due to one loop insertions at a specific level in the tree are suppressed, because of the extra energy denominators in the radiative corrections, by the factor $g^2/((2\pi)^3 n m^2)$, where n is the number of particles at this level.

We can conclude that, while the lowest Fock states can change much due to radiative corrections, this is not the case for the higher Fock states. The scale is naturally given by the wave functions of the lowest Fock state. Therefore, radiative corrections are restricted to the energy, corresponding to this scale. Hard processes do not occur, therefore no other scale is introduced. We saw that the higher Fock states, which are highly virtual, are not influenced much by the quantum corrections.

6.5 Conclusions

If we want to understand the bound state in field theory we will have to replace the potential picture by the virtual cloud picture. The Hamiltonian formulation is most suited to gain insight into the virtual cloud picture. The virtual cloud is the unseen part of the bound state, and, for that matter, the unseen part of all particles. Because of the interaction, a particle couples to multi-particle states which spread around the original particle. These higher Fock states belong to actual content of the physical particle. Although we describe the constituent by the

coordinate of the particle in the lowest Fock state, we must be aware that this particle is not the constituent but only a part of the constituent, i.e. the lowest Fock state. The higher Fock states determine the range of influence; the strength and the range of the interaction.

The connection between Hamiltonian field theory and covariant Langrangian field theory has been unclear. The local Lagrangian density leads to a nonlocal Hamiltonian as the result of causality. Causality results in the implementation of the second boundary condition, eq. (6.7), of the relativistic wave equation. The additional phase-space factors improve the short-distance behavior of the theory. These phase-space factors make some of the so-called nonperturbative form factors superfluous.

We have seen that to low orders in particle number this wave function picture gives a good approximation for the Coulomb potential. The infrared singularity of the Coulomb potential is regulated by the binding energy. Additional corrections occur when the binding energy is of the same order as the constituent mass.

The features of the virtual cloud, which can be a relatively large part of the physical wave function, is studied in the light-front formalism. The kinematics will outweigh the coupling constant for high Fock states such that these high Fock states are suppressed even for a coupling constant of the order one. In a bound state there is only one scale; the scale of the lowest Fock state wave function. This scale determines the constituent masses, which is the particle mass with self-energy corrections due to binding, since the particles are bound they are off-shell. The sum of the masses is larger than the mass of the bound state. In a covariant formulation the dynamics is related to scales. In the virtual cloud picture one has to ask the question how much the clouds are part of each constituent and how much is shared as a background in which all the constituents move. If the clouds are parts of the separate constituents they will be described by the properties of the lowest Fock state particles separately and thus can be interpreted as self-energy corrections and screening, i.e. as scaling of the particle properties. The breakdown of the scale picture in the covariant theory signifies which part of the cloud is shared among the constituents. At very large length scales the system is chargeless and the virtual cloud vanishes.

In the last section we have seen that the high Fock states form a background with respect to the lower Fock states. The overall distribution of the longitudinal momentum is determined by the Fock states occupations, while the distribution of the transverse momenta remains the same for all the Fock states.

The Hamiltonian formulation is consistent with known results. It increases our understanding of field theory, and allows for implementation beyond the realm of perturbation theory. The potential picture can be replaced by a more accurate picture of higher Fock states. In terms of higher Fock states, the potential is the energy density change due to the interference between the virtual clouds which surround each of the constituents.

Summary and conclusions

In this thesis different aspects of Hamiltonian field theory are discussed. The greater part of the thesis deals specifically with light-front Hamiltonian field theory. Although, as is shown in the second chapter, classical light-front field theory is ill-defined, still it is possible to establish a proper one-to-one correspondence between light-front perturbation theory and covariant perturbation theory. This correspondence constitutes a proof of equivalence between covariant field theory and light-front field theory, and is dealt with in the third chapter.

Chapters 4 and 5 deal with renormalization. A general discussion of dimensional regularization and its application to time-ordered perturbation theory forms the essence of chapter four. Chapter 5 deals specifically with the features of divergences in light-front perturbation theory. A renormalization procedure is proposed which deals with the transverse and the longitudinal singularities in the same manner. The procedure is illustrated with a number of examples.

Some conceptual problems are discussed in chapter six. We derive a relativistic Schrödinger equation from Feynman's space-time approach. This motivates the rules for "old-fashioned" perturbation theory as given by Weinberg (Weinberg, 1966), and establishes a relation with quantum mechanics and phase-space factors in scattering theory. The results from Feynman's space-time approach and stationary perturbation theory, *à la* Lippman-Schwinger, are equivalent using this Hamiltonian.

Conceptual problems were already present from the onset of light-front field theory, when Weinberg showed (Weinberg, 1966) that only some physical processes, each represented by an ordinary time-ordered diagram, contribute to the Feynman diagram if this diagram was calculated in a frame that moves with the speed of light (Kogut & Susskind, 1973). This so called *infinite momentum frame* (IMF) cannot be connected to any other reference frame by a finite Lorentz transformation. Thus, a limiting procedure is involved. This limit has to compete with other limits present in field theory: infinite space integration, regularization of singular expressions. Besides, problems might arise when we are dealing with fermions (Ahluwalia, 1992). That the IMF is naturally described with light-front coordinates is only apparent for coordinates and momenta (Leutwyler et al., 1970). That only some diagrams survive (Chang & Ma, 1969) is puzzling. However, we have shown that this, in general, is indeed true. Another possible approach to light-front field theory is the direct quantization on a light-front. There are many different ways to do this, which become more elaborate if the theories are supposed to incorporate more features (Kalloniatis & Robertson, 1994). As a classical theory, light-front field theory is ill-defined; the standard initial value problem on the light-front is overdetermined. In addition, it leads to a non-unique evolution in time (Hörmander, 1963) (see also chap. 2). The first problem can be solved in principle through methods devised for the quantization of constrained systems (Dirac, 1964; Hanson et al., 1976; Sundermeyer, 1982; Henneaux &

Teitelboim, 1993). The second problem is more serious. One needs to separate degrees of freedom associated with different evolutions, from the same initial value, in l.c. time and then introduce constraints which can restrict the space of solutions to the one considered physical on some grounds. This, in essence, is what people are dealing with when they introduce zero-modes, degrees of freedom of which the evolution is unknown (zero or infinite?). This problem is often disguised in practical calculations where a $(p^+)^{-1}$-singularity occurs (Maskawa & Yamazaki, 1976; Tang, 1988; Burkhardt & Langnau, 1991; Griffin, 1992; Burkhardt, 1993).

Another way to quantize a light-front theory is to use axiomatic commutation relations on a complete set of free fields (Jackiw, 1972; Ida, 1977; Schlieder & Seiler, 1972), an approach guided by the results of current algebra (de Alfaro $\mathrm{et\ al.}$, 1973). On the light front, different points with $(\Delta x_\perp = 0)$ are light-like separated. The question arises what is the equal-time commutator between fields: a delta function in x^- which violates covariance, or a sign function in x^- which leads to non-integrable fields (except at the loss of covariance) (Nakanishi & Yamawaki, 1977). Whether such theories can describe physical processes has not been established. This approach became less favorable in the late seventies.

The approach most favored nowadays is based on two methods: with the covariant results in mind derive a "constrained Hamiltonian" (Kogut & Soper, 1970; Brodsky $\mathrm{et\ al.}$, 1973; Mustaki, 1990). Due to zero-modes it is hard to make a one-to-one correspondence between normalized states on a space-like surface and a light-like surface. As long as one deals only with tree graphs all these problems are rather formal. The presence of loops makes them acute. In loops one has to "sum over all states". This rule forces one to consider states with $p^+ \to 0$. The advantages of light-front field theory are paid for by the occurrence of problems. In the approaches discussed here the problems arise in different forms and are dealt with in different ways. They might be disguised as technical difficulties. Due to the fundamental nature of these problems the final results depend strongly on the choices one has to make when defining the (finite) theory, e.g., boundary conditions of fields quantized in a box (Neville & Rohrlich, 1971; Huang & Lin, 1993), or regularization of the $(p^+)^{-1}$ singularity (Maskawa & Yamazaki, 1976; Tang, 1988; Burkhardt & Langnau, 1991; Griffin, 1992; Burkhardt, 1993). We also had to make some choices. Wherever we had to do so, we emphasized the relation with Feynman diagrams. In a manifestly covariant approach there is no $(p^+)^{-1}$ singularity. It is a distinct advantage of our approach that this singularity is absent too (see sect. 3.5). We seem to have cured one of the diseases of light-front field theory. However, presently we do not know whether our regularization procedure leads in all cases to the same answer as the covariant approach.

In the fifth chapter we have shown that using the proper regularization procedure we recover the covariant results from divergent diagrams. The additional divergences, which occur in light-front perturbation theory, cannot correspond to Lorentz invariant objects and are automatically removed when the finite part of the amplitude is determined. It seems that the longitudinal singularities are similar to the gauge dependent parts in gauge field theories; they complicate the calculations, but they should not influence the physical observables.

We have shown (see sect. 3.5.1) that in some cases there are $\delta(p^+)$ contributions to the S matrix. Maybe these terms indicate a coupling to the "vacuum" or they may represent contributions which relate one version of light-front field theory to another by a finite renormalization. However, it would be good practice to try to separate the mathematical question "how to calculate?", from the physical one "how to interpret?".

We consider the present situation in light-front field theory to be confused. We give three

reasons for this point of view:

(i) The paucity of comparisons to standard covariant theories;

(ii) The mixing of mathematical problems with physical ones;

(iii) The lack of consensus on what are the established results (with proper, mathematically rigorous derivations).

Still, there are a five good reasons to work on light-front field theory:

(a) It is the only theory distinctly different from covariant field theory which allows for a comparison at intermediate levels. Such a comparison increases the understanding of both theories;

(b) It is the most natural way to describe nucleons in terms of quarks;

(c) Our understanding increases with each answer to questions that light-front field theory raises;

(d) The spectrum condition suppresses the higher Fock states.

(e) It is a Hamiltonian formulation with states and time evolution. It invokes the same the intuitive picture inherent in elementary quantum mechanics.

The sixth chapter presents an outlook. Here we discuss some of the aspects of (d) and (e). First, we derive a consistent quantum mechanical picture and show that it leads to the correct results for weak-coupling scalar electrodynamics. Secondly, we combine the quantum mechanical picture with the light-front formalism and illustrate, with some calculations, the intuitive picture that arises for bound states.

The explanation of experimental results is the main success of light-front field theory (Brodsky & Pauli, 1991; Brodsky & Robertson, 1996). Mainly due to the work of Hans-Christian Pauli, Brodsky and collaborators, calculations in a Hamiltonian framework with a Fock state expansion are feasible and competitive, however, the methods are not so elegant. The direct numerical implementation makes the physics less transparent, in addition a large basis is often necessary. Apart from extension of the basis it is difficult to systematically improve the approximations. Other improvements of the scheme are based on the analysis of the numerical results. Conceptual developments of light-front field theory require a firm foundation and elegant, transparent methods. Exact results rarely exist for physical systems, therefore systematic approximations must be possible within the framework chosen.

Publications

Some of the results of this thesis have been published in a slightly different form. When this dissertation was printed the following articles had appeared:

1. Equivalence of light-front and covariant field theory, N.E. Ligterink and B.L.G. Bakker, Phys. Rev. **D** 52, 5954 (1995).

2. Renormalization of light-front Hamiltonian field theory, N.E. Ligterink and B.L.G. Bakker, Phys. Rev. **D** 52, 5917 (1995).

3. Feynman Diagrams and Light-Cone Time-Ordered Diagrams, Norbert E. Ligterink and B.L.G. Bakker, in *Theory of Hadrons and Light-Front QCD*, St. D. Głazek (ed.), World Scientific, Singapore, 1995.

Samenvatting

Licht-front Hamiltoniaanse veldentheorie covariantie en renormalisatie

Licht-front Hamiltoniaanse veldentheorie is de methode om processen die zich op zeer kleine schalen afspelen te beschrijven, door een waarnemer die met de snelheid van het licht reist. Maar een stoffelijke waarnemer kan niet met de snelheid van het licht reizen dus de beschrijving is abstract. De voordelen van een dergelijke beschrijving zijn vooral praktisch van aard en bovendien nog niet erg goed begrepen. Men zegt vaak dat het vacuum triviaal is, of ontkoppeld is van de fysische toestanden.
Hadronische materie, dat is de materie waar kernen uit bestaan, is desondanks het best begrepen in het licht-frontformalisme. De materie lijkt te bestaan uit een paar puntdeeltjes en een zachte wolk die de puntdeeltjes samenhoudt. Met enige experimentele informatie over de zachte wolk kunnen veel experimenten verklaard worden en processen voorspeld.
In dit proefschrift worden de grondslagen van de licht-front Hamiltoniaanse veldentheorie onderzocht. Ondanks het feit dat de quantisatie, dat is de bewerking die van golven tevens deeltjes maakt, een slecht gedefinieerd procedure is op het licht-front, is het toch mogelijk de licht-front veldentheorie een stevig fundament te geven door haar te relateren aan de covariante veldentheorie. De covariante veldentheorie wordt algemeen beschouwd als de correcte beschrijving van processen op kleine schalen, omdat het verstrooiingsexperimenten, het botsen van puntdeeltjes, uitstekend beschrijft. Maar de covariante veldentheorie faalt in de beschrijving van de karakteristieken van hadronen. De karakteristieken die wij terugvinden en waarderen in het licht-frontformalisme, namelijk, die van puntdeeltjes met de zachte wolk.
In het aantonen van de equivalentie van de covariante en de licht-front veldentheorie worden veel problemen van de licht-front-veldentheorie opgerakeld; sommige problemen waren reeds door anderen in een andere context gevonden. In dit proefschrift worden de meeste problemen eenduidig opgelost door naar de relatie met de covariante veldentheorie te kijken, op sommige vragen wordt er alleen een ander licht geworpen door dit verband te onderzoeken. In het bijzonder worden een aantal standaardtechnieken van renormalisatie kritisch onderzocht.
Dit proefschrift dient twee hoofddoelen. Ten eerste, het oplossen, of begrijpen, van de problemen die specifiek zijn voor licht-front-veldentheorie. Ten tweede, het bewijzen dat in onze aanpak de licht-front-veldentheorie een goed gedefinieerde theorie is.

Hoofdstuk 1: Introductie

We geven een beschouwing over veldentheorie in het algemeen, en beargumenteren waarom een Hamiltoniaanse aanpak beter dan covariante aanpak, op zijn plaats is voor de beschrijving

van gebonden toestanden. We geven een simpel voorbeeld waarin de karakteristieken van licht-front-veldentheorie naar voren komen.

Hoofdstuk 2: Partieële differentiaalvergelijkingen en licht-front-veldentheorie

In dit hoofdstuk beschouwen we welke consequenties de keuze van beginvoorwaarden op het licht-front hebben. Die consequenties zijn vergaand. De evolutie van een systeem is niet uniek, en sommige oplossingen zijn singulier op het licht-front en kunnen daarom daar niet beschreven worden. Het verschil tussen twee evoluties met dezelfde beginvoorwaarden is een nul-oplossing. Deze oplossingen worden expliciet geconstrueerd voor de Klein-Gordon en de Dirac-vergelijking. Tevens wordt aangetoond dat de singuliere oplossingen buiten de gebruikelijke integreerbare functieruimten liggen. Deze eigenschappen voor licht-achtige beginvoorwaarden hebben grote consequenties voor quantisatie en renormalisatie.

Hoofdstuk 3: Equivalentie van licht-front en covariante veldentheorie

In dit hoofdstuk wordt de relatie aangetoond tussen de storingstheorie voor de covariante beschrijving van verstrooiing en de lichtkegel-tijdgeordende beschrijving van verstrooiing. Met een algemeen algoritme kunnen Feynman diagrammen geschreven worden als lichtkegel-tijdgeordende diagrammen. De technische problemen en uitzonderingsgevallen zijn opgespoord en geanalyseerd.

Hoofdstuk 4: Een andere kijk op dimensionele regularisatie

We analyseren de dimensionele regularisatie en komen tot de conclusie dat met behulp van dimensionele analyse en differentiatie, de dimensionele regularisatie geformuleerd kan worden zonder te referen naar een niet-geheeltallige dimensie. De regularisatie geeft eindige integralen, zonder regulatoren. Het praktisch nut van deze techniek ligt vooral in de toepasbaarheid voor Hamiltoniaanse theorieën. Tevens geeft het een andere kijk op dimensionele regularisatie.

Hoofdstuk 5: Renormalisatie van licht-front Hamiltoniaanse theorieën

In dit hoofdstuk geven we een regularisatiemethode om het eindige deel te bepalenvan lichtkegel-tijdgeordende diagrammen. Hierbij maken we geen onderscheid tussen de longitudinale en de transversale dimensies. De methode is gebaseerd op de Taylor-reeksontwikkeling van de amplitude naar de externe impulsen. De instantane termen en de andere longitudinale singulariteiten worden automatisch verwijderd. We trekken hieruit de conclusie dat deze geen betekenis hebben, maar een artefact zijn van de licht-frontformulering. We geven een aantal voorbeelden; het blijkt dat altijd het correcte covariante resultaat gevonden wordt.

Hoofdstuk 6: De relativistische Hamiltoniaan in de gebonden toestand

In dit hoofdstuk wordt de relatie tussen de covariante veldentheorie en de Hamiltoniaanse veldentheorie nader beschouwd. We concluderen dat de Hamiltoniaan die correspondeert met een lokale Lagrange-dichtheid niet-lokale faseruimte-factoren bevat. Voor zwakke koppeling in de scalaire electrodynamica leiden we de relativistische versie van de Coulomb-Schrödinger vergelijking af. In het licht-frontformalisme onderzoeken we voor sterkere koppelingen de bezettingsgraad van de hogere Fock-toestanden in een gebonden toestand. Het blijkt dat de hogere Fock-toestanden kinematisch onderdrukt zijn.

Curriculum vitae

Norbert Ligterink was born in the red-brick industry town Enschede in 1968 as the son of Johan Ligterink and Geesje Ligterink-Snippe. He has one elder brother: Frank Ligterink. In 1972 the family moved to Delden where Norbert lived all throughout his childhood. He visited the primary school, the Rannink School, in Delden and the secondary school, the Twickel College, in Hengelo. Much of this spare time he spend with the scouting group in the forests which surround the village Delden.

In 1987 he moved to Amsterdam to study physics at the Vrije Universiteit and taste the city life. During his study he spend half a year at the University of Uppsala in Sweden, autumn-term 1990, and studied various subjects. Another half year he spend at the Non-linear Systems Laboratory of the mathematics department of the University of Warwick in Coventry, England, in 1992. In England he studied classical nonlinear systems and the appropriate mathematical methods for their study. After the study of current of a composite boson consisting of two fermions for his graduation thesis he graduated September 1992.

Immediately after his graduation he was employed by the FOM (Stichting voor Fundamenteel Onderzoek der Materie) to study the possibilities to use light-front field theory for the description of relativistic bound states, the product of which you have before you. This study was carried out at the Vrije Universteit under the guidance of Ben Bakker.

Apart from his interest in physics he has a broad interest in film, theater and art, and spend many hours in theaters and cinemas. From 1992 he was volunteer for the art-house cinema: Filmhuis Uilenstede. He found it necessary to have an active cultural life besides the mentally demanding study of physics.

Dankwoord

Ik moet de neiging bedwingen om iedereen en alles te bedanken. In plaats daarvan wil ik alleen zeggen dat ik de laatste jaren veel plezier heb beleefd aan mijn omgeving. De mensen om mij heen, ook de vreemden die ik op straat tegenkom, worden deel van mijn innerlijke gesprekspartner. Elk paar ogen helpt mij bij het onder woorden brengen van mijn vaste overtuiging; dwingen mij om mijn gedachten te formuleren en zo deel te zijn van de collectieve werkelijkheid.

Een paar mensen wil ik met name bedanken. Ten eerste Ben Bakker, beste Ben, voor mijn gevoel hebben we uitstekend kunnen samenwerken; ik ben weinig mensen tegengekomen met

wie ik zoveel dezelfde wetenschappelijk instelling deel. Ik denk dat dat grotendeels door jouw toedoen is. Ik heb de gemoedelijke sfeer zeer kunnen waarderen.
I would like to thank Stan Brodsky for the attention he gave to my work.
Daarnaast wil ik mijn kamergenoten Ferry Blaazer en Nico Schoonderwoerd bedanken voor de kameraadschap; het was prettig vertoeven op de werkvloer. Ik wil mijn broer bedanken voor alles. I also like to thank two girls, Katarina Elofsson and Bettina Lange, who, each in her own way, gave a new twist to my life.
I also would like to thank Thomas Heinzl, Vladimir Karmanov, Dave Robertson, Alex Kalloniatis, Piet Mulders, Rik Tangerman, Daniel Boer, Rainer Jacob, Thomas Kraan, Jozef Namysłowski, Gerald Miller, Klaas Allaart, Misha Polikarpov, Harrie Boersma, Tung-Mow Yan, Pierre van Baal, Henk Blok, Franz Gross, Ovid Jacob, Taco Nieuwenhuis, Daniel Phillips, Carlo Acerbi, Antonio Bassetto, Maxim Chernodub, Yuri Simonov, Rik Naus, John Tjon, Theo Ruijrok, Robert Perry, Gerke Nieuwland, Stan Głazek, Averoth Harindranath for many stimulating discussions.
Ik wil ook graag mijn werkgever, de stichting FOM, bedanken voor de hulp en de ruime taakopvatting. Tevens wil ik SHELL-Nederland bedanken voor de reisbeurs die het mogelijk maakte om gedurende vier weken in Amerika conferenties te bezoeken.
Als laatste wil ik mijn ouders bedanken, die de randvoorwaarden hebben geschapen die alles mogelijk maakten. Jullie gaven mij zowel de vrijheid om eigen keuzes te maken, als een onvoorwaardelijke steun.

Mijn wollen jas is doorweekt en zwaar.
Een geeuw eindigt in een koude rilling.
Het werd tijd dat ik verder ging.
Maar ik kom toch nimmer daar.
Want ik weet niet waar
dit gevoel mij heen wil leiden.
De wind waait over woeste weiden.
Het zonlicht weerkaatst in de plassen op het pad.
Ik ben vergeten wat
ik zeggen wou.
Het lopen verjaagt de kou.
Al lopend word ik een onuitsprekelijke waarheid gewaar.

References

Achtzehnter, J., & Wilets, L. 1988. Wave equation for a composite nucleon. Phys. Rev., **C 38**, 5.

Ahluwalia, D. V. 1992. Interpolating Dirac spinors between instant and light front forms. Phys. Lett., **B 277**, 243.

Baym, G. 1959. Inconsistency of cubic boson-boson interactions. Phys. Rev., **117**, 886.

Bergère, M. C., & Zuber, J. B. 1974. Renormalization of Feynman amplitudes and parametric integral representations. Commun. math. Phys., **35**, 113.

Bergstra, J. A., & Klop, J. W. 1989. Termherschrijfsystemen. Deventer, The Netherlands: Kluwer Bedrijfswetenschappen.

Bethe, H. A., & de Hoffmann, F. 1955. Mesons and fields. Vol. II. Evanston: Row, Peterson and Comp.

Bogoliubov, N. N., & Shirkov, D. V. 1959. Introduction to the theory of quantized fields. New York: Interscience.

Bollini, C. G., & Giambiagi, J. J. 1972. Dimensional renormalization: The number of dimensions as a regularization parameter. Nuovo Cim., **12 B**, 20.

Brodsky, S. J., & Langnau, A. 1993. Perturbation theory in light-cone quantization. J. Comp. Phys., **109**, 84.

Brodsky, S. J., & Pauli, H. C. 1991. Light cone quantization of quantum chromodynamics. In: The 30th Schladming winter school; Recent aspects of quantum fields. Berlin: Springer-Verlag.

Brodsky, S. J., & Robertson, D. G. 1996. Light cone quantization and QCD phenomenology. In: Bass, S. D., & Guichon, P. A. M. (eds), Confinement physics school, Cambridge, 1995. Cambridge: Editions Frontières.

Brodsky, S. J., Roskies, R., & Suaya, R. 1973. Quantum electrodynamics and renormalization theory in the infinite momentum frame. Phys. Rev., **D 8**, 4574.

Burkhardt, M. 1993. Light-front quantization of the sine-Gordon model. Phys. Rev., **D 47**, 4628.

Burkhardt, M., & Langnau, A. 1991. Rotational invariance in light-cone quantization. Phys. Rev., **D 44**, 3857.

Caswell, W. E., & Kennedy, A. D. 1982. Simple approach to renormalization theory. Phys. Rev., **D 25**, 392.

Chang, S. J., & Ma, S. K. 1969. Feynman rules and quantum electrodynamics at infinite momentum. Phys. Rev., **180**, 1506.

Chang, S. J., & Yan, T. H. 1973. Quantum field theories in the infinite momentum frame. II. Scattering matrices of scalar and Dirac fields. Phys. Rev., **D 7**, 1147.

Chang, S. J., Root, R. G., & Yan, T. M. 1973. Quantum field theories in the infinite momentum frame. I . Quantization of scalar and Dirac fields. Phys. Rev., **D 7**, 1173.

Collins, J. 1984. Renormalization. Cambridge: Cambridge University Press.

de Alfaro, V., Fubini, S., Furlan, G., & Rossetti, C. 1973. Currents in hadron physics. Amsterdam: North-Holland.

de Wit, B., & Smith, J. 1986. Field theory in particle physics. Amsterdam: North-Holland.

Dirac, P. A. M. 1949. Forms of relativistic dynamics. Rev. Mod. Phys., **21**, 392.

Dirac, P. A. M. 1964. Lectures on quantum mechanics. New York: Yeshiva University Press.

Dirac, P. A. M. 1974. The principles of quantum mechanics. Oxford: Clarendon Press.

Feynman, R. P. 1949. Space-time approach to quantum electrodynamics. Phys. Rev., **76**, 769.

Fulton, W., & Harris, J. 1991. Representation theory. New York: Springer-Verlag.

Gel'fand, I. M., & Shilov, G. 1964. Generalized functions. New York: Academic Press.

Gradshteyn, I. S., & Ryzhik, I. M. 1980. Table of integrals, series and products. New York: Academic Press.

Griffin, P. 1992. Sine-Gordon model and the small k^+-region in light-cone perturbation theory. Phys. Rev., **D 46**, 3538.

Głazek, St. D., & Wilson, K. G. 1993. Renormalization of Hamiltonians. Phys. Rev., **D 48**, 5863.

Gross, F. 1993. Relativistic quantum mechanics and field theory. New York: Wiley.

Hagen, C. R., & Yee, J. H. 1976. Light-cone quantization: Study of a soluble model with q-number anti-commutator. Phys. Rev., **D 10**, 2789.

HAHN, Y., & ZIMMERMANN, W. 1968. An elementary proof of Dyson's power counting theorem. Commun. math. Phys., **10**, 330.

HANSON, A.J., REGGE, T., & TEITELBOIM, C. 1976. Constrained Hamiltonian systems. Roma: Accademia Nazionale dei Lincei.

HEINZL, T., KRUSCHE, S., & WERNER, E. 1991a. Non-trivial vacuum structure in light-cone quantum field theory. Phys. Lett., **B 256**, 55.

HEINZL, T., KRUSCHE, S., SIMBURGER, S., & WERNER, E. 1991b. Spontaneous symmetry breaking in light cone quantum field theory. Phys. Lett., **B 272**, 54.

HEINZL, T., KRUSCHE, S., SIMBURGER, S., & WERNER, E. 1992. Nonperturbative light cone quantum field theory beyond tree level. Z. Phys, **C 56**, 415.

HEITLER, W. 1954. The quantum theory of radiation. Oxford: Clarendon Press.

HENNEAUX, M., & TEITELBOIM, C. 1993. Quantization of gauge systems. Princeton: Princeton University Press.

HEPP, K. 1966. Proof of the Bogoliubov-Parasiuk theorem on renormalization. Commun. math. Phys., **2**, 301.

HÖRMANDER, L. 1963. Linear partial differential operators. Berlin: Springer-Verlag.

HUANG, S., & LIN, W. 1993. On the zero mode problem of the light-cone quantization. Ann. of Phys., **226**, 248.

IDA, M. 1977. Canonical formalism on a lightlike hyperplane. Nuovo Cim., **A 40**, 354.

JACKIW, R. 1972. Canonical light-cone commutators and their applications; Springer tracts in modern physics. Vol. 62. New York: Springer-Verlag.

JAROSZEWICZ, T., & BRODSKY, S. J. 1991. Z-diagrams of composite objects. Phys. Rev., **C 43**, 1946.

JAUCH, J. M., & ROHRLICH, F. 1955. The theory of photons and electrons. Cambridge (Mass.): Addison-Wesley.

KADYSHEVSKY, V. G. 1964. Relativistic equation for the S matrix in the p representation. I & II. Sov. Phys. JETP, **19**, 443, 597.

KALLONIATIS, A. C., & ROBERTSON, D. G. 1994. Discretized light-cone quantization of electrodynamics. Phys. Rev., **D 50**, 5262.

KARMANOV, V. A. 1988. Relativistic composite systems in light-front dynamics. Sov. J. Part. Nucl., **19**, 228.

KOGUT, J., & SUSSKIND, L. 1973. The parton picture of elementary particles. Phys. Rep., **8**, 75.

KOGUT, J. B., & SOPER, D. E. 1970. Quantum electrodynamics in the infinite momentum. Phys. Rev., **D 1**, 2901.

KOLTUN, D. S., & EISENBERG, J. M. 1988. Quantum mechanics of many degrees of freedom. New York: Wiley.

KUTI, J., & WEISSKOPF, V. F. 1971. Inelastic lepton-nucleon scattering and lepton pair production in the relativistic quark-parton model. Phys. Rev., **D 4**, 3418.

LEE, B. W. 1976. Methods in field theory; Les Houches Summer School in Theoretical Physics. Vol. XXVIII. Amsterdam: North-Holland.

LEIBBRANDT, G. 1975. Introduction to the technique of dimensional regularization. Vol. 1975-25. Universty of Guelph, Can.: Dep. Math. Stat. Mathematical Series.

LEIBBRANDT, G. 1987. Introduction to noncovariant gauges. Rev. Mod Phys., **59**, 1067.

LEPAGE, G. P., & BRODSKY, S. J. 1980. Exclusive processes in perturbative quantum chromodynamics. Phys. Rev., **D 22**, 2157.

LERAY, J. 1953. Lectures on hyperbolic differential equations. Princeton: The Institute for Advanced Study.

LEUTWYLER, H., & STERN, J. 1978. Relativistic dynamics on a null plane. Ann. Phys., **112**, 94.

LEUTWYLER, H., KLAUDER, J. R., & STREIT, L. 1970. Quantum field theory on lightlike slabs. Nuovo Cim., **LXVI A**, 536.

LEV, F. M. 1993. Relativistic quantum mechanics and its application to few-nucleon systems. Rivista del Nuovo Cim., **16**, 1.

LEVINE, M. J., WRIGHT, J., & TJON, J. A. 1967. Effect of self-energy terms in the Bethe-Salpeter equation. Phys. Rev., **157**, 1416.

LIPPMANN, B. A., & SCHWINGER, J. 1950. Variational principles for scattering processes I. Phys. Rev., **79**, 469.

MACDONALD, I. G. 1979. Symmetric functions and Hall polynomials. Oxford: Clarendon Press.

MASKAWA, T., & YAMAZAKI, K. 1976. The problem of $P^+ = 0$ mode in the null plane field theory and Dirac's method of quantization. Prog. Theor. Phys., **56**, 270.

MCCARTOR, G. 1988. Light cone quantization for massless fields. Z. Phys., **C 41**, 271.

MILLS, R. L., & YANG, C. N. 1966. Treatment of overlapping divergences in the photon self-energy function. Suppl. Prog. Theor. Phys., **37 & 38**, 507.

MUSTAKI, D. 1990. Null plane quantization of fermions. Phys. Rev., **D 42**, 1184.

MUSTAKI, D., PINSKY, S., SHIGEMITSU, J., & WILSON, K. 1991. Perturbative renormalization of null-plane QED. Phys. Rev., **D 43**, 3411.

MUTA, T. 1987. Foundations of quantum chromodynamics. Singapore: World Scientific.

NAKANISHI, N., & YAMAWAKI, K. 1977. A consistent formulation of the null plane quantum field theory. Nucl. Phys., **B122**, 15.

NEVILLE, R. A., & ROHRLICH, F. 1971. Quantum field theory off null planes. Nuovo Cim., **1A**, 625.

NEWTON, T. D., & WIGNER, E. P. 1949. Localized states of elementary particles. Rev. Mod. Phys., **21**, 400.

PERRY, R. J. 1993. Asymptotic freedom in Hamiltonian light-front quantum chromodynamics. Phys. Lett., **B 300**, 8.

PERRY, R. J. 1994a. Hadrons 94: Topics on the Structure and interaction of hadronic systems. Singapore: World Scientific.

PERRY, R. J. 1994b. A renormalization group approach to Hamiltonian light-front field theory. Ann. of Phys., **232**, 116.

PERRY, R. J., & WILSON, K. G. 1993. Perturbative renormalizability with an infinite number of relevant and marginal operators. Nucl. Phys., **B403**, 587.

PINSKY, S. S., & VAN DE SANDE, B. 1994. Spontaneous symmetry breaking of (1+1)-dimensional ϕ^4 theory in light-front field theory. II. Phys. Rev., **D 49**, 2001.

ROBERTSON, D. G. 1993. Spontaneous symmetry breaking in discretized light-cone field theory. Phys. Rev., **D 47**, 2549.

ROBERTSON, D. G., & MCCARTOR, G. 1992. An equal-time quantized field theory on the light cone. Z. Phys., **C 53**, 661.

SCHLIEDER, S., & SEILER, E. 1972. Some remarks on the "null plane development" of a relativistic quantum field theory. Comm. math. Phys, **25**, 62.

SCHMIDT, M. G. 1974. Simple connection between covariant Feynman formalism and time-ordered perturbation theory in the infinite-momentum frame. Phys. Rev., **D 9**, 408.

SCHWINGER, J. (ed). 1958. Selected papers on quantum electrodynamics. New York: Dover.

SPEER, E. R. 1967. Analytic renormalization. J. Math. Phys., **9**, 1404.

SUNDERMEYER, K. 1982. Constrained dynamics; Lecture notes in physics. Vol. 169. Berlin: Springer-Verlag.

SYMANZIK, K. 1981. Schrödinger representation and Casimir effect in renormalizable quantum field theory. Nucl. Phys., **B190**, 1.

'T HOOFT, G., & VELTMAN, M. 1972. Regularization and renormalization of gauge fields. Nucl. Phys., **B44**, 189.

TAKAHASHI, Y. 1957. On the generalized Ward identity. Nuovo Cim., **6**, 371.

TANG, A. C. 1988. Regulating $1/(k^+)^n$ singularities in discrete light-cone quantization. Phys. Rev., **D 37**, 3014.

THIES, M. 1985. New interpretation of the Dirac approach to proton-nucleus scattering. Phys. Lett., **B 162**, 255.

THORN, C. B. 1979. Asymptotic freedom in the infinite momentum frame. Phys. Rev., **D 20**, 1934.

WARD, J. C. 1950. An identity in quantum electrodynamics. Phys. Rev., **78**, 182.

WEINBERG, S. 1966. Dynamics at infinite momentum. Phys. Rev., **150**, 1313.

WEINBERG, S. 1967. Dynamical approach to current algebra. Phys. Rev. Lett., **18**, 188.

WEINBERG, S. 1995. The quantum theory of fields. Vol. 1. Cambridge: Cambridge University Press.

WHITTAKER, E. T., & WATSON, G. N. 1927. A course of modern analysis. Cambridge: Cambridge University Press.

WILSON, K. G., WALHOUT, T. S., HARINDRANATH, A., ZHANG, W. M., PERRY, R. J., & GŁAZEK, ST. D. 1994. Nonperturbative QCD: A weak coupling treatment on the light front. Phys. Rev., **D 49**, 6720.

WU, T. T. 1962. Perturbation theory of pion-pion interaction.I. Renormalization. Phys. Rev., **125**, 1436.

YAN, T. H. 1973a. Quantum field theories in the infinite momentum frame. III. Quantization of the coupled spin-one fields. Phys. Rev., **D 7**, 1760.

YAN, T. H. 1973b. Quantum field theories in the infinite momentum frame. IV. Scattering matrix of vector and Dirac fields and perturbation theory. Phys. Rev., **D 7**, 1780.

ZIMMERMANN, W. 1968. The power counting theorem for Minkowski metric. Commun. math. Phys., **11**, 1.

ZIMMERMANN, W. 1969. Convergence of Bogoliubov's method of renormalization in momentum space. Commun. math. Phys., **15**, 208.